CLUSTER THEORIES FOR SUBSTITUTIONALLY DISORDERED ALLOYS

THESIS
submitted to the University of Roorkee
for the award of the degree
of
DOCTOR OF PHILOSOPHY
in
PHYSICS

By
VIJAY KUMAR

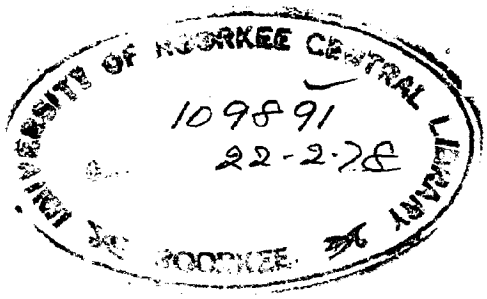

DEPARTMENT OF PHYSICS
UNIVERSITY OF ROORKEE
ROORKEE (INDIA)
June, 1977

TO

MY PARENTS

C E R T I F I C A T E

This is to certify that the thesis entitled 'CLUSTER THEORIES FOR SUBSTITUTIONALLY DISORDERED ALLOYS' which is being submitted by Mr. Vijay Kumar in fulfilment for the award of the degree of Doctor of Philosophy in Physics from the University of Roorkee, is a record of his own work carried out by him under my supervision and guidance. The matter embodied in this thesis has not been submitted for the award of any other degree.

This is further to certify that he has worked for a period equivalent to 24 months full time research for preparing his thesis for Ph.D. Degree at this University.

S.K. Joshi

Dated: June 20,1977

(S.K. Joshi)
Professor and Head,
Physics Department
University of Roorkee
Roorkee, 247672
INDIA.

ACKNOWLEDGEMENTS

It is a great pleasure to express my sincere gratitude to my teacher and supervisor Prof. S.K. Joshi who has always been a source of inspiration for me. His constant encouragement and valuable suggestions, specially during the less productive periods, were a great help for me for the completion of this work.

I am grateful to Drs. Deepak Kumar and A.Mookerjee for their interest in the problem and for their cooperation in several phases of this work. I am thankful to Drs.F.Brouers and M.H. Engineer for fruitful discussions and to Drs.W.H.Butler and F. Ducastelle for several helpful suggestions. I thank Dr. M.J. Kelly for sending me continued fraction coefficients for the simple cubic and the diamond lattices. Thanks are also due to all the members of the Physics Department, University of Roorkee, Roorkee and the Physics Department, D.B.S. Post-Graduate College, Dehradun for their cooperation.

I also take this opportunity to thank the authorities of the Structural Engineering Research Centre, Roorkee, the Computer Centre, Delhi University, Delhi and the Computer Division, Institute of Petroleum Exploration, Dehradun for allowing the use of their computer facilities.

Finally the financial support from the Council of Scientific and Industrial Research, India is gratefully acknowledged.

SYNOPSIS

This thesis is devoted to the study of substitutionally disordered alloys (mainly binary alloys). The contents are divided into two parts. The first part deals with the theories developed for the elementary excitations in disordered systems. In particular, a single band tight binding model Hamiltonian for electrons in disordered systems has been studied in detail. The single site coherent potential approximation (SSCPA), most commonly used in the study of elementary excitations in disordered systems, is not suitable for realistic systems where the constituents have different band widths and the system possesses some short-range-order. It is also inadequate in situations where the mean free path of excitations is small. The SSCPA has, therefore, been generalized by many people in many ways so as to suit various situations. These cluster generalizations are usually very tedious. We have studied a cluster generalization of SSCPA, which is computationally simple so that a numerical calculation of the density of states is possible. We considered clusters made up of a central atom and its Z nearest neighbours. Then analogous to the SSCPA scattering from one such cluster embedded in an otherwise effective medium is considered. The effective medium is determined in different ways namely (i) in the self-consistent central site approximation, (ii) in the self-consistent boundary site approximation and (iii) by imposing self-consistency conditions on the averaged T-matrix elements. The main assumption which reduces the computational

effort to a manageable level without effecting the final results much, is that the various configurations for a fixed number of different kinds of atoms on the shell of nearest neighbours are taken to be indistinguishable. We have considered off-diagonal disorders of Shiba type where the hopping integral h^{AB} is the geometric mean of h^{AA} and h^{BB}, as well as, the general case where h^{AA}, h^{AB} and h^{BB} can take arbitrary values. In the former case the problem reduces to that of the diagonal disorder when one uses a renormalized propagator formulation. We have calculated the densities of states and the spectral densities of states for a wide range of parameters. Our results are in good agreement with the exact results obtained from computer simulation or from the method of moments. A critical study of various approximate cluster methods developed so far by various workers, has also been done.

This cluster method has further been applied to the problem of mixed Heisenberg ferromagnets. In essence the problem is quite similar but a bit more complicated. The constituents have been taken to have different spins and the exchange integrals takes on three values for a binary alloy. The theory describes very well the behaviour of excitations for all values of wave-vector, energy and concentration. Some difficulties have been encountered in the low energy region where the Goldstone theorem is not satisfied.

The second part of the thesis deals with the problem

of surface segregation in alloys. It has been observed that the surface concentration in alloys is different from that of the bulk. A quasi-chemical model has been employed to develop a formalism to calculate concentration in various layers parallel to the surface assuming the alloy to simulate a regular solution. Several interesting aspects of the problem like the effects of foreign atom adsorption and surface relaxation on surface segregation have been considered in a phenominological manner. In addition to some model calculations, results have been obtained for Ni-Au and Ag-Au alloys. Good agreement has been obtained with experimental results obtained from Auger electron spectroscopy. This calculation is further extended to incorporate the short-range-order in alloys (alloys following non-regular solution model). We are able to formulate a method which can predict the short-range-order at the surfaces of alloys.

PUBLICATIONS

1. Electronic structure of disordered alloys-Generalized coherent-potential approximation and effects of environment (with D.Kumar and S.K. Joshi), Phys. Rev. B11, 2831(1975).

2. On the cluster theories of disordered alloys (with S.K.Joshi), J. Phys. C8, L148(1975)

3. Electronic structure of disordered alloys-local environment effects (with D.Kumar and S.K.Joshi), J.Phys.C9, 2733(1976).

4. Surface segregation in random alloys (with D.Kumar and A.Mookerjee), J.Phys.F6, 725(1976).

5. Theory of substitutionally disordered Heisenberg ferromagnets (with D.Kumar and S.K. Joshi), J.Phys.C10,1741(1977).

6. The self-consistent boundary site approximation in the cluster theories of disordered alloys (with S.K.Joshi), Phys. Rev.B16, (in press).

7. Surface segregation in Gold-Silver alloys (with D.Kumar and S.K. Joshi) in the proceedings of International Symposium on Solid State Physics, Calcutta Jan.10-14(1977).

8. Prediction of surface short-range-order parameter and concentration in alloys from bulk data (with D.Kumar and S.K. Joshi), communicated to J.Phys.F.

9. Review article: Electronic States in disordered alloys (with S.K.Joshi), Ind. J.Phys. and the Proc. of Ind. Association for the cultivation of Science, Commemoration Volume, Part II (1977).

C O N T E N T S

CHAPTER I

I N T R O D U C T I O N

For several good reasons* the study of elementary excitations in disordered materials has attracted lot of attention of solid state physicists in recent years[1-8]. Though the subject is not new[9,10] but significant advancement has taken place only within the last two decades. The reason for this slow progress in this exciting field is obvious. In ordered materials, a great simplification is achieved[10,11] because of the presence of translational symmetry in the underlying arrangement described by the positions, composition and orientation of the constituent units. As a consequence of the translational symmetry one only needs information about a unit cell of the crystal to calculate the behaviour of the whole system. This makes the study of ordered materials manageable. The quasi-momentum $\vec{k}$ (we put $\hbar = 1$) of the elementary excitations is a good quantum number and the energy spectrum (which consists of continua separated by regions of forbidden energies) of different kinds of elementary excitations in crystals is determined by the dispersion relation $E = E(\vec{k})$. The eigenstates of quasi-momentum $\vec{k}$ are, according to Bloch's theorem, described by a modulated plane wave with wave vector $\vec{k}$.

---

* In fact, in our practical life, most of the time we deal with systems which do not have the periodicity found in ordered materials. Examples of such systems are doped semiconductors, disordered alloys and magnetic materials, amorphous semiconductors, glasses and liquids.

On the other hand the disordered materials lack the periodicity of the crystal. As a result of which the states of a given quantum number are non-stationary. Strictly speaking the concept of dispersion relation giving energy in terms of the quasi-momentum does not make any sense. As a whole the description of states in disordered materials is quite different and difficult as compared to that in ordered materials.

The central question in the construction of a quantum theory of disordered materials is the study of the structure of the energy spectrum of elementary excitations and the explanation of the character of quantum states possible in such systems. This thesis deals with the theories which try to answer the first question. We shall deal with the class of disordered materials known as substitutionally disordered alloys where on a perfect point lattice, atoms of more than one kind are distributed randomly. Most of our discussion will be confined to binary alloys. Generalizations to an n-component alloy will be straightforward.

The constituents of an alloy will, in general, have different masses and electronic configurations. For a study of the electronic excitations[7,8], one considers the dynamics of an electron moving in a random aperiodic potential field of static ion cores and an effective potential of all other electrons. The problem of vibrations of atoms[3,4], having different masses (mass disorder) and coupled with each other through spring constants which can have different values depending on the occupancy of the sites (force constant disorder), can be transformed to look quite

similar to the electronic problem. The problem of the spin waves in disordered alloys is again very similar[5] to the one of lattice vibrations. A complete solution of such a problem has not yet been achieved. Progress has been made in three directions:

(i) Highly simplified models have been investigated and exact results have been obtained from analytic methods in some cases.[12]

(ii) Machine calculations[13-19] have been carried out for some simple models. In these calculations one solves the equation of motion by constructing a Hamiltonian for a tiny piece of the alloy which is taken to represent the whole system. Most of such calculations have been performed on one dimensional systems. These machine calculations have played a very important role for providing checks on the validity of various approximate theories.

(iii) Study of more realistic models where one has to depend on a number of simplifying assumptions. In this thesis we shall be dealing mostly with problems which fall in this category.

A basic problem which one faces in disordered systems is the lack of detailed information about the microscopic configurations of the atoms in the system. What we know about the disordered materials is some macroscopic parameters such as

the concentration in the case of the alloys. To meet the difficulty of lack of information about the microscopic configurations in formulating a microscopic theory of a disordered system, we take all possible configurations consistent with the macroscopic parameters of the system and then average over all these configurations. Suppose we have a quantity $O(e_1, e_2, \ldots e_k, \ldots)$ which is a function of random variables $e_1, e_2, \ldots e_k, \ldots$. Let these random variables be distributed according to the joint probability distribution function $\pi(e_1, e_2, \ldots e_k, \ldots)$. Then the configurational average of O is given by

$$\langle O \rangle = \int\int \ldots \int \ldots O(e_1, e_2, \ldots e_k, \ldots)\pi(e_1, e_2, \ldots e_k, \ldots) \times de_1\, de_2 \ldots de_k \ldots \quad \ldots (1.1)$$

The symbol $\langle \ldots \rangle$ represents a configuration average. If the random variables $e_1, e_2, \ldots e_k, \ldots$ are independently distributed as in the case of random alloys then $\pi(e_1, e_2, \ldots e_k, \ldots)$ can be written as the product $p_1(e_1)p_2(e_2)\ldots p_k(e_k)\ldots$. This configurational averaging is inherent in all theories of disordered materials.

The mathematical tools (or the theoretical methods) for the study of various types of elementary excitations in disordered systems are the same. In fact, to a good approximation, electron, phonon, magnon and exciton problems reduce to the same formulation[6]. To be specific, here, we shall consider the problem of electronic states in disordered alloys in detail. As stated earlier, this requires solution of the Schrödinger equation with an aperiodic potential. Various approximations have been made to solve this problem[7]. The simplest approximation

is the virtual-crystal approximation (VCA) where the actual configuration dependent crystal potential is replaced by an averaged concentration dependent potential $\langle V \rangle$ constructed out of the potentials of the constituents. For a binary alloy A_xB_{1-x},

$$\langle V \rangle = x\ V_A + (1-x)\ V_B. \qquad \ldots (1.2)$$

V_A and V_B are the crystalline potentials which one would have for a crystal of pure materials A and B respectively. The potential $\langle V \rangle$ is periodic and the resulting Schrödinger equation can be solved using the standard methods of the band theory.[20,21] In practice the VCA provides good agreement with experiments when V_A and V_B do not differ appreciably, such as GeSi alloys.[22,33] In other words we can say that the VCA is good for systems where the mean free path is quite large compared to the interatomic separation.

Recent theories of disordered alloys, which take into account disorder at a realistic level, are usually viewed within the multiple scattering framework [24,25] which regards the propagation of an electron in an alloy as a succession of elementary scatterings on the random atomic scatterers. Conventionally such a description uses Green's functions.[26] Several experimental quantities like the density of states, the specific heat, the neutron scattering cross-sections etc. are related[6] to the Green's function. Therefore, a knowledge of the Green's function will make a comparison between theory and experiments possible.

The most important development in the theory of elementary excitations in disordered alloys has been the introduction of the coherent potential approximation (CPA) by Soven[27] (for electrons) and Taylor[28] (for phonons) in 1967. The CPA is a mean-field theory. The simplicity of the CPA arises from the fact that formally it can be viewed as a reduction of the alloy problem to one of a single impurity in a self-consistently determined effective medium. The CPA has been studied at length for a simple single band tight-binding model Hamiltonian. Though this simple model is not of much interest as far as the realistic systems are concerned, but it has played an important role in our understanding of the energy-spectrum of elementary excitations in disordered alloys. In a very significant contribution Velicky et al[29] studied this model Hamiltonian by considering disorder only in the diagonal term and established the supremacy of the CPA over all the other early theories. Lateron numerous papers have appeared[30] where people have tried to improve upon this model. These improvements have been done mainly in three directions:

(i) Attempts have been made to incorporate the off-diagonal disorder alongwith the diagonal disorder. This represents a more realistic situation. But even with this improvement we are far from reality as far as electrons in disordered systems are concerned. However, these developments proved helpful in the study of phonons[31,32] and magnons[33-35] in disordered systems.

(ii) From machine calculations[13-19] it has been found that

the energy spectrum of excitations presents a fine structure which is a characteristic of various configurations of clusters of atoms. This fine structure is more pronounced in the case of a linear chain. The CPA washes away this fine structure because it is a single site approximation and is incapable of seeing any potential fluctuations due to clusters of atoms.[29,36] The energy spectrum of disordered systems has exact bounds, according to the Saxon-Hutner conjecture[37-41]. This states that there can be no states in the energy region simultaneously forbidden to the energy spectrum of each constituent. The CPA spectrum is cut-off sharply and there are regions where the CPA does not give any states but a finite density of states is allowed. Further, in general, alloys are not completely random but there exist some sort of local order. Such local order can be incorporated in generalizations of the CPA where instead of a single site one considers scattering from a cluster of atoms embedded in an effective medium.

(iii) Finally attempts have been made to improve upon the single band models so as to account for the realistic systems. This has led to the extension of the CPA for degenerate d bands[40, 42-44] and the two-band s-d models[45-48]. Recently attempts have also been made[49-57] to construct alloy theories based on the familiar KKR method in the band structure calculations but using a simpler approximation such as the averaged T-matrix approximation (ATA).

In the first part of the thesis we present some of our attempts towards improving the CPA. We have developed cluster

theories which incorporate the diagonal as well as the off-diagonal disorders in a single band tight binding model Hamiltonian. Efforts have been made to mould the theory in such a way that we get good agreement with exact results obtained from machine calculations. The theory has been applied to the disordered Heisenberg ferromagnetic binary alloys- a problem of correlated site and bond disorders.

The organisation of the first part of the thesis is as follows. In Chapter II we recapitulate some of the ideas of the multiple scattering theory. The single site CPA and the ATA are introduced and discussed for a single band tight binding model. The merits and the demerits of the single site approximation (SSA) are presented and a need for the improvements over the SSA is emphasized. Chapter III deals with the theories which improve upon the calculation of the single particle Green's function. A critical study of the various prevalent cluster theories is made. In this chapter we have restricted ourselves to problems with the diagonal disorder only. Two simple cluster theories, the self-consistent central site approximation (SCCSA) and the self-consistent boundary site approximation (SCBSA) have been studied in detail. The density of states has been calculated for various values of parameters. The analytic behaviour of the Green's function has been studied. Finally we have studied a cluster generalization based on a new configuration averaging technique of Mookerjee[58,59]. In Chapter IV we present formulations where both the diagonal and the off-diagonal disorders are taken into

account. These theories are capable of dealing with alloys having some short-range-order. Two cases have been considered. (i) When the hopping integral h^{AB} is a geometric mean[57] of h^{AA} and h^{BB}, the problem reduces to that of a diagonal disorder if one uses a renormalized propagator formalism[60,61].

(ii) The general case when the hopping integrals h^{AA}, h^{BB} and h^{AB} can have any values, is more difficult to treat. As an example of our approach to this general case, the problem of disordered Heisenberg ferromagnets is studied in Chapter V. The constituents are supposed to have different spins coupled through exchange integrals which can have three different values. The problem is first reduced to an analogous electronic problem. A calculation of the spin wave density of states and the spectral functions has been carried out for the whole concentration range and for various values of exchange integrals.

The second part of the thesis deals with the problem of surface segregation in alloys. In recent years this problem has attained great importance and has attracted attention of several experimentalists and theoreticians.[62] It has been found that the chemical composition in multicomponent systems may be very different at the surface from its bulk value. It can be understood easily from the following simple thermodynamic arguments. Creation of a surface requires work and it is always accompanied by a positive free energy change. Thus, in order to minimize the positive surface free energy, the surface will be enriched by the constituent which has the lowest surface free energy. This results, for many multicomponent

systems, in gross imbalance between the surface composition in the topmost layer and in the bulk. Even when we are dealing with monatomic solids, this surface thermodynamic driving force is the cause of the segregation of impurities at the surface that lowers the total surface free energy.

There are several important surface phenomena such as heterogeneous catalysis, passivation of the surface by suitable protective coatings, corrosion etc. where the chemical composition of the topmost layer controls the surface properties and not the composition in the bulk. Yet another important class of solids is semiconductor alloys which are now used in semiconductor devices in the form of thin films where the surface plays an important role. Most experimental processes like LEED (low energy electron diffraction)[63], photoemission[64] etc. essentially probe surfaces no more than a few Ångstroms deep. Theoretical interpretation of these experimental results should therefore involve surface properties. In order to determine the various properties of surfaces it is essential to know the chemical composition at the surface.

It is expected from a crude calculation involving the Gibbs equation[65] that the component with the lower 'surface tension' accumulates on the alloy surface. The expression which gives the surface concentration is[66]

$$\frac{x^s}{1-x^s} = \frac{x^b}{1-x^b} \exp\left[(\gamma_B - \gamma_A)\, a/kT\right] . \qquad \ldots (1.3)$$

Suffixes s,b denote respectively the surface and the bulk, x the concentration of the solute A in solvent B, γ the surface tension of the pure elements and a the average surface area occupied per atom. Other symbols have their usual meaning. Equation (1.3) is valid for alloys in which the surface segregation is confined to the first atomic plane of the surface (the socalled monolayer model) and the entropy is ideal. There are many surface active organic liquids which demonstrate this surface accumulation of the lower surface tension component in a random binary alloy[67]. Auger electron spectroscopy (AES) provides a direct measurement of surface composition[68,69]. Results have been reported for a large number of alloys e.g. Cu-Ni[70-73], Ag-Pd[74-76], Pb-In[77], Au-Ni[78,79], Fe-Cr[80], Ag-Cu[81], Cu-Au[82-84], Ag-Au[85-87], Au-Sn[88], Ni-Pd[89], Pt-Au[90], Pt-Sn[91,92], Cu-Al[93,94] etc. Temperature and energy dependance of Auger peak intensities give a very sensitive measure of the surface concentration. It is obvious from Eq.(1.3) that although the bulk concentration is independent of temperature, the surface composition depends on it. Such dependence has been borne out by the above experiments. Further, the environment of a surface can have a decisive effect on surface segregation. For example surfaces of Pt-Ag and Pd-Au alloys[95] in vacuum are enriched in Ag and Au respectively. However, the presence of CO in the surface environment causes enrichment of Pt and Pd. The explanation given is the formation of strong carbonyl bonds with Pt and Pd, driving them to the surface.

As most of the solid solutions are not ideal, the

monolayer surface model is not good enough. Instead multi-layer models[96-100] have been developed for regular solutions. Most studies completed so far have been carried out on binary systems which have fairly simple bulk thermodynamic properties that can be described by the regular solution model. In these models the two component crystal is treated as an infinite set of layers of atoms and each layer is treated as having a possibly different composition. An expression is then written for the free energy of the system in the quasi-chemical approach (or the pair bonding model)[101] with the atom fractions of each layer inserted as variable parameters which are varied to obtain the minimum free energy for the whole system. Such an attempt has been made by us[100] and is discussed in Chapter VI. In this model the constituent having the lower heat of vaporization, segregates at the surface. Several interesting aspects such as chemisorption and surface relaxation effects on the surface segregation have been studied. The theory has been applied to Ni-Au system which gives good agreement with the AES experiments[78].

This theory does not always provide good agreement with the experiments. For example in Cu-Au system significant enrichment of the first layer with Au occurs over the whole concentration range, though the heat of vaporization of Au is more than that of Cu. This has been explained on the basis of strain theory of McLean[102] which predicts that segregation should occur whenever the size difference between the constituents is large. Here the driving force for segregation is

the lowering of the elastic strain energy in the bulk which arises from lattice mismatch.

Both of these theories of surface segregation have proven useful in interpreting catalytic[97] and metallurgical[103] phenomenon. But in some cases these theories do not agree with the experiments, e.g. the size difference theory does not predict surface segregation of Au in Au-Pt alloys while it does occur. Similarly the quasi-chemical theory gives quite wrong results for Fe-Zr and both theories fail for Pt-Ni and Pt-Fe alloys. Recently Burton and Machlin[104] have suggested a simple criterion for surface segregation. It is related to the equilibrium distribution of a solute in an alloy in its solid and liquid phases. They observed the analogy of a liquid phase with the surfaces of solids. The two have in common - lower symmetry, lower coordination and no elastic strain. Therefore, segregation should occur in the solid/surface equilibrium if and only if distribution occurs in the solid/liquid equilibrium so that the liquid is richer in solute than the solid phase. With this simple argument they noticed that most of the experimental results could be explained. But this type of observation if at all true, would be able to tell the constituent which will segregate at the surface. To develop a microscopic theory one has to know the chemical composition in various layers. Therefore, one can think of modifying the quasi-chemical theory to explain the experiments.

Another important factor in the case of alloys is the

presence of short-range-order. There has so far been no theory which can predict the short-range-order at the surfaces. We have developed a theory[105] based on the pair bond energy description (quasi-chemical approach) of heat of formation. The theory can predict short range order parameter in different layers parallel to the surface and also between two adjacent layers. This is described in Chapter VII. There are no experimental results. It will be a significant step to determine the short-range-order parameters because the values of interlayer short-range-order parameters may be significantly different from the corresponding bulk value because of the significant difference in the composition of various layers. Such studies will also be of importance in calculating the contact potential and the work function.

PART I

ELEMENTARY EXCITATIONS IN DISORDERED SYSTEMS

CHAPTER II

MULTIPLE SCATTERING THEORY

§2.1 General Considerations:

This section develops a formalism for describing the motion of electrons in disordered substitutional alloys. The results derived in this section are valid for any single particle Hamiltonian in which the disorder term can be decomposed into a sum of contributions associated with each site.

We start with a simple substitutionally disordered binary alloy A_xB_{1-x} in which atoms of two kinds A and B are distributed in a random way on a lattice having N equivalent sites. The probability of finding an A or B atom at any site is x or (1-x) respectively. The one electron Hamiltonian is

$$\underline{H} = -\frac{\hbar^2}{2m}\nabla^2 + V(\vec{r}) \qquad \ldots (2.1)$$

where $V(\vec{r})$ is the total single particle potential which varies from cell to cell. $V(\vec{r})$ can be expressed as a sum of potentials $v_n(\vec{r}-\vec{R}_n)$ contributed by each cell centered at $\vec{R}_n$,

$$V(\vec{r}) = \sum_n v_n(\vec{r}-\vec{R}_n). \qquad \ldots (2.2)$$

v_n takes the value v^A or v^B depending upon whether the site n is occupied, respectively, by an A or B atom. In general v_n may depend on the configuration of the neighbouring atoms,

but this configuration dependence will be neglected in our discussion. It is convenient to express the single particle Hamiltonian (2.1) as a sum of two terms

$$\underline{H} = \underline{H}_o + \underline{H}_1 \qquad \ldots (2.3)$$

where $\underline{H}_o$ is a suitably chosen periodic unperturbed Hamiltonian. For example, it may be a free particle Hamiltonian in which case $\underline{H}_1$ is just V. In the case of a dilute alloy where a small number of A impurities are present in a host B, it is preferred to take $\underline{H}_o$ as the pure host B crystal Hamiltonian $\underline{H}_B$ and deviations from $\underline{H}_o$, on sites A, may be treated in a similar way as in the point impurity case because the probability of finding two impurity atoms close to each other will be very small. Another special case is where the crystal potentials of pure A and pure B crystals do not differ appreciably (weak scattering limit). In this case we may use the virtual-crystal model as the unperturbed Hamiltonian $\underline{H}_o$

$$\underline{H}_o = -\frac{\hbar^2}{2m} \nabla^2 + \langle V(\vec{r}) \rangle \qquad \ldots (2.4)$$

and treat the deviation $\underline{H}_1$ as small perturbation. For the general case,[29] one replaces the ensemble of random systems (characterized by $\underline{H}$) with various configurations by a periodic average crystal which is characterized by an effective Hamiltonian $\underline{H}_{eff}$(yet to be determined). We shall be interested in quantities such as the averaged density of states, the partial density of states and the spectral function which gives information about the life time of excitations. These

quantities are related to the single particle Green's function (see Appendix A) defined as

$$\underline{G}(z) = (z\underline{I} - \underline{H})^{-1} \qquad \ldots (2.5)$$

where $z = E + i\eta$ is the complex energy having an infinitesional imaginary part η. One can similarly define an effective medium Green's function,

$$\langle \underline{G}(z) \rangle \equiv \bar{\underline{G}} = [z\underline{I} - \underline{H}_{eff}(z)]^{-1}. \qquad \ldots (2.6)$$

$\langle \underline{G}(z) \rangle$ and $\underline{H}_{eff}(z)$ both have the full crystal symmetry. As stated earlier in the case of the disordered systems, the excitations have finite life time (as compared to infinite life time in the case of ordered materials). This fact can be incorporated into a theory if we consider that the eigenvalues of the effective Hamiltonian are complex so that the eigenstates decay with time. From the analytic properties of the averaged Green's function[55] if follows that

$$H_{eff}(z^*) = H^{\dagger}_{eff}(z). \qquad \ldots (2.7)$$

$H_{eff}(z)$ will thus be non-Hermitian and energy dependent. In order to determine $\langle \underline{G} \rangle$ for our general problem, we search for some approximate $\tilde{\underline{H}}$ which may be regarded as the starting approximation to the exact effective Hamiltonian and which has the same analytic properties as $\underline{H}_{eff}(z)$. The corresponding Green's function is defined as

$$\tilde{\underline{G}}(z) = [z\underline{I} - \tilde{\underline{H}}]^{-1}. \qquad \ldots (2.8)$$

The configuration dependent Green's function $\underline{G}$ can now be written in terms of the reference Green's function $\tilde{\underline{G}}$ to obtain the following Dyson equation

$$\underline{G} = \tilde{\underline{G}} + \tilde{\underline{G}}\,\underline{U}\,\underline{G} \qquad \ldots (2.9)$$

where $$\underline{U} = \underline{H} - \tilde{\underline{H}}\,. \qquad \ldots (2.10)$$

Iterating (2.9) we obtain

$$\underline{G} = \tilde{\underline{G}} + \tilde{\underline{G}}\,\underline{T}\,\tilde{\underline{G}} \qquad \ldots (2.11)$$

where $\underline{T}$ is the total T-matrix and satisfies the following relation

$$\underline{T} = \underline{U}(\underline{I} + \tilde{\underline{G}}\,\underline{T}). \qquad \ldots (2.12)$$

Taking the configurational average in (2.11) we obtain

$$\langle \underline{G} \rangle = \tilde{\underline{G}} + \tilde{\underline{G}} \langle \underline{T} \rangle \tilde{\underline{G}}. \qquad \ldots (2.13)$$

Also from (2.6) and (2.8) we have

$$\langle \underline{G} \rangle = \tilde{\underline{G}} + \tilde{\underline{G}}(\underline{H}_{eff} - \tilde{\underline{H}}) \langle \underline{G} \rangle. \qquad \ldots (2.14)$$

Comparing (2.13) and (2.14) we have

$$\langle \underline{T} \rangle \tilde{\underline{G}} = (\underline{H}_{eff} - \tilde{\underline{H}}) \langle \underline{G} \rangle \qquad \ldots (2.15)$$

or $$\underline{H}_{eff} = \tilde{\underline{H}} + \langle \underline{T} \rangle (\underline{I} + \tilde{\underline{G}} \langle \underline{T} \rangle)^{-1}. \qquad \ldots (2.16)$$

This equation represents the correction to our initial approximation $\tilde{\underline{H}}$ for $\underline{H}_{eff}$ and can be used in two ways. Either the $\langle \underline{T} \rangle$ corresponding to a given $\tilde{\underline{H}}$ can be inserted into (2.16) or the equation

$$\langle \underline{T} \rangle = 0 \qquad \ldots (2.17)$$

may be used to determine $\underline{H}_{eff}$. These two possibilities define two different classes of approximate calculation of $\underline{H}_{eff}$. The former is known as a non-self-consistent approximation and the latter is a self-consistent approach. For all practical purposes it is impossible to solve (2.17) exactly. Therefore, approximations have been made which simplify the condition (2.17). For this purpose we express the total T-matrix in terms of atomic T-matrices using the multiple scattering theory.

The basic requirement of the multiple scattering theory[24,106] is that the perturbation term $\underline{U}$ can be decomposed as a sum of contributions from each site i.e.

$$\underline{U} = \sum_n \underline{u}_n . \qquad \ldots (2.18)$$

Therefore, from (2.12) we have

$$\underline{T} = \sum_n \underline{u}_n (\underline{I} + \underline{\tilde{G}}\, \underline{T}) \equiv \sum_n \underline{T}_n . \qquad \ldots (2.19)$$

This expresses the T-matrix as a sum of contributions arising from the individual scatterers.

Now $$\underline{T}_n = \underline{u}_n (\underline{I} + \underline{\tilde{G}} \sum_m \underline{T}_m) \qquad \ldots (2.20)$$

or $$\underline{T}_n = \underline{t}_n (\underline{I} + \underline{\tilde{G}} \sum_{m \neq n} \underline{T}_m) \qquad \ldots (2.21)$$

where $$\underline{t}_n = (\underline{I} - \underline{u}_n \underline{\tilde{G}})^{-1} \underline{u}_n \qquad \ldots (2.22)$$

is the atomic T-matrix.

Inserting (2.21) into (2.19) and iterating we obtain the standard multiple scattering series[107]

$$\underline{T} = \sum_n \underline{t}_n + \sum_n \underline{t}_n \tilde{\underline{G}} \sum_{m\neq n} \underline{t}_m + \sum_n \underline{t}_n \tilde{\underline{G}} \sum_{m\neq n} \underline{t}_m \tilde{\underline{G}} \sum_{p\neq m\neq n} \underline{t}_p + \ldots . \quad \ldots (2.23)$$

This expresses the total T-matrix as a sum of terms in which an electron undergoes successive scatterings at various sites. The exclusions in the summations are due to the fact that the atomic T-matrix $\underline{t}_n$ represents the complete scattering from the site n. An electron can scatter again from n only after it has undergone at least one intermediate scattering process. Equation (2.20) physically expresses the strength of a scatterer in the alloy as a product of the strength of an isolated scatterer and a factor describing the transformation of an unperturbed incident wave on the site n into an effective wave because of the multiple scattering in the alloy.

§ 2.2 The Single Site Approximation (SSA)[29]

In the last section we developed a general expression (2.20) or equivalently (2.23) for the total T-matrix. Taking the configurational average in (2.20) we obtain

$$\langle \underline{T}_n \rangle = \langle \underline{t}_n (\underline{I} + \tilde{\underline{G}} \sum_{m\neq n} \underline{T}_m) \rangle \quad . \quad \ldots (2.24)$$

The second term in the bracket on the right hand side involves correlated scattering from two and more sites. Eq.(2.24) can be rewritten as follows:

$$\langle \underline{T}_n \rangle = \langle \underline{t}_n \rangle (\underline{I} + \tilde{\underline{G}} \sum_{m\neq n} \langle \underline{T}_m \rangle) + \langle \underline{t}_n \tilde{\underline{G}} \sum_{m\neq n} (\underline{T}_m - \langle \underline{T}_m \rangle) \rangle \quad . \quad \ldots (2.25)$$

The first term in this equation describes the effect of the averaged effective wave seen by an atom at the site n and the second term corresponds to fluctuations of the effective wave. In the single site approximation one neglects the fluctuation term. We then obtain a closed set of equations

$$\langle \underline{T}_n \rangle = \langle \underline{t}_n \rangle (\underline{I} + \underline{\tilde{G}} \sum_{m \neq n} \langle \underline{T}_m \rangle). \qquad \ldots (2.26)$$

Using the fact that $\sum_{m \neq n} \underline{T}_m = \underline{T} - \underline{T}_n$ we obtain

$$\langle \underline{T}_n \rangle = (\underline{I} + \langle \underline{t}_n \rangle \underline{\tilde{G}})^{-1} \langle \underline{t}_n \rangle (\underline{I} + \underline{\tilde{G}} \langle \underline{T} \rangle). \qquad \ldots (2.27)$$

Substituting (2.27) into (2.16), we obtain

$$\underline{H}_{eff} = \underline{\tilde{H}} + \sum_n (\underline{I} + \langle \underline{t}_n \rangle \underline{\tilde{G}})^{-1} \langle \underline{t}_n \rangle . \qquad \ldots (2.28)$$

The quantity $(\underline{I} + \langle \underline{t}_n \rangle \underline{\tilde{G}})^{-1} \langle \underline{t}_n \rangle$ is the effective scattering potential corresponding to the average scattering arising from the scatterer at the site n. This is known as the average T-matrix approximation[108] (ATA) and is non-self-consistent. On the other hand the self-consistency requirement (2.17) simplifies to

$$\langle \underline{t}_n \rangle = 0 \qquad \ldots (2.29)$$

for all n. Because of the periodicity of the averaged quantities, it is sufficient to consider only one, say the zeroth site. This self-consistent approximation is referred to as the single site coherent potential approximation[27] (CPA). We shall consider this approximation in detail and will later consider some improvements over the single site approximation.

We can have a physical picture of the CPA as follows. Our problem originally was to find a reasonable procedure to determine the effective medium characterized by $\underline{H}_{eff}$. According to the CPA, one considers a system where each site except for one (say the origin) is occupied by the average atom and the origin by either A or B. Then the problem is that of a single impurity embedded in the effective medium (We see from equations (2.24) and (2.26) that the configuration dependent incident wave on site n has been replaced by an effective wave describing the surrounding alloy in an averaged way). The effective medium is then determined in a self-consistent manner by requiring the average T-matrix from this site to be zero.

The fluctuation term neglected in Eqn. (2.25) corresponds to the neglect of all statistical correlations between the site n and all other sites m. These correlations are of two types, (i) those resulting from short-range-order and (ii) those due to multiple scattering. The first of these can be eliminated by assuming the alloy to be completely random. The other correlations, on the other hand, are always present. These correlations play important role when the scattering potential is appreciably large (strong scattering regime). These will be considered in Chapters III and IV. In the next section we present some of the calculations of the density of states for a single band tight binding model Hamiltonian. This has also been used to discuss the demerits of the single site approximation.

§2.3 Critiques of the SSA

Here we study a simple single band tight binding model Hamiltonian in the framework of the SSA. This model Hamiltonian has been very popular in the study of disordered systems and will also be adopted by us in this thesis. Using the Wannier states $|m\rangle$ ($\langle n|m\rangle = \delta_{nm}$) as a basis, the one electron Hamiltonian in the tight binding approximation is[109]

$$\underline{H} = \sum_n |n\rangle \varepsilon_n \langle n| + \sum_{m \neq n} h_{nm} |n\rangle\langle m|, \qquad \ldots (2.30)$$

$$= \underline{D} + \underline{W} \ . \qquad \ldots (2.31)$$

The diagonal term ε_n is the atomic energy level (This includes a term h_{nn} which has the effect of shifting the atomic energies.) associated with the state $|n\rangle$ at the site n and the off-diagonal element h_{nm} represents the hopping integral between the sites n and m. The diagonal term ε_n is a random variable depending on the type of atom occupying the site n i.e. it may be either ε^A or ε^B. The hopping integral h_{nm} is also a random variable and depends, in general, not only on the configuration of the pair of sites n and m but also on the configuration of other sites. The most common assumption here is to neglect the dependence of h_{nm} on sites other than n and m and to restrict to hopping between nearest neighbours. h_{nm} can, therefore, take the values h^{AA}, h^{BB}, $h^{AB} = h^{BA}$ depending on the configuration of sites n and m. In this section we shall further assume that the hopping integrals are translationally invariant so that the only randomness is in the diagonal term $\underline{D}$.

The general case where both the diagonal and the off-diagonal terms are random will be considered in Chapter IV. With this assumption the density of states of the two pure constituents will be identical except for the shift of the energy scale. The matrix elements of $\underline{W}$ in the Bloch representation can be written as

$$\langle \vec{k}|\underline{W}|\vec{k}'\rangle = \delta_{\vec{k}\vec{k}'}\omega s(\vec{k}) \qquad \ldots (2.32)$$

where $$|\vec{k}\rangle = \frac{1}{\sqrt{N}} \sum_n e^{i\vec{k}.\vec{R}_n} |n\rangle \qquad \ldots (2.33)$$

relates the Bloch and the Wannier basis. $\omega = Z|h|$ is the half band width and $s(\vec{k}) = \frac{1}{Z} \sum_n e^{i\vec{k}.\vec{\delta}}$ describes the $\vec{k}$-dependence of the band energy and is dimensionless. $\vec{\delta}$ is the nearest neighbour lattice vector. In the case of simple cubic lattice $s(\vec{k})$ is given by the following expression

$$s(\vec{k}) = \frac{1}{3}(\cos k_x a + \cos k_y a + \cos k_z a). \qquad \ldots (2.34)$$

We choose the energy scale such that

$$\varepsilon^A = \frac{1}{2}\omega\delta = -\varepsilon^B \qquad \ldots (2.35)$$

which defines a dimensionless parameter δ. Now we define the self-energy operator $\underline{\Sigma}(z)$ such that $\underline{H}_{eff} = \underline{W} + \underline{\Sigma}$ and $\underline{\tilde{H}} = \underline{W} + \underline{\sigma}(z)$. The effective Hamiltonian and the averaged Green's function are diagonal in $\vec{k}$-representation,

$$\langle \vec{k}|\underline{H}_{eff}|\vec{k}'\rangle = \delta_{\vec{k},\vec{k}'}\left[\omega s(\vec{k}) + \Sigma(\vec{k},z)\right] \qquad \ldots (2.36)$$

and $\bar{G}(\vec{k},z) = \langle \vec{k}|\underline{\bar{G}}(z)|\vec{k}\rangle$

$$= \left[z - \omega_s(\vec{k}) - \sum(\vec{k},z)\right]^{-1} . \qquad \ldots (2.37)$$

$\bar{G}(\vec{k},z)$ is fully specified by the spectral functions

$$A(\vec{k},E) = -\pi^{-1} \operatorname{Im} \bar{G}(\vec{k},E+i0) \qquad \ldots (2.38)$$

because of the integral representation

$$\bar{G}(\vec{k},z) = \int_{-\infty}^{\infty} \frac{dE}{z-E} A(\vec{k},E) . \qquad \ldots (2.39)$$

From (2.38) and (2.37) we have

$$A(\vec{k},E) = -\frac{1}{\pi} \frac{\operatorname{Im} \sum(\vec{k},E)}{\left[E-\omega_s(\vec{k}) - \operatorname{Re} \sum(\vec{k},E)\right]^2 + \left[\operatorname{Im} \sum(\vec{k},E)\right]^2} . \qquad \ldots (2.40)$$

This shows that the spectral functions are of Lorentzian shape having the half width $-\operatorname{Im} \sum(\vec{k},E)$. The location and the width of the peaks determine, respectively, the quasiparticle energy and the life time. $\operatorname{Re} \sum(\vec{k},z)$ gives the shift in the quasiparticle energy from its value in the perfect crystal specified by $\underline{W}$.

Within the SSA, $\sum(\vec{k},z)$ is independent of $\vec{k}$ and therefore $\underline{\sum}$ is a number operator,

$$\underline{\sum}(z) = \sum_n |n\rangle \sum(z) \langle n| . \qquad \ldots (2.41)$$

(2.31) can now be written as

$$\underline{H} = \underline{W} + \sum_n |n\rangle\, \bar{\sigma} \langle n| + \sum_n |n\rangle\, (\varepsilon_n - \bar{\sigma})\, \langle n|$$

$$= \underline{\tilde{H}} + \sum_n |n\rangle\, (\varepsilon_n - \bar{\sigma})\, \langle n|$$

$$= \underline{\tilde{H}} + \sum_n \underline{u}_n \,. \qquad \ldots (2.42)$$

Now proceeding analogous to Section § 2.1 one obtains the following expression[46] for the self-energy

$$\sum(z) = \bar{\sigma}(z) + \frac{\langle t \rangle}{1 + \langle t \rangle \tilde{F}(z)} \qquad \ldots (2.43)$$

where $\tilde{F}(z) = \langle n|\, \underline{\tilde{G}}(z)\, |n\rangle$ $\qquad \ldots (2.44)$

and $\langle t \rangle$ is the averaged T-matrix. The self-consistency condition (2.29) reduces to

$$\frac{x(\varepsilon^A - \sum)}{1-(\varepsilon^A - \sum)\tilde{F}} + \frac{(1-x)(\varepsilon^B - \sum)}{1 - (\varepsilon^B - \sum)\tilde{F}} = 0. \qquad \ldots (2.45)$$

Eqns. (2.43) and (2.45) have been studied by Velicky et al[29] and later on by Schwartz et al[46] for a semi-elliptical model density of states. The CPA which gives the first eight moments of the density of states correctly[110], is the best single site approximation.[29,111] The ATA may be viewed as the first iteration[46,113] of (2.43) towards self-consistency. Within the appropriate limits, both the CPA and the ATA, exhibit dilute alloy[114], virtual-crystal[107] and atomic limits[115] and therefore represent an interpolation scheme that reduces[29] properly to the exact solutions in very diverse limiting cases. To check the accuracy of the CPA

we compare the CPA density of states for a linear chain (Fig.2.1) and for a simple, cubic lattice (Fig.2.2) with the exact results(histogram)[18,36]. The CPA density of states is obtained from the relation

$$\rho(E) = -\frac{1}{\pi} \mathrm{Im} \langle 0 | \langle G(E+i\varepsilon) \rangle | 0 \rangle \ . \qquad \ldots (2.46)$$

It is easily noticed from the figures 2.1 and 2.2 that the exact results of the density of states have some fine structure, particularly, in the minority band. The CPA gives a smooth density of states. For small values of δ the CPA gives a reasonably good description of an alloy over a wide range of parameters. In other words, the CPA works best when the mean free path of excitations is large. However, it becomes inadequate when the scattering potential δ is large in which case the mean free path is short or the energy of interest lies in the impurity band. The fine structure in the impurity band of the density of states may be attributed to isolated clusters of impurity atoms. Furthermore, the CPA spectrum has a sharp cut-off and there is no band tailing. The tails in the minority band are due to very large clusters of impurity atoms, and play a central role in determining the electronic properties of amorphous semiconductors. Obviously the CPA will be unable to give such behaviours because of its single site nature. The width of the band in the CPA is narrower than the one obtained from the exact results. In the CPA, the band splits for a much smaller value of δ than predicted by the localization theorem[40]. These effects may be included in a

self-consistent manner by applying the CPA formalism to a cell containing several sites rather than to a single site. The foregoing discussion clearly illustrate the need for cluster generalizations of the CPA. This becomes more important when one is interested in alloys where there exist some short-range-order and instead of diagonal disorder alone, there is off-diagonal (extended) disorder as well- a situation one faces in the study of real alloys.

FIGURE CAPTIONS

Fig.2.1 Density of States from the CPA compared with the exact density of states (histogram). (a) $x = 0.5$, $h = 1.0$, $\delta = 0.25$ (b) $x = 0.5$, $h = 1.0$, $\delta = 1.0$. The curves are symmetric about $E = 0$.

Fig.2.2 Density of states from the CPA (---) compared with the exact density of states (——). For all curves $h = 1/6$. (a) $\delta = 0.8$, $x = 0.05$; (b) $\delta = 0.8$, $x = 0.16$; (c) $\delta = 0.8$, $x = 0.5$ and (d) $\delta = 1.5$, $x = 0.1$.

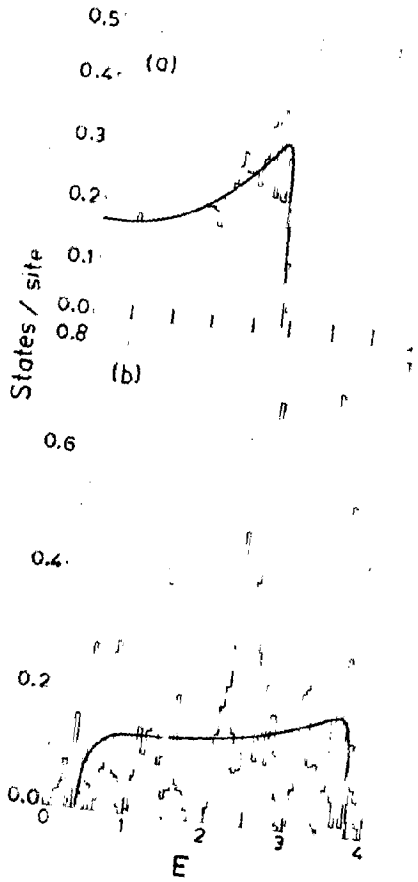

FIG.2.1

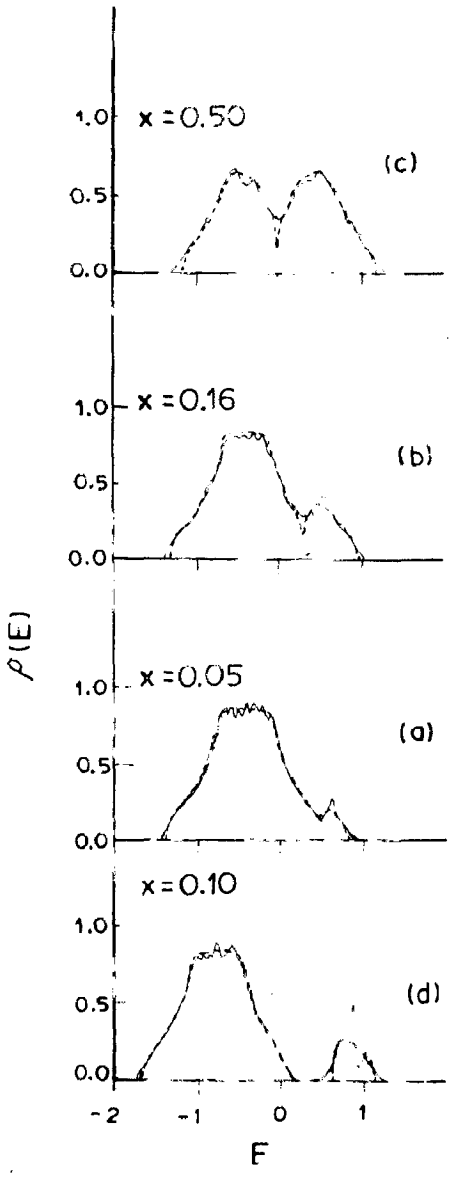

FIG. 2.2

CHAPTER III

CLUSTER THEORIES

In the last section we emphasized the need for cluster generalizations of the CPA to get a better agreement with the exact results and to account for situations one faces in real systems. Further, a large number of experiments[116-120] on concentrated alloys have shown the importance of the local environment on the magnetic and electrical properties of several alloys. These experiments are generally interpreted using a semi-empirical model[116] which assumes that the electronic state of each atom is mainly dependent on the chemical nature of its Z nearest neighbours.

The inadequacy of the CPA for large δ can be understood from the fact that for large values of δ, the fluctuation term (see Eqn. 2.25) neglected in the derivation of the CPA will become important. Therefore, in order to obtain a better estimate of the configurationally averaged Green's function, it is necessary to include this fluctuation term i.e. to consider scattering due to pairs, triplets etc. in a self-consistent manner. In this chapter we shall consider theories which are improvements over the CPA. In what follows, here we shall first consider the work done by us in this direction. A critical study of various cluster theories will be presented in the last section of this chapter.

§ 3.1 The Molecular CPA

The method of molecular CPA (MCPA) also referred to as the cell method, was first introduced by Tsukada[121,122]. It has been, thereafter, used by several workers[8]. This method is based on the fact that if the mean free path is small (a case for which the cluster effects are important), then the main effects of the microscopic configurations of the whole system can be taken into account by considering only the correlations between neighbouring atoms lying within a sphere of radius equal to the mean free path of the excitations. As in this case an electron at a point $\underline{r}$ can see configurations in a small neighbourhood and not the atoms sitting far enough from it. Similar ideas were used by Matsuda and coworkers[123] in their method of MEAPS (Method of Ensemble Average of Periodic Systems) in the calculation of frequency distribution function for random lattices. Very similar proposal was made by Butler and Kohn[124] in their locality principle. They emphasized the fact that the density of states of a disordered system is a local property. Therefore, according to the locality principle a properly performed cluster calculation of the density of states will be exact in the limit of short mean free path.

In the cell method[121] the crystal is divided into small identical non-overlapping cells each containing several sites. The atomic configuration in different cells may be quite different. Then analogous to the single site CPA, the

behaviour of an electron is studied in one of these cells approximating the effects of all the other cells by an averaged medium which is determined self-consistently by requiring the average T-matrix from this cell to vanish.

To derive the MCPA we rewrite the Hamiltonian (2.30) in the following form[70]

$$\underline{H} = \sum_c |c\} \underline{\varepsilon}_c \{c| + \underline{W}. \qquad \ldots (3.1)$$

Here again we are considering only the diagonal disorder. $|c\}$ is a column vector consisting of $\underline{n}$ of the states $|i\rangle$; $\underline{n}$ being the number of sites in the cell. The diagonal matrix $\underline{\varepsilon}_c$ contains the energies of the orbitals centered at the $\underline{n}$ sites in the cell c.

$$\{c| = (\langle ci_1|, \langle ci_2|, \langle ci_3|, \ldots \langle ci_n|) \qquad \ldots (3.2)$$

and

$$\underline{\varepsilon}_c = \begin{bmatrix} \varepsilon_{ci_1} & & & \\ & \varepsilon_{ci_2} & & \\ & & \ddots & \\ & & & \varepsilon_{ci_n} \end{bmatrix} . \qquad \ldots (3.3)$$

Then the results of the multiple scattering theory may be used by changing the single site operators into single cell operators. Proceeding parallel to the section § (2.1) we can write

$$\underline{T} = \sum_c \underline{T}_c \qquad \ldots (3.4)$$

with $\underline{T}_c = \sum_{i\varepsilon c} |i\rangle \langle i|\underline{T} = |c\}\{c|\underline{T}.$ ... (3.5)

The multiple scattering equations for $\underline{T}_c$ are

$$\underline{T}_c = \underline{t}_c(\underline{1} + \underline{\tilde{G}} \sum_{c' \neq c} \underline{T}_{c'}) \quad \text{... (3.6)}$$

where $\underline{t}_c$ is given by

$$\underline{t}_c = (\underline{1} - \underline{V}_c\underline{\tilde{G}})^{-1}\underline{V}_c \quad \text{... (3.7)}$$

with $\underline{V}_c = \sum_{i\varepsilon c} |i\rangle \varepsilon_i \langle i| - \underline{\sigma}_c$ ... (3.8)

$$\underline{\sigma}_c = |c\} \underline{\sigma}(z)\{c|. \quad \text{... (3.9)}$$

Taking the configurational average in (3.6) and decoupling the averages in the right hand side, the exact self consistency condition (2.17) now reduces to

$$\langle \underline{t}_c \rangle = 0 \quad \text{... (3.10)}$$

within the single cell approximation. In this generalization of the CPA, the self-energy $\underline{\Sigma}(z)$ is cell diagonal[36,121,125] i.e. the only non-zero matrix elements of the self-energy are those which connect sites in the same cell whereas the matrix elements between sites lying in different cells are zero. By the introduction of this cell diagonality of the self-energy, the translational invariance of the configurationally averaged medium is broken. However, by the introduction of the cell diagonality of the self-energy several interesting and desired features have been introduced into the theory. These will be

discussed in Section § 3.5. The drawback of broken translational symmetry is perhaps not very important while dealing with local properties such as the density of states. The method can be generalized to any arbitrarily large size of the cell, thereby improving the accuracy of the method. The lowest order approximation will be the one atom cluster which is the CPA. However, in this case the translational invariance of the effective medium is preserved.

The self-consistency condition (3.10) may be alternatively written in terms of the matrix elements of the configurationally averaged Green's function, if we observe that the Green's function for a system with the averaged medium every where except the cell $\underline{c}$, can be written as

$$\underline{G}_c = \overline{\underline{G}} + \overline{\underline{G}}\,\underline{t}_c\overline{\underline{G}}. \qquad \ldots (3.11)$$

Therefore the condition (3.10) becomes

$$\langle \underline{G}_c \rangle = \overline{\underline{G}} \qquad \ldots (3.12)$$

or $$\{c|\langle \underline{G}_c \rangle|c\} = \{c|\overline{\underline{G}}|c\}\ . \qquad \ldots (3.13)$$

Equation (3.13) is an $\underline{n}x\underline{n}$ matrix equation and requires solution of n^2 non-linear simultaneous equations in n^2 unknown matrix elements of the cluster diagonal self-energy. In general, these equations will be quite complicated and difficult to solve without further approximations. For the one dimensional nearest neighbour tight binding model, the density

of states has been calculated by Tsukada[121] and Butler[36]. From these calculations it is observed that as the size of the cluster is increased, the calculated density of states matches with the exact density of states. For two or three dimensional systems, no such calculations have been carried out. Simple cluster theories have been developed and are discussed in the next section.

§ 3.2 Simple Self-Consistent Cluster Theories

To simplify the calculations of the MCPA, people have approximated the form of the cell diagonal self-energy. The simplest approximation[122,126] is to choose a scalar self-energy i.e. $\underline{\Sigma}_c = \Sigma \underline{I}_c$ (where $\underline{I}_c$ is an nxn unit matrix) just like in the single site CPA. Therefore, there will be only one adjustable parameter in the effective Hamiltonian making it impossible to satisfy equation (3.10) which demands that all the n^2 matrix elements of $\langle \underline{t}_c \rangle$ must vanish or the equation (3.12) which demands equality of each matrix element of of $\langle \underline{G}_c \rangle$ with the corresponding one of $\overline{\underline{G}}$. Within the limitations of the scalar coherent potential ansatz, Butler[126] suggested a self-consistent central site approximation (SCCSA) which was later on used by several workers.[61,122,127-131] In this approximation Σ is chosen self-consistently in such a manner that the averaged density of states per site at the center of the cluster is consistent with the external medium i.e.,

$$\langle 0 | \langle \underline{G}_c \rangle | 0 \rangle = \langle 0 | \overline{\underline{G}} | 0 \rangle . \qquad \ldots (3.14)$$

Here the orbital $|0\rangle$ is centered at the center of the cluster. The numerical calculations in this approximation are easy and are in fact similar to that of the CPA except that here one treats a cluster of sites embedded in an effective medium rather than a single site. With the choice of the scalar coherent potential, the effective medium retains its translational invariance. The density of states calculated in this approximation, compares well[126] with the exact results on a linear chain obtained from the Schmidt integral-equation technique[132]. For three dimensional systems this method was applied by Brouers et al[129,130] to the calculation of the phonon frequency spectra of lattices with mass defects for which exact histogram calculations[17] are available. According to their findings, the agreement between the two is fairly reasonable. Unfortunately, this approximation suffers from some severe drawbacks[133] and it is not useful in the strong scattering regime. In this regime the configurationally averaged Green's function $\bar{G}(z)$ is not an analytic function[134] of the energy parameter z. For large values of δ branch points appear in $\bar{G}(z)$ off the real z axis. The density of states may not be a single valued function of energy or for certain values of the energy the density of states may not be defined. These difficulties do not show up for small values of δ. But for large values of δ, one should be cautious while performing numerical calculations. Butler[36] has pointed out that the branch points occur for values of real z which lie near the peaks in the density of states. In this region

of energy the averaged Green's function $\bar{G}(z)$ changes rapidly and therefore one may easily overlook the fact that ones numerical algorithm has switched branches. The origin of these difficulties in the SCCSA has been explained by Butler[36] who also gave a physical argument for the failure of the SCCSA in the strong scattering regime. When the mean free path is shorter than the distance from the center of the cluster to its boundary, then the density of states at the center of the cluster will be almost independent of the external medium. Consequently, it will not be always possible to determine the medium by making the density of states at the center of the cluster consistent with the external medium. On the other hand a boundary site in the cluster is in intimate contact with the external medium. Therefore by requiring the consistency between the averaged diagonal element of the cluster Green's function at the boundary of the cluster and a diagonal element of the Green's function for the uniform external medium, one should avoid the most obvious difficulty with the SCCSA. This has led to the emergence of the self-consistent boundary site approximation (SCBSA)[36]. Like the SCCSA, the SCBSA is also an ad hoc theory and the numerical calculations are very simple. To check the usefulness of the SCBSA, Butler[36] calculated the density of states at the center of the cluster for a linear chain. Surprisingly enough it was found that the SCBSA is identical to the MCPA on a linear chain though the later employed a full matrix self-energy. Butler[36] was able to reproduce the fine structure in

the density of states observed in the exact machine calculations. The equivalence of the SCBSA and the MCPA is, however, true only for a linear chain and not for two and three dimensional lattices. Because in two and three dimensions, the cells which reproduce the lattice when periodically continued, do not have all the boundary sites equivalent. Nonetheless, with this unexpected success of the SCBSA on a linear chain, it was naturally quite encouraging to check the usefulness of the SCBSA in three dimensions. We[135] suggested a simple successive cluster reduction method which enables us to apply the SCBSA to a system of any dimensionality.

3.2a Successive cluster reduction method

In this method we considered clusters made up of a central site and its Z nearest neighbours (This choice is not restricted and one can choose clusters of any size). Then one such cluster is thought to be immersed in an effective medium which is to be determined self-consistently. The Green's function $\underline{G}^c$ for such a system can be written in terms of a Green's function $G^{c(n)}$ of a system in which an atom at the site n in the cluster has been replaced by a fictitious atom with site energy Σ.

$$\underline{G}^c = \underline{G}^{c(n)} + \underline{G}^{c(n)} \underline{t}^{(n)} \underline{G}^{c(n)} \qquad \ldots (3.15)$$

where $$\underline{t}^{(n)} = \underline{V}^{(n)} / (\underline{1} - \underline{G}^{c(n)} \underline{V}^{(n)}) \qquad \ldots (3.16)$$

is the T-matrix corresponding to the potential fluctuation $\underline{V}^{(n)}$

($\underline{V}^{(n)} = (\varepsilon_n - \sum)|n\rangle\langle n|$) at the site n. Now $\underline{G}^{c(n)}$ can be expressed in terms of a Green's function $\underline{G}^{c(nm)}$ of a system in which two atoms at the sites n and m in the cluster have been replaced by fictitious atoms.

$$\underline{G}^{c(n)} = \underline{G}^{c(nm)} + \underline{G}^{c(nm)}\underline{t}^{(m)}\underline{G}^{c(nm)} . \qquad \ldots (3.17)$$

$\underline{t}^{(m)} = \underline{V}^{(m)}/(\underline{1}-\underline{G}^{c(nm)}\underline{V}^{(m)})$ is the T-matrix corresponding to the potential fluctuation $\underline{V}^{(m)}$ at the site m. This process is repeated until all the (Z+1) atoms in the cluster are replaced by fictitious atoms. This method of successively writing the cluster Green's function $\underline{G}^{c}$ in terms of Green's functions of smaller and smaller clusters and ultimately in terms of a perfectly coherent medium Green's function $\overline{\underline{G}}$ enables us to calculate its matrix element at the boundary site of the cluster.

We applied this method to a substitutionally disordered binary alloy A_xB_{1-x} having the diamond lattice structure. The cluster considered consists of a central site (o) and its four nearest neighbours (1,2,3,4). The following set of equations is obtained by repeating the process of Eqn.(3.15):

$$\underline{G}^{c} = \underline{G}^{c(o)} + \underline{G}^{c(o)}\,\underline{t}^{(o)}\,\underline{G}^{c(o)} \qquad \ldots (3.18a)$$

$$\underline{G}^{c(o)} = \underline{G}^{c(o1)} + \underline{G}^{c(o1)}\,\underline{t}^{(1)}\,\underline{G}^{c(o1)} \qquad \ldots (3.18b)$$

$$\underline{G}^{c(o1)} = \underline{G}^{c(o12)} + \underline{G}^{c(o12)}\,\underline{t}^{(2)}\,\underline{G}^{c(o12)} \qquad \ldots (3.18c)$$

$$\underline{G}^{c(o12)} = \underline{G}^{c(o123)} + \underline{G}^{c(o123)}\,\underline{t}^{(3)}\,\underline{G}^{c(o123)}, \qquad \ldots (3.18d)$$

$$\underline{G}^{c(o123)} = \overline{\underline{G}} + \overline{\underline{G}}\,\underline{t}^{(4)}\,\overline{\underline{G}} . \qquad \ldots (3.18e)$$

This process is quite arbitrary and one can write equation (3.18) in many different ways without effecting the final results.

Now suppose we want to calculate the matrix element of $\underline{G}^c$ at the boundary site 1 of the cluster, then from equation (3.18a) we have

$$G^c_{11} = G^{c(o)}_{11} + G^{c(o)}_{10} t^{(o)}_{oo} G^{c(o)}_{01} \quad \ldots (3.19)$$

where $$t^{(o)}_{oo} = V^{(o)}_{oo}(1 - V^{(o)}_{oo} G^{c(o)}_{oo})^{-1}. \quad \ldots (3.20)$$

Expressions for $G^{c(o)}_{11}$, $G^{c(o)}_{10}$ and $G^{c(o)}_{oo}$ are easily obtained from equation (3.18) and can be finally expressed in terms of the matrix elements $\bar{G}(o)$, $\bar{G}(R_1)$ and $\bar{G}(R_2)$ of the effective medium Green's function $\underline{\bar{G}}(z)$. Here we have made use of the fact that for a single band, the matrix elements of $\underline{\bar{G}}$ depend only on the separation between the two sites. Here 0, R_1 and R_2 in the argument of $\bar{G}$ denote 0, the first nearest neighbour and the second nearest neighbour separations. Now $\bar{G}(R_1)$ and $\bar{G}(R_2)$ can be expressed in terms of $\bar{G}(o)$ as follows:

The effective medium Green's function $\underline{\bar{G}}$ can be written as

$$\underline{\bar{G}} = \underline{g} + \underline{g}\,\underline{W}\,\underline{\bar{G}} \quad \ldots (3.21)$$

where $\underline{g}$ is the effective medium locator and is given by

$$\underline{g} = \sum_n (z - \Sigma)^{-1} |n\rangle\langle n|. \quad \ldots (3.22)$$

Therefore

$$\bar{G}(o) = g_{oo} + \sum_i g_{oo} W_{oi} \bar{G}_{io}$$

$$= g_{oo} + g_{oo} h Z \bar{G}(R_1)$$

or $$\bar{G}(R_1) = \{(z - \Sigma)\bar{G}(o) - 1\} / \omega. \quad \ldots (3.23)$$

Also from (3.21)

$$\bar{G}(R_1) = \sum_i g_{oo} W_{oi} \bar{G}_{ij}$$

$$= g_{oo} W_{oi} \bar{G}_{ii} + g_{oo} h(Z-1)\bar{G}(R_2)$$

or $$\bar{G}(R_2) = \{Z(z-\Sigma)\bar{G}(R_1) / \omega - \bar{G}(o)\} / (Z-1). \quad \ldots (3.24)$$

The effective medium is then determined self-consistently by satisfying the following condition

$$\sum_{P_c} P_c G^c_{11} = \bar{G}(o). \quad \ldots (3.25)$$

We calculated G^c_{11} for all the 32 configurations of the 5 atom cluster. P_c is the probability of a particular configuration of the cluster. The half band width of the pure constituents is taken to be 4. Equation (3.25) was solved by an iterative procedure. The density of states calculated in this manner is shown in figure (3.1). We have calculated the density of states at the center of the cluster and at the boundary of the cluster. The density of states at the boundary site is here calculated from the relation

$$\rho(E) = -\frac{1}{\pi} \mathrm{Im}\, \bar{G}(o) \quad \ldots (3.26)$$

and is denoted by SCBSA(B).

The density of states at the center of the cluster is calculated from

$$\rho(E) = -\frac{1}{\pi} \mathrm{Im} \sum_{P_c} P_c G^c_{oo} \qquad \ldots (3.27)$$

and is denoted by SCBSA(C). Expression for G^c_{oo} is obtained from (3.18a) and is given by

$$G^c_{oo} = G^{c(o)}_{oo} + G^{c(o)}_{oo} t^{(o)}_{oo} G^{c(o)}_{oo}. \qquad \ldots (3.28)$$

$G^{c(o)}_{oo}$ and $t^{(o)}_{oo}$ can again be calculated from (3.18b) and (3.20) respectively and can be ultimately written in terms of the matrix elements of the effective medium Green's function.

We have compared our results with the results obtained from the SCCSA[126], the CPA[29] and the disordered field formalism (DFF).[136] The following conclusions can be immediately drawn from the figure:

(i) The SCCSA, the DFF and the CPA show splitting of the band for $\delta = 1$ and $x = 0.5$ while the SCBSA does not. One could see from qualitative arguments of Kirkpatrick et al[40] that inclusion of correlated scattering from a cluster should cause the band split at a higher δ than the one in the CPA.

(ii) There is not much difference in the structure of the SCBSA(B) and the CPA density of states except that the band in the SCBSA (B) has broadened on both the upper and the lower edges. The SCBSA(C) shows a peak in the density of states which agrees well with the results of the DFF. The DFF shows two peaks in the density of states. However, there are some mistakes in the calculations of the environment in the DFF (See Section 3.4).

This effects the band edges and the middle of the band. The DFF has been shown[137] to be equivalent to using full cluster self-energy, whereas here in the SCBSA we used a scalar self-energy. This shows that the SCBSA is also a good approximation even for three dimensional systems. The SCCSA density of states also shows a peaky structure but it has a discontinuity at $E \approx 2.25$. This is because the Green's function has a spurious branch cut in the complex energy plane (for more details see Section § 3.3).

3.2b An approximate configuration counting method

From above calculations it is apparent that the SCBSA reproduces well the fine structure in the density of states if applied to the center of the cluster. The procedure followed here in the derivation of the SCBSA becomes a bit laborious as the number of nearest neighbours increases (e.g. the cubic lattices). The computational effort needed increases a lot because the configurational averages have to be performed over a large number of configurations. We[138] proposed another simpler method in which the number of distinct configurations is greatly reduced by making an assumption that for a fixed number of different kinds of atoms on the shell of nearest neighbours, the different configurations of the atoms on the shell are not distinguished. This approximation in counting configurations was earlier made by Brouers et al[128] in their study of the SCCSA. With this simplifying assumption, the density of states comes out to be the same as the one obtained by recognising and

counting all the different configurations. This will mean that the total averaged density of states is not sensitive to the detailed configuration of the atoms in the cluster.

As before we considered clusters consisting of a central site and its Z nearest neighbours. Then analogous to the single site CPA, one such cluster $\underline{c}$ is thought to be immersed in the effective medium. The Green's function $\underline{G}^c$ for such a system can be written as

$$\underline{G}^c = \{\underline{\bar{G}}^{-1} - \sum_{i\varepsilon c} |i\rangle (\varepsilon_i - \bar{\Sigma}) \langle i|\}^{-1}. \qquad \ldots (3.29)$$

This can be expressed in terms of a Green's function $\underline{G}^s$ of a system in which the central site is also occupied by a fictitious atom with site energy $\bar{\Sigma}$. Then,

$$\underline{G}^c = \underline{G}^s + \underline{G}^s \underline{V}^o \underline{G}^c \qquad \ldots (3.30)$$

where
$$\underline{V}^o = |0\rangle (\varepsilon_o - \bar{\Sigma}) \langle 0| \qquad \ldots (3.31)$$

and 0 denotes the central site.

Now the Green's function $\underline{G}^s$ can easily be expressed in terms of the effective medium Green's function $\underline{\bar{G}}$:

$$\underline{G}^s = \underline{\bar{G}} + \underline{\bar{G}}\, \underline{T}^s \underline{\bar{G}} \qquad \ldots (3.32)$$

where
$$\underline{T}^s = \underline{V}^s (\underline{I} + \underline{\bar{G}}\, \underline{T}^s) \qquad \ldots (3.33)$$

and
$$\underline{V}^s = \sum_i{}' |i\rangle (\varepsilon_i - \bar{\Sigma}) \langle i|, \qquad \ldots (3.34)$$

s denotes the shell of nearest neighbours. Prime denotes that the sum is taken over the shell sites.

In order to determine the effective medium within the SCBSA, we choose the following condition

$$\sum_{P_c} \left(\frac{1}{Z} \sum_{i}' G^c_{ii}\right) P_c = \bar{G}(o) \quad . \qquad \ldots (3.35)$$

Here P_c is the weighted probability of a cluster configuration. Since the various configurations for a fixed number of A and B types of atoms on the shell s are not distinguished, we have summed over all the shell sites and divided by Z to obtain an average matrix element of $\underline{G}^c$ at the boundary site.

The matrix elements of $\underline{G}^c$ are obtained from (3.30)

$$\frac{1}{Z} \sum_{i}' G^c_{ii} = \frac{1}{Z} \sum_{i}' G^s_{ii} + \left\{V^o_{oo}/(1-V^o_{oo}G^s_{oo})\right\} \times \frac{1}{Z} \sum_{i}' G^s_{oi}G^s_{io}. \qquad \ldots (3.36)$$

Equation (3.32) is then solved to obtain

$$\begin{aligned} G^s_{oo} &= \bar{G}(o) + \bar{G}^2(R_1) \sum_{ij}' T^s_{ij} \\ &= \bar{G}(o) + \bar{G}^2(R_1)T \cdot \end{aligned} \qquad \ldots (3.37)$$

where

$$T = \frac{1}{Z} \sum_{ij}' T^s_{ij}. \qquad \ldots (3.38)$$

Also,

$$\begin{aligned} G^s_{ii} &= \bar{G}(o) + \sum_{jk}' \bar{G}_{ij}T^s_{jk}\bar{G}_{ki} \\ &= \bar{G}(o) + \bar{G}(o) \sum_{k}' T^s_{ik}\bar{G}_{ki} + \bar{\Gamma} \sum_{\substack{j\neq i \\ k}}' T^s_{jk}\bar{G}_{ki} \\ &= \bar{G}(o) + (\bar{G}(o)-\bar{\Gamma})^2 T^s_{ii} + (2\bar{\Gamma}\bar{G}(o)-\bar{\Gamma}^2) \sum_{k}' T^s_{ik} \\ &\quad - \bar{\Gamma}^2 \sum_{j}' T^s_{ji} + Z\,\bar{\Gamma}^2\, T. \end{aligned}$$

Summing over i and dividing by Z, we obtain

$$\frac{1}{Z}\sum_i{}' G^s_{ii} = \bar{G}(o) + \frac{1}{Z}(\bar{G}(o)-\bar{\Gamma})^2 \sum_i{}' T^s_{ii} + \{2\bar{\Gamma}\bar{G}(o)+(Z-2)\bar{\Gamma}^2\}T \,. \qquad \ldots (3.39)$$

In a similar manner we also obtain

$$\frac{1}{Z}\sum_i{}' G^s_{oi}G^s_{io} = \bar{G}^2(R_1)(1+Z\bar{\Gamma}T)^2\{1+\frac{2}{Z}(\bar{G}(o)-\bar{\Gamma})\sum_i{}' t_{ii} + \frac{1}{Z}(\bar{G}(o)-\bar{\Gamma})^2\sum_i{}' t^2_{ii}\} \qquad \ldots (3.40)$$

where

$$t_{ii} = V^s_{ii}/(1-V^s_{ii}(\bar{G}(o)-\bar{\Gamma})). \qquad \ldots (3.41)$$

Here the matrix elements of the effective medium Green's function between two different sites of the shell s are approximated by $\bar{\Gamma}$ which is defined as[129]

$$\bar{\Gamma} = \frac{1}{(Z-1)}\sum_{i\neq j}{}' \bar{G}_{ij}. \qquad \ldots (3.43)$$

This approximation is equivalent to the hypothesis that the various configurations for a fixed number of A and B types of atoms on the shell are not distinguished. Expressions for T and T^s_{ii} are obtained from Eq.(3.33),

$$T^s_{ij} = V^s_{ii}(\delta_{ij} + \sum_k{}' \bar{G}_{ik}T^s_{kj})$$

$$= V^s_{ii}(\delta_{ij} + \bar{G}(o)T^s_{ij} + \bar{\Gamma}\sum_k{}' T^s_{kj} - \bar{\Gamma}T^c_{ij})$$

or $$T^s_{ij} = t_{ii}(\delta_{ij} + \bar{\Gamma} \sum_k{}' T^s_{kj}).$$

Therefore

$$T = \frac{1}{Z}(1 + Z\,\bar{\Gamma} T) \sum_i{}' t_{ii}. \qquad \ldots (3.43)$$

Similarly

$$\frac{1}{Z} \sum_i{}' T^s_{ii} = \frac{1}{Z} \sum_i{}' t_{ii} + \frac{\bar{\Gamma}}{Z}(1+Z\,\bar{\Gamma} T) \sum_i{}' t^2_{ii}. \qquad \ldots (3.44)$$

Expression for $\bar{G}(R_1)$ is given by (3.23) and for $\bar{\Gamma}$ it is the same as (3.24),

$$\bar{\Gamma} = \left[Z(z-\bar{\Sigma})\,\bar{G}(R_1)/\omega - \bar{G}(o)\right]/(Z-1). \qquad \ldots (3.45)$$

Once the effective medium is determined by solving the condition (3.35), the partial and the total averaged densities of states are then determined as before in two ways:

(i) At the boundary of the cluster the partial densities of states are calculated from

$$\rho^c(E) = -\frac{1}{\pi Z}\,\mathrm{Im} \sum_i{}' G^c_{ii}. \qquad \ldots (3.46)$$

The total averaged density of states $\rho(E)$ is obtained from (3.26).

(ii) At the center of the cluster these are obtained from

$$\rho^c(E) = -\frac{1}{\pi}\,\mathrm{Im}\, G^c_{oo} \qquad \ldots (3.47)$$

and $$\rho(E) = \sum_{P_c} P_c\, \rho^c(E). \qquad \ldots (3.48)$$

Expression for G^c_{oo} is obtained from (3.30)

$$G^c_{oo} = G^s_{oo}/(1-G^s_{oo}V^o_{oo}), \qquad \ldots (3.49)$$

where G^s_{oo} is given by Eqn.(3.37).

This procedure has been used to calculate the densities of states for binary alloys having the simple cubic and the diamond lattice structures. The input density of states $\rho^{(o)}(E)$ for the pure constituents, needed in the calculation of the Green's function matrix elements, is shown in figure 3.2 for a simple cubic lattice. For the diamond lattice it was calculated using the continued fraction coefficients a_i and b_i's tabulated in table 3.1.

$$\rho^{(o)}(E) = -\frac{1}{\pi} \operatorname{Im} G^{(o)}_{oo}(E)$$

where $G^{(o)}_{oo}(E)$ can be expressed as an infinite continued fraction[139]

$$G^{(o)}_{oo}(E) = \cfrac{1}{E-a_o-\cfrac{b_1^2}{E-a_1-\cfrac{b_2^2}{E-\ldots}}} \qquad (3.50)$$

The Simple Cubic Lattice

Our results for alloys having the simple cubic lattice structure are shown in Figs.3.3-3.7. The half band width of the pure constituents is taken to be unity. In Fig.3.3 we have shown the minority band of an alloy with δ=1.25 and x=0.05. There is not much difference in the results of the CPA and other methods (considered here) as far as the majority band is concerned. The CPA result and the results obtained from

Table 3.1

Continued fraction coefficients for diamond lattice bulk s-band, 21 levels exact.

All a_i's are zero.

	b_i
1	2.0000
2	1.7321
3	2.2361
4	1.8439
5	2.0892
6	1.9358
7	2.0718
8	1.9140
9	2.0861
10	1.9295
11	2.0517
12	1.9571
13	2.0458
14	1.9475
15	2.0533
16	1.9538
17	2.0367
18	1.9679
19	2.0338
20	1.9620
21	2.0348
22	2.0
∞	2.0

two other cluster theories, the SCCSA and the BPA of Brouers et al[128] and the method of moments[140], have also been shown for comparison. The central peak in these results corresponds to an isolated impurity cluster configuration. The other peaks similarly correspond to two impurity, three impurity.... resonance levels. It can be easily noticed that the various peaks in the SCBSA(B) and the SCBSA(C) are centered at about the same energies as in the SCCSA, the BPA and the method of moments. However, there is a marked distinction between the results obtained from the SCBSA(B) and the SCBSA(C). In the case of the SCBSA(B), the various peaks are less prominent as compared to the results obtained from the SCBSA(C). Particularly, the central peak in the SCBSA(B) looks very similar to the one in the CPA and is not well defined. Whereas the results of the SCBSA(C) agree fairly well with the SCCSA, the BPA and the method of moments except that the peaks in the SCBSA(C) are more intense. The method of moments gives a band which is wider than the one obtained from any other method mentioned here. This is because of the smaller size of the cluster considered in the SCBSA or the SCCSA as compared to the method of moments where a cluster of 7175 atoms has been used. Lifshitz[39] has argued that the tailing becomes more prominent as we increase the cluster size very much. The results of the moments method given here are more or less the same as the exact results obtained by Alben et al[18]. The only difference between the two is that the curves in the moment method are smoother due to the fact that the continuation of the continued fraction eliminates the finite size effects. From these we

conclude that the SCBSA(C) results are in good agreement with the exact results.

Figure 3.4 corresponds to an alloy with $\delta = 1.0$ and $x = 0.5$. The SCBSA(B) results are more or less the same as the CPA results (not shown in the figure). The SCBSA(C) result shows peaks at $E \simeq \pm 0.635$ which agrees fairly well with the one obtained from the method of moments. This corresponds to cluster configurations where an A(B) atom is surrounded by 6B or 5B (6A or 5A) atoms as can be seen from figure 3.5 where we have plotted the partial densities of states. However, the SCBSA(C) misses peaks at $E \simeq \pm .325$ and shows some unphysical results in the energy interval $E \simeq -0.02$ to $E \simeq +0.02$. In this region some of the partial densities of states become negative which is obvious from figure 3.5. It is also noticed from figure 3.5 that the partial densities of states do not match at $E = 0.0$ i.e. there are discontinuities in the partial densities of states curves. This is a sign of non-analyticity (see the next section) which makes an approximation unacceptable.

In figure 3.6, we have shown the minority band of an alloy with $\delta = 2.2$ and $x = 0.1$. This corresponds to a split band case. It is obvious from the figure that the SCBSA(B) result is not much different from the CPA result. However, the SCBSA(C) reproduces the fine structure as observed in the result of the moment method. The central peak in the SCBSA(C) is more intense compared to the result of the moment method, whereas the other peaks are subdued. The partial densities of states are found to become negative in the energy region below $E \simeq -.91$.

At certain energies even the total averaged density of states is found to be negative. The results in this energy region are not reliable at all.

The Diamond Lattice

Our results for alloys having the diamond lattice structure are shown in Figs.3.7-3.9. The half band width of the pure constituents has been taken to be 4. The results for alloys with $\delta = 1.0$ and $x = 0.5$ are the same as shown in figure 3.1. In contrast to the simple cubic lattice, here for $x = 0.5$ there are no difficulties of non-analyticities or negative partial densities of states. In figure 3.7 we have shown the minority band of relatively dilute alloy with $\delta = 2.0$ and $x = 0.1$. This corresponds to the split band region. The SCBSA(B) as well as the SCBSA(C) both show fine structure in the densities of states. However, the peaks are more intense in the case of the SCBSA(C). There are no results available for this particular case from other methods. As in the case of the simple cubic alloys, here also we face the problem of negative partial densities of states. In the case of the SCBSA(B), the partial densities of states are shown in figure 3.8. In a small region of energy between $E \approx 3.461$ and $E \approx 3.473$, some of the partial densities of states become negative, (This feature is shown in an insert in the lower part of the figure) whereas the total averaged density of states is positive. In the case of the SCBSA(C), the partial densities of states are positive in this region. But near $E \approx 3.2$, in

both the SCBSA(B) and the SCBSA(C) some of the partial densities of states are negative. In the SCBSA(C) even the total averaged density of states is negative.

In figure 3·9, results have been presented for an alloy with $\delta = 2.0$ and $x = 0.5$. The SCBSA(B) result is more or less similar to the CPA result but the SCBSA(C) shows a peaky structure. Here we do not face any problem of non-analyticity or the negative partial densities of states.

From these results it is clear that though the SCBSA is quite simple and reproduces the fine structure well, yet it suffers from the difficulties of negative partial densities of states and non-analytic behaviour of the Green's function (See Section 3.3) in the strong scattering regime. Further, it is apparent that the SCBSA is superior to the SCCSA as the region of analyticity of the SCBSA is much greater than that of the SCCSA. This region of analyticity also depends on the underlying lattice structure of the alloy. For the diamond lattice the SCBSA is found to be successful over a larger range of parameters in contrast to the simple cubic lattice. Moreover, for a linear chain the SCBSA always yields analytic results whereas the SCCSA does not. We conclude that the SCBSA(C) is reasonably good approximation for the calculation of the electronic structure of disordered alloys, but it should be applied with care in the strong scattering regime.

§3.3 Analytic Properties of Averaged Green's Function

From the analytic properties[134] of the Green's function, every exact configuration dependent Green's function (2.5) contributing to the average has singularities only on the real axis. Therefore, the exact averaged Green's function is analytic in the complex energy plane (Im $z \gtrless 0$) except for a cut along the real axis. The configurationally averaged Green's function may be written as follows:

$$\langle \underline{G} \rangle = \langle (z-\underline{H})^{-1} \rangle = (z-\underline{W}-\underline{\Sigma})^{-1} ; \qquad \ldots(3.51)$$

where the self-energy $\underline{\Sigma}$ has the same analytic behaviour as $\langle \underline{G} \rangle$. Further, both the $\langle \underline{G} \rangle$ and $\underline{\Sigma}$ satisfy the 'reality condition':

$$\underline{\bar{G}}^{*}(z) = \underline{\bar{G}}(z^{*})$$
$$\text{and} \quad \underline{\Sigma}^{*}(z) = \underline{\Sigma}(z^{*}). \qquad \ldots (3.52)$$

In the following we shall work in the upper half-plane (Im $z > 0$) of the complex energy plane. From equation (A.4) of appendix A, it is clear that in this case the imaginary part of the Green's function is negative definite and therefore, from equation (A.11), the density of states is +ve definite. This also leads to the result that the imaginary part of Σ is negative definite.[125]

The question of analyticity of the configurationally averaged Green's function has become an important issue in the theories of disordered systems (especially the cluster theories). In fact the analyticities are very hard to establish analytically and it becomes easier to locate nonanalyticities through a

numerical computation of the Green's function in the complex energy plane. Here from the non-analyticities of the averaged Green's function we shall mean branch points off the real axis. Approximations which lead to $\langle G \rangle$ with such nonanalytic behaviour would be unacceptable.

Müller-Hartmann[141] for the first time gave a general proof that the single site CPA always leads to analytic Green's functions. Later on Ducastelle[125] proved the analyticity of the MCPA. Since the MCPA is hard to apply, an important question is whether the approximate self-consistent theories lead to analytic Green's functions or not. Nickel and Butler[133] carried out numerical calculations of the average Green's function for real as well as complex energies. These calculations were based on two different approximations (i) the pair approximation of Nickel and Krumhansl[142] and (ii) the SCCSA. It was shown that both of these approximations suffer from non-analyticities in the strong scattering regime. At those values of Rez where singular points appear off the real axis, the density of states is not uniquely defined.

We[138] have studied the analytic behaviour of the SCBSA by solving the condition (3.35) self-consistently in the complex energy plane. This equation is highly non-linear and yields many solutions. The correct solution was chosen by starting at a very large value of the energy where we know the asymptotic behaviour of the Green's function ($G(z) \approx 1/z$; $z \to \infty$). This root was then followed towards the energy region of interest. Our results for a simple cubic alloy with $\delta = 2.2$

and $x = 0.1$, are shown in figure 3.10 where we have drawn contours of equal real and imaginary parts of the configurationally averaged Green's function. We started with a large value of Im z and tried to approach the real axis. It was found that for Im $z < 0.05$ as we go from $E = +\infty$ towards the band region the root does not join continuously to the value it will have if we approach the band region from $E = -\infty$. (If every thing works well then there should be only one root which joins continuously onto $G = 1/z$ as $|z| \to \infty (\text{Im } z > 0)$). A discontinuity in the value of the root is an indication for the existence of branch-point singularities off the real axis and forces us to draw branch cuts off the real axis. Here the cut has been drawn parallel to the imaginary z axis at Re $z \approx .91$. The density of states is different if we cross $E \approx .91$ from right to left and from left to right. From this calculation it is apparent that the SCBSA is non-analytic in the strong scattering regime. We also noticed earlier that in this region some of the partial densities of states were negative. It is our conjecture that one will face the problem of non-analyticity of the averaged Green's function in a region where the partial densities of states become negative. The negative partial densities of states observed in both the simple cubic and the diamond lattices, are unphysical and should not be there in any theory. We feel that this defect is inherent in the boundary site condition and it does not stem from the additional approximation that we introduced through equation (3.42). This approximates the matrix elements of $\bar{\bar{G}}$ between two different sites of the shell by their averaged

value $\bar{\Gamma}$ and is exact on a diamond lattice. We have not searched for the lowest value of δ and x at which the non-analytic behaviour of the averaged Green's function (or the negative partial densities of states) starts showing up; but for the simple cubic alloys with $\delta = 1.0$ and $x = 0.5$ and for alloys having the diamond lattice structure with $\delta = 2.0$ and $x = 0.1$, these features are seen in figures 3.4 and 3.7 respectively. It is also concluded from this calculation that the SCBSA is not equivalent to the MCPA in three dimensions as the later always yields analytic Green's functions, but the SCBSA does not. We feel that the problem of non-analyticity will be unavoidable in any cluster theory where the coherent potential matrix is approximated by a scalar coherent potential. Perhaps one should use smaller clusters with proper symmetries and then treat these exactly.

§ 3.4 The Disorder Field Formulation (DFF)

From the discussion of the last section we noticed that most of the cluster theories except the MCPA suffer from the difficulty of non-analytic behaviour of the averaged Green's function. These difficulties arise because of the improper choice of the form of the self-energy matrix. Mookerjee[58] in 1973, introduced a new formalism known as the disorder field formalism (DFF) which preserves the correct 'herglotz' property* of the averaged Green's function. This is because, unlike other conventional techniques, here the averaging is done exactly prior to any perturbation expansion and subsequent approximations. There is no direct introduction of a self-energy

* A function $f(z)$ is called herglotz if for $\mathrm{Im}\, z > 0$, $f(z)$ is analytic and $\mathrm{Im}\, f(z) < 0$.

concept. Whereas all the conventional perturbation approaches construct an effective Hamiltonian by defining a self-energy operator, in the DFF one obtains an effective Hamiltonian by enlarging the initial Hilbert space $\mathcal{H}$ (in which the Hamiltonian operator of the system $\underline{H}$ is described) through the introduction of another Hilbert space Φ which describes the disorder field. The product space $\Psi = \mathcal{H} \otimes \Phi$ is referred to as the 'augmented space'. This method has been discussed in detail by Mookerjee[58] in the case, when the Hamiltonian has only the diagonal disorder. It was shown by Bishop and Mookerjee[143] that within the single site approximation the new formalism reproduces the results of the CPA. In this paper they also showed the way to construct cluster-CPA. The method reproduced the fine structure in the spectrum of a disordered linear chain. Later, Mookerjee[136] applied this formalism to three dimensional systems, namely, alloys having the diamond lattice structure. Unfortunately, in this calculation, some mistakes crept in the calculation of the environment. In this section we shall point out these mistakes and describe some numerical results. We shall not reproduce all the details of the formalism here, but start with the expression[143] for the configurationally averaged Green's function defined as

$$\underline{\bar{G}}(z) = (z\underline{I}_{\Psi} - \underline{\bar{H}})^{-1} \qquad \ldots (3.53)$$

where $\underline{I}_{\Psi}$ is the identity operator in Ψ and $\underline{\bar{H}}$ is the effective medium Hamiltonian which acts in the augmented space Ψ and is defined as

$$\underline{\bar{H}} = \sum_i \underline{P}_i \otimes \underline{Q}_i + \sum_{ij} h_{ij} \underline{T}_{ij} \otimes \underline{I} \qquad \ldots (3.54)$$

where $\underline{Q}_i = \underline{I}_1 \otimes \underline{I}_2 \otimes \ldots \underline{I}_{i-1} \otimes \underline{M}_i \otimes \underline{I}_{i+1} \otimes \ldots$ ... (3.55)

$\underline{Q}_i \epsilon \underline{\Phi}, \underline{M}_i \epsilon \Phi_i$; $\underline{P}_i = |i\rangle\langle i|$ is a projection operator in $\mathcal{H}$.

$\therefore \quad \underline{T}_{ij} = |i\rangle\langle j|$,

$$\underline{\Phi} = \Phi_1 \otimes \Phi_2 \otimes \ldots \quad \Phi_i \otimes \ldots \quad . \qquad \ldots (3.56)$$

and $\underline{I}_i$ is the identity operator in the space Φ_i. $\otimes$ denotes the direct or tensor product. We have yet to define Φ_i and $\underline{M}_i$. For each random variable ϵ_i, we find a Hilbert space Φ_i, a unit vector v_o^i (in Φ_i) and a self-adjoint operator $\underline{M}_i$ (in Φ_i) such that

$$p_i(\epsilon_i) = -\frac{1}{\pi} \operatorname*{Lim}_{\epsilon \to \epsilon_i + io} \operatorname{Im} \langle v_o^i | (\epsilon \underline{I}_i - \underline{M}_i)^{-1} | v_o^i \rangle . \qquad \ldots (3.57)$$

In other words, v_o^i and $\underline{M}_i$ are chosen such that the spectral density of $\underline{M}_i$ with respect to v_o^i is the given probability distribution p of the random variable. Such a relation can always be found for any probability density p. For the binary alloy the probability distribution is given by

$$p_i(\epsilon_i) = x\delta(\epsilon_i - \epsilon_A) + (1-x)\delta(\epsilon_i - \epsilon_B). \qquad \ldots (3.58)$$

For this distribution, Φ_i is a Hilbert space of dimension 2 and the ropresentation of the operator $\underline{M}_i$ in a basis v^i is a 2x2 matrix

$$\underline{M}_i = \begin{pmatrix} a & b \\ b & c \end{pmatrix} , \qquad \ldots (3.59)$$

where
$$\begin{aligned} a &= x\epsilon_A + (1-x)\epsilon_B \\ b &= (\epsilon_A - \epsilon_B)\sqrt{x(1-x)} \\ c &= (1-x)\epsilon_A + x\epsilon_B . \end{aligned} \qquad \ldots (3.60)$$

The eigen values of the matrix $\underline{M}_i$ are ε_A and ε_B and the corresponding eigen vectors are

$$\begin{pmatrix} \sqrt{\frac{x}{1-x}} \\ 1 \end{pmatrix}, \begin{pmatrix} \sqrt{\frac{1-x}{x}} \\ -1 \end{pmatrix} .$$

These eigenvectors can be obtained from a linear combination of the unit vectors

$$\begin{pmatrix} 1 \\ 0 \end{pmatrix} \quad \text{and} \quad \begin{pmatrix} 0 \\ 1 \end{pmatrix} .$$

Therefore the appropriate unit vectors are

$$v_o^i = \begin{pmatrix} 1 \\ 0 \end{pmatrix} \quad \text{and} \quad v_1^i = \begin{pmatrix} 0 \\ 1 \end{pmatrix} . \qquad \ldots (3.61$$

The fact that $\underline{Q}_i$ is equal to the identity operator on all except the i^{th} component of $\underline{\Phi}$ is an expression of the independence of the random variables ε_i's. We further define

$$\gamma_o = v_o^1 \otimes v_o^2 \otimes \ldots \quad v_o^i \otimes \ldots \quad . \qquad \ldots (3.62$$

With these definitions we can now write the matrix elements of the effective Hamiltonian in the augmented space $\bar{\underline{\Psi}}$;

$$\bar{H}_{if,jf'} = \langle if|\bar{\underline{H}}|jf'\rangle = M_i^{ff'}\delta_{ij} + h_{ij}\delta_{ff'} \; ; \qquad \ldots (3.63$$

where the vectors $\{|if\rangle\}$ in the augmented space $\bar{\underline{\Psi}}$ are defined as

$$|\psi_i \otimes v_{\alpha_1}^1 \otimes v_{\alpha_2}^2 \otimes v_{\alpha_3}^3 \otimes \ldots \quad v_{\alpha_k}^k \otimes \ldots \rangle$$

where i denotes the atomic site index and $\alpha_k = 0$ or 1.

Following the notation of Mookerjee we set

$$|if\rangle = |\Psi_i \otimes \gamma_o\rangle \qquad \ldots (3.64)$$

$$|if_j\rangle = |\Psi_i \otimes v_o^1 \otimes v_o^2 \otimes \ldots \; v_o^{j-1} \otimes v_1^j \otimes v_o^{j+1} \otimes \ldots\rangle$$

$$|if_{j\ell}\rangle = |\Psi_i \otimes v_o^1 \otimes \ldots \; v_o^{j-1} \otimes v_1^j \otimes v_o^{j+1} \otimes \ldots \; v_o^{\ell-1} \otimes v_1^\ell \otimes v_o^{\ell+1} \otimes \ldots\rangle$$

and so on. Here $f_{j\ell}$ .... denotes the field states and $\Psi_i \equiv |i\rangle$. The matrix elements of the averaged Green's function are then determined from the relation

$$\bar{G}_{nm}(E) = \langle \Psi_n \otimes \gamma_o | \{(E+io)\underline{I}_{\underline{\Psi}} - \bar{\underline{H}}\}^{-1} | \Psi_m \otimes \gamma_o \rangle . \qquad \ldots (3.65)$$

So far we have described the augmented space formalism for determining the configurationally averaged Green's function of an alloy having only the diagonal disorder. Equation (3.65) is exact and is applicable to one, two or three dimensional alloys. Essentially what we have done so far is that we have transformed the initial Hamiltonian $\underline{H}$ which involves some random variables to $\bar{\underline{H}}$ that has no random variables. We shall now employ a graphical method which gives us physical insight into the nature of the new formalism. In this method one reduces the evaluation of $\bar{G}_{nm}(z)$ to the calculation of the contributions from all 'self-avoiding walks' between $|nf\rangle$ and $|mf\rangle$ available in the whole augmented space $\underline{\Psi}$. This graphical method was introduced by Anderson[144] to study diffusion in random lattices and was later used by Bishop and Mookerjee[143] to calculate the density of states

of diagonally disordered alloys. In order to calculate the density of states in the augmented space formalism we need to evaluate the inner product $\langle \psi_i \otimes \gamma_o | (z\underline{I}_{\underline{\Psi}} - \underline{\bar{H}})^{-1} | \psi_i \otimes \gamma_o \rangle$. Before we actually calculate it, it is instructive to see what equation (3.63) means descriptively in terms of 'walks' in the augmented space. An electron at a site labelled by i and field state f can be induced by $\underline{\bar{H}}$ either to make spatial hops to one of the nearest neighbours j of i with matrix element h_{ij}, keeping the field state the same or it can remain on the same spatial site while the field at the site i changes according to M_i, the fields at all other spatial sites remaining unchanged.

The Graphical Method:

Our problem now is to develop an approximation for the determination of $\bar{G}_{oo}$. The exact graph for this in the augmented space $\underline{\Psi}$ is impossible to think of as it involves an enormously large variety of closed, self-avoiding loops from 'Of' and back. Here we shall discuss the pair approximation in detail and will make only some comments on the higher order approximations. In the pair approximation we retain all the closed self-avoiding paths in $\underline{\Psi}$ between a nearest neighbour pair of spatial sites and delink all closed loops (which involve both spatial and field hops) involving three, four or more spatial sites. In other words in this approximation, two spatial vertices one within and one outside the cluster (here the pair under consideration) cannot be linked in a loop involving field hops. In the multiple scattering

terminology we account exactly the multiple scattering within the cluster whereas the scattering from vertices within the cluster and outside the cluster is treated independently. This is essentially the idea behind the cluster CPA's.

The graph corresponding to a pair approximation is shown in Fig.3.11. Here 'Of' denotes that an electron is at a spatial site '0' and in the field state $|f\rangle$. It can go to the site 1 with an h hop keeping the field same. This is denoted as lf. Then it can change the field at the site 1. This field hop has been denoted by b and the corresponding vertex is denoted as lf_1 corresponding to the state $|lf_1\rangle$. Now it can again come to site '0' in the state $|0f_1\rangle$ without changing the field at 1 and then a field hop to come to state $|0f_{10}\rangle$ and so on. This graph is the same for one, two or three dimensional solids. The only change will be in the calculation of the environment attached to each vertex of the graph. This environment corresponds to walks in the delinked part of the original graph and involves vertices outside the cluster. For a linear chain this procedure was used by Bishop and Mookerjee[143] and for the diamond lattice by Mookerjee[136]. In the application to the diamond lattice there are some mistakes in the calculation of the environment. In Fig.3.12 we show the correct graph for the environment on a diamond lattice. This environment is the same whether one considers a pair or a cluster of a central site and its Z nearest neighbours (as considered by Mookerjee). In the augmented space $\tilde{\Psi}$, the graph corresponding to $\underline{\bar{G}}(E)$ has five fold coordination (for the diamond lattice) at each vertex: four

of them with link factor h (single line) to the four nearest neighbour spatial sites and one with link factor b (double line) corresponding to a 'field' hop. The circles 'g' represent graphs which we call the 'environment'. To begin with we observe that in the graph for g', one spatial hop and a field hop should be missing as we have already included these in the main graph (Fig.3.11). Now we denote by $\hat{g}$ a graph with four h hops to each of which we attach g' and a b link which is again connected by $\hat{g}$. This ensures a five fold coordination at each vertex of the graph. Mookerjee missed this later $\hat{g}$ attached to each b link. None of the $\hat{g}$'s attached to b links from different vertices are interconnected; 'delinking' is, therefore, assured.

When disorder is absent i.e. b = 0, g' is just $3h^2G_{oo}^{(o)}$ on the diamond lattice, where the superscript(o) on G denotes that the Green's function has been calculated in the situation where there is a 'vacancy' in the neighbourhood of the vertex 'O'. The best method of calculating this is the recursion method where we calculate a set of coefficients $\{\beta_n\}$ such that

$$g_{n-1}(E) = 1/[E - \beta_n^2 g_n(E)]$$

$$G_{oo}^{(o)}(E) = g_o(E). \qquad \ldots (3.66)$$

The values of β_n in tables 3.2 and 3.3 were supplied to us by M.J.Kelly.

Table 3.2

Continued fraction coefficients for the diamond lattice (with a vacancy) s-band, 21 levels exact.

All a_i's are zero

	b_i
1	1.732051
2	1.732050
3	2.081665
4	1.954610
5	1.990033
6	2.011724
7	2.001086
8	1.989212
9	2.004332
10	2.011427
11	1.976354
12	2.024587
13	1.982179
14	2.012238
15	1.986095
16	2.020713
17	1.973568
18	2.026295
19	1.978129
20	2.017886
21	1.979012
22	2.0
∞	2.0

Table 3.3

Continued fraction coefficients for the simple cubic lattice (with a vacancy) s-band, 12 levels exact. All a_i's are zero.

	b_i
1	2.236068
2	2.863563
3	3.035561
4	2.933415
5	3.034377
6	2.990541
7	2.988242
8	3.021068
9	2.980383
10	3.010758
11	3.000135
12	2.991404
13	3.0
∞	3.0

In the presence of disorder($b \neq 0$) and referring to Fig.3.12, we have

$$g' = 3h^2 G_{oo}^{(o)}(E-a-b^2\hat{g}) \; ; \qquad \ldots (3.67)$$

$$\hat{g} = \cfrac{1}{E-c-\cfrac{4h^2}{E-a-g'-b^2\hat{g}}} \; . \qquad \ldots (3.68)$$

Here we choose h to be unity. and define

$$X = E-a-b^2\hat{g} \; , \qquad \ldots (3.69)$$

so that $g' = 3h^2 G_{oo}^{(o)}(X)$

and $$X = E - a - \cfrac{b^2}{E-c-\cfrac{4h^2}{X - g'}}$$

The last equation simplifies to

$$(E-c)X^2 - \{(E-c)g' + 4 + (E-a)(E-c) - b^2\} X + (E-a)(E-c)g' + 4(E-a) - b^2 g' = 0 \; . \qquad \ldots (3.70)$$

The solution of (3.67) for $b \neq 0$ can be affected by a Newton-Raphson type iterative procedure. We choose some value of E in the band and start with the known solution for $b = 0$. Then by varying b in small steps we successively reach the point $b = b_o$ by applying the Newton-Raphson technique on the variable b. Then by varying the variable E in small steps we calculate $g'(E,b)$. For $\delta = 1.0$ and $x = 0.5$, the real and imaginary parts of g' are shown in Fig.3.13 for the diamond lattice. A comparison with Mookerjee's result[136](Fig.9) shows that the results are almost identical except near $E = 0.0$ and the band edges. Once the environment is calculated, the diagonal element of the averaged Green's function $\bar{G}_{oo}$ is

obtained from the following relation

$$\bar{G}_{oo} = \frac{1}{z-a-g'-\sum_{P} C(P)} \qquad \ldots (3.71)$$

where C(P) denotes the contribution of a self-avoiding walk. Now from Fig.3.11 there are only four self-avoiding paths which start from vertex 1 (Of) and come back to 1(Of) without repeating any vertex. These are (121), (181), (123456781) and (187654321). Also[143,144]

$$C(121) = h^2 G^{(1)}_{22}$$

$$C(181) = b^2 G^{(1)}_{88}$$

$$C(123456781) = hG^{(1)}_{22}\ bG^{(21)}_{33}\ hG^{(321)}_{44}\ bG^{(4321)}_{55}\ x\ hG^{(54321)}_{66}\ bG^{(654321)}_{77}\ hG^{(7654321)}_{88} b$$

$$\equiv h^4 b^4 G^{(1)}_{22} G^{(21)}_{33} G^{(321)}_{44} G^{(4321)}_{55} G^{(54321)}_{66}\ x\ G^{(654321)}_{77}\ G^{(7654321)}_{88} \qquad \ldots (3.72)$$

and

$$C(187654321) = h^4 b^4 G^{(1)}_{88} G^{(18)}_{77} G^{(187)}_{66}\ G^{(1876)}_{55}\ x\ G^{(18765)}_{44} G^{(187654)}_{33} G^{(1876543)}_{22}.$$

If we exclude 1 then the rest of the graph (Fig.3.11) is just a linear chain shown in Fig.3.14. From this graph it is easy to write the following expressions for various Green's functions.

$$G^{(1)}_{22} \ldots = \frac{1}{z-a-g'-b^2 G^{(21)}_{33}}$$

$$G_{33}^{(21)} = \frac{1}{z-c-g'-h^2 G_{44}^{(321)}}$$

$$G_{44}^{(321)} = \frac{1}{z-a-g'-b^2 G_{55}^{(4321)}}$$

$$G_{55}^{(4321)} = \frac{1}{z-c-g'-h^2 G_{66}^{(54321)}}$$

$$G_{66}^{(54321)} = \frac{1}{z-c-g'-b^2 G_{77}^{(654321)}}$$

$$G_{77}^{(654321)} = \frac{1}{z-a-g'-h^2 G_{88}^{(7654321)}}$$

$$G_{88}^{(7654321)} = \frac{1}{z-c-g'} \qquad \ldots (3.73)$$

$$G_{88}^{(1)} = \frac{1}{z-c-g'-h^2 G_{77}^{(18)}}$$

$$G_{77}^{(18)} = \frac{1}{z-a-g'-b^2 G_{66}^{(187)}}$$

$$G_{66}^{(187)} = \frac{1}{z-c-g'-h^2 G_{55}^{(1876)}}$$

$$G_{55}^{(1876)} = \frac{1}{z-c-g'-b^2 G_{44}^{(18765)}}$$

$$G_{44}^{(18765)} = \frac{1}{z-a-g'-h^2 G_{33}^{(187654)}}$$

$$G_{33}^{(187654)} = \frac{1}{z-c-g'-b^2 G_{22}^{(1876543)}}$$

$$G_{22}^{(1876543)} = \frac{1}{z-a-g'} \,.$$

The corresponding density of states has been shown in Fig.3.15 along with the CPA results. The DFF shows a two peaked structure. Densities of states for other parameters are shown in Fig.3.16. The DFF shows a peaky structure which becomes more prominent as disorder is increased and a wider band as compared to the CPA. We have not been able to complete calculations for clusters consisting the central site and its four nearest neighbours, because of inadequate computer facilities. This problem requires an inversion of a complex 160x160 matrix. The main graph corresponding to the cluster remains the same as given by Mookerjee. We have also performed pair calculations for a simple cubic lattice. The graph for the environment is shown in Fig.3.17. In general the equation (3.67) may be written as follows:

$$g' = (Z-1)h^2 G_{oo}^{(o)}(X) \qquad \ldots (3.74)$$

where X satisfies the equation

$$(E-c)X^2 - \{(E-c)g' + Zh^2 + (E-a)(E-c) - b^2\} X + (E-a)(E-c)g' + Zh^2(E-a) - b^2 g' = 0 \qquad \ldots (3.75)$$

The results of the pair calculation for the simple cubic lattice are similar to the one for the diamond lattice. A cluster (consisting of (Z+1)sites) calculation for the simple cubic lattice will require inversion of a $(7x2^7)x(7x2^7)$ complex matrix and the main graph for calculating $\bar{G}_{oo}$ will be much more complicated than the corresponding graph for the diamond lattice.

The DFF has been shown[137] to be equivalent to using a full cluster diagonal self-energy. In this sense we can say that the cluster calculations in DFF are equivalent to the MCPA. Both of these always yield analytic Green's functions. The DFF has recently been applied to alloys having diagonal as well the off-diagonal disorders[145] and to situations where there exist some short-range-order[146] in the alloys. A single bond approximation for alloys having off-diagonal disorder alone was formulated by us[147]. These formulations have been used to calculate density of states for a linear chain. An application of the DFF to three dimensional lattices will be quite involved. This necessitates, therefore, a need for simpler cluster generalizations which preserve the herglotz propery of the Green's function.

§ 3.5 A Critical Study of Various Cluster Theories

After the introduction of the CPA by Soven[27] it was reformulated in a variety of ways, e.g., the locator method[148,149], the diagrammatic technique[150], the cumulant expansion method[151], the moment method[152], the recursion method[153], and the DFF[143]. All of these methods led to the same results in the single site approximation. But unlike the single site CPA there is no unique way for cluster generalizations of the CPA. The early attempts in this direction were based on improving the CPA by considering correlated scatterings from pairs, triplets etc. But conflicting ideas came into picture. In some of these generalizations[154,155] based on the multiple scattering approach people have considered all the pairs which

connect a site n with all the rest of the sites in the system. The self-energy in this approximation is no longer diagonal in the site representation but has off-diagonal matrix elements between every pair of sites. Whereas in some of the other pair generalizations[150,156] based on diagrammatic techniques people have considered multiple scatterings from a nearest neighbour pair embedded in an effective medium. The self-energy in this approximation is a 2x2 matrix. Though these generalizations produced some fine structure in the density of states but were not quite satisfactory. In these generalizations the equivalence between the locator and the propagator expansions as observed in the single site CPA, is no longer preserved[148]. The numerical calculations by Nickel and Butler[133] show that these generalizations suffer from the difficulty of non-analytic behaviour of the averaged Green's function in the strong scattering regime. Further the formulae of Nickel and Krumhansl[142] and that of Cyrot-Lackmann and Ducastelle[154] do not have the appropriate split band limit. The pair approximations also fail to take into account the correlation effects arising from the symmetry of the underlying lattice. This has led to generalizations like the MCPA already discussed. In these generalizations one usually considers instead of a pair, a cluster of central site and its Z nearest neighbours. This cluster generalization has proved quite fruitful, as it preserves[157] the equivalence between the locator and the propagator expansions and yields analytic Green's functions[125]. Numerical calculations[36] on a linear chain also give excellent agreement

with the exact results. But the MCPA is quite difficult to apply to three dimensional lattices. The DFF also appears to be equivalent to the MCPA though it has not been rigorously proved. The only drawback of the MCPA is that the effective medium does not have the property of translational symmetry of the empty lattice. But it is supposed not to be a severe drawback while evaluating local properties such as the densities of states.

The difficulty in applying the MCPA to three dimensional lattices has led to the emergence of simple approximations like the SCCSA and the SCBSA. Though the two approximations give quite reasonable density of states which agrees well with the available exact results but suffer from the difficulties of non-analytic behaviour of the averaged Green's function and the negative partial densities of states in the strong scattering regime. The DFF too becomes very much involved as we go towards higher order approximations and its general applicability seems to be very restricted. Recently Desjonqueres and Cyrot-Lackmann[140] have done calculations using the method of moments. This promising method gives an excellent agreement with the exact results[18]. The important point in this method is that it does not use the Bloch's theorem or the detailed band structure. It works for both the bulk as well as the local properties at the surfaces of ordered and disordered materials. However, this method has not so far been applied to any real alloy*.

* This method has been applied to several transition metals by Cyrot-Lackmann and coworkers and excellent results have been obtained.

Yet another method, which is similar in nature to the method of moments in the sense that it also does not require the use of detailed band structure calculations, is the recursion method. This method was initially introduced by Haydock et al[139] to study the electronic structure of transition metals which can be well described in the tight binding approximation. Later, it was applied to disordered alloys by Mookerjee[58], Jacobs[153], Cubiotti et al[158], and Kerker[153]. This method, in principle, allows one to treat exactly the problem of a cluster embedded in a given Cayley-tree or linear chain effective medium. In their application of the recursion method, Jacobs[153] and Cubiotti et al[158] chose an effective medium characterized by a Green's function which is a weighted average of the Green's functions for the two pure components of an alloy. Since such an effective VCA type medium is known to yield less accurate densities of states, it is expected that using such a medium should yield less accurate cluster Green's functions. Also for a dilute alloy Jacobs and coworkers obtained an unexpected triangular shaped majority band which is certainly due to an inadequate termination of their continued fraction. They truncated the continued fraction at the fourth level which will not give the proper shape of the density of states curves.

We feel that the MCPA and the method of moments are the best approaches todate for cluster generalizations. But for general applicability some simpler methods have yet to be developed which would preserve the desired herglotz

property of the Green's function. Here it will be of interest to mention that the SCCSA and the SCBSA give very good results for moderately disordered alloys and are the simplest of any other cluster generalization of the same order.

FIGURE CAPTIONS

Fig.3.1 Density of states curves for a binary alloy having the diamond lattice structure. $\delta = 1.0$, $x = 0.5$ and $\omega = 4.0$. The curves are symmetric about $E = 0$.

Fig.3.2 Density of states for a simple cubic bulk s-band.

Fig.3.3 Minority band of the density of states curves for a binary alloy having the simple cubic lattice structure. $\delta = 1.25$, $x = 0.05$, $\omega = 1.0$.

Fig.3.4 Density of states curves for a binary alloy with $\delta = 1.0$, $x = 0.5$ and having the simple cubic lattice structure. The arrow shows the region where non-physical results are obtained in the SCBSA.

Fig.3.5 Representative plots of the partial densities of states. The curves are discontinuous at $E = 0.0$.

Fig.3.6 Minority band of the density of states curves for a simple cubic alloy with $\delta = 2.2$ and $x = 0.1$. The vertical arrow shows the region where the branch point occur off the real axis. The horizontal arrow shows the region where some of the partial densities of states are negative.

Fig.3.7 Minority band of the density of states curves for a binary alloy having the diamond lattice structure with $\delta = 2.0$ and $x = 0.1$. The horizontal arrow shows the region where some of the partial densities of states are negative.

Fig.3.8 Plots of the partial densities of states in the minority band in the SCBSA (B). The parameters are the same as in Fig.3.7(——), (— —), (- - -), (—·—) and (—··—) respectively correspond to cluster configurations in which an impurity atom A is surrounded by 4A, 3A and 1B, 2A and 2B, 1A and 3B and 4B. See the missing

peak near $E \approx 3.2$. The arrow indicates the region where some of the partial densities of states become negative. This has been shown on an enlarged scale in the lower part of the figure. Also in the region near $E \gtrsim 3.2$, some of the partial densities of states are negative.

Fig.3.9 The density of states curves for binary alloys having the diamond lattice structure with $\delta = 2.0$ and $x = 0.5$. The curves are symmetric about $E = 0$.

Fig.3.10 Contours of equal real and imaginary parts of the averaged Green's function $\bar{G}(o)$ in the SCBSA. The various parameters are the same as in Fig.3.6. The solution has been chosen in such a manner that $\bar{G}(z) \approx 1/z$ as $z \to \infty$ ($Imz > 0$). A branch cut has been drawn at $Rez \gtrsim 0.91$.

Fig.3.11 The graph showing exactly all closed loops in the augmented space connecting two nearest neighbour sites for an alloy whose site energies have a bimodal distribution.

Fig.3.12 The graph g' corresponding to the environment on a diamond lattice.

Fig.3.13 Real (----) and imaginary (——) parts of environment g' for a binary alloy with $\delta = 1.0$ and $x = 0.5$ on a diamond lattice.

Fig.3.14 Part of the graph 3.11 when the vertex 1 is excluded.

Fig.3.15 Density of states in the pair approximation (——) and the CPA(----) for a binary alloy having the diamond lattice structure. The curves are symmetric about $E = 0$.

Fig.3.16 Minority band of the density of states curves for an alloy having the diamond lattice structure.

Fig.3.17 The graph g' corresponding to the environment on a simple cubic lattice.

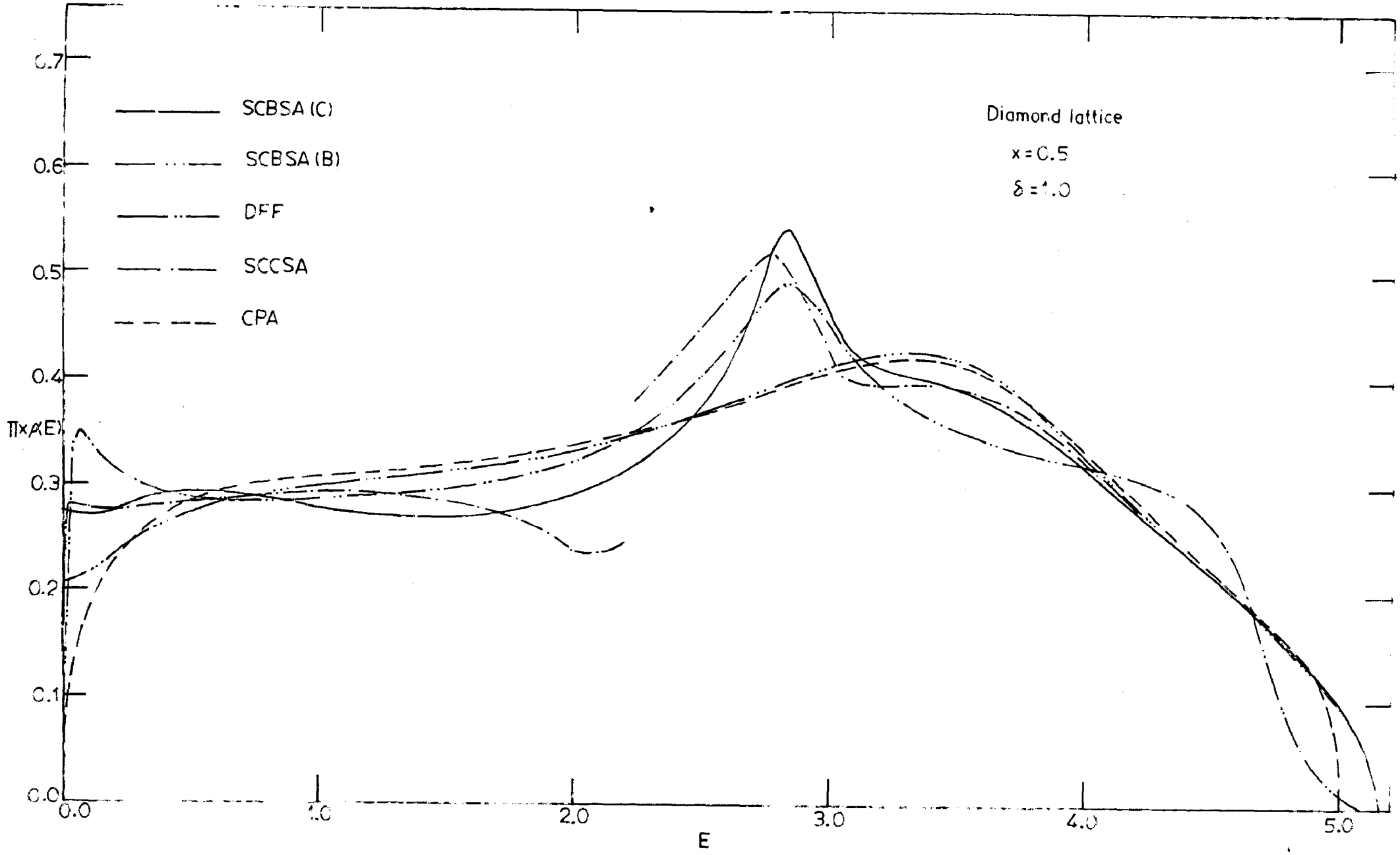
SCBSA (C)
SCBSA (B)
DFF
SCCSA
CPA
Diamond lattice
x = 0.5
δ = 1.0
πxA(E)
E
0.0
0.1
0.2
0.3
0.4
0.5
0.6
0.7
1.0
2.0
3.0
4.0
5.0

FIG. 3.1

Density of states of simple cubic lattice

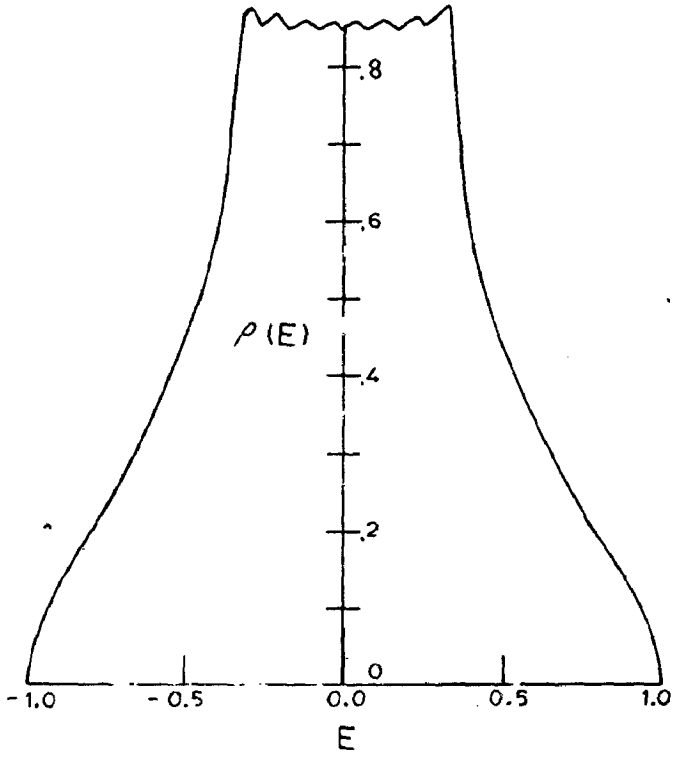

FIG.3.2

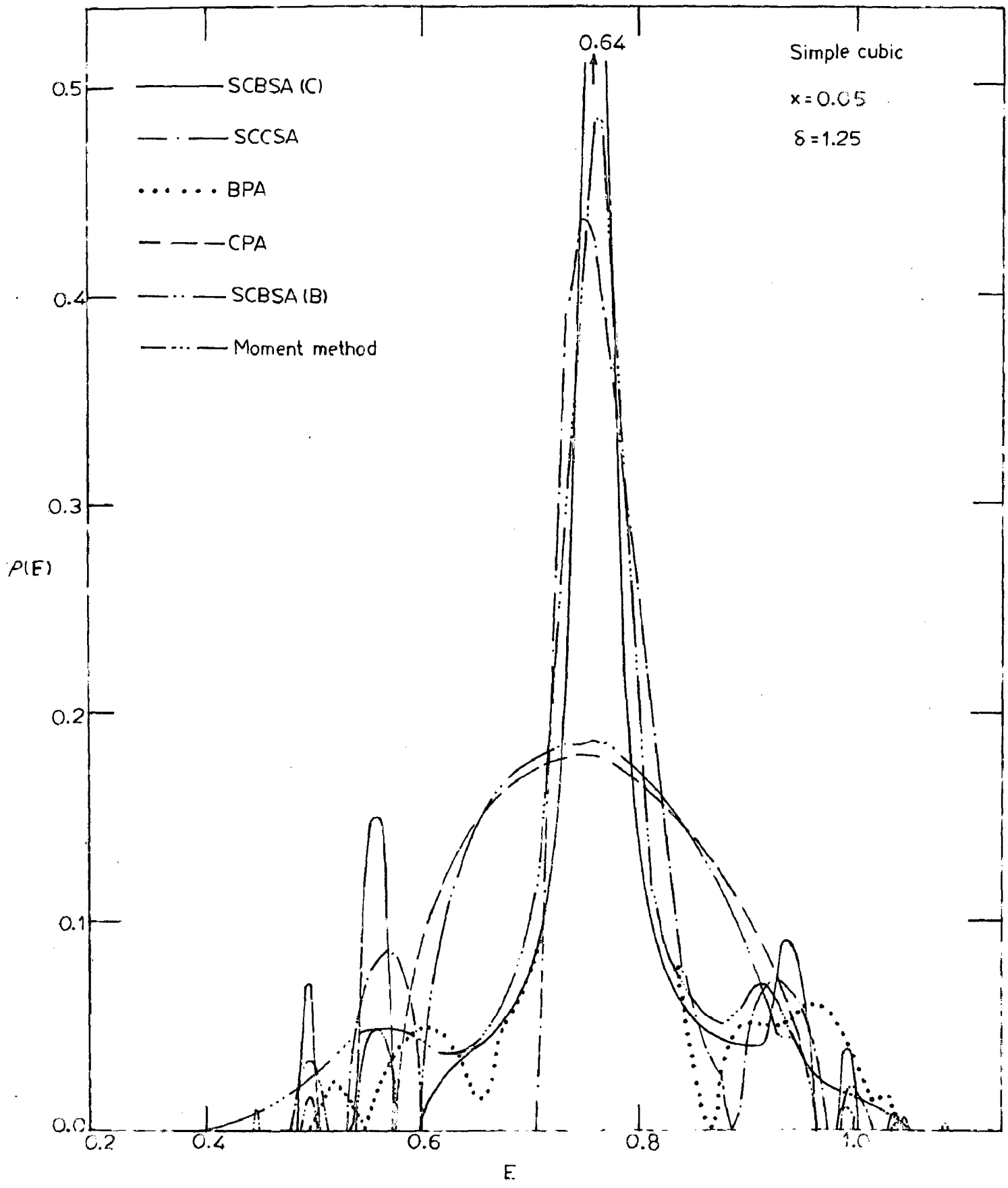
0.64
Simple cubic
x = 0.05
δ = 1.25
SCBSA (C)
SCCSA
BPA
CPA
SCBSA (B)
Moment method
P(E)
E
0.0
0.1
0.2
0.3
0.4
0.5
0.2
0.4
0.6
0.8
1.0

FIG.3.3

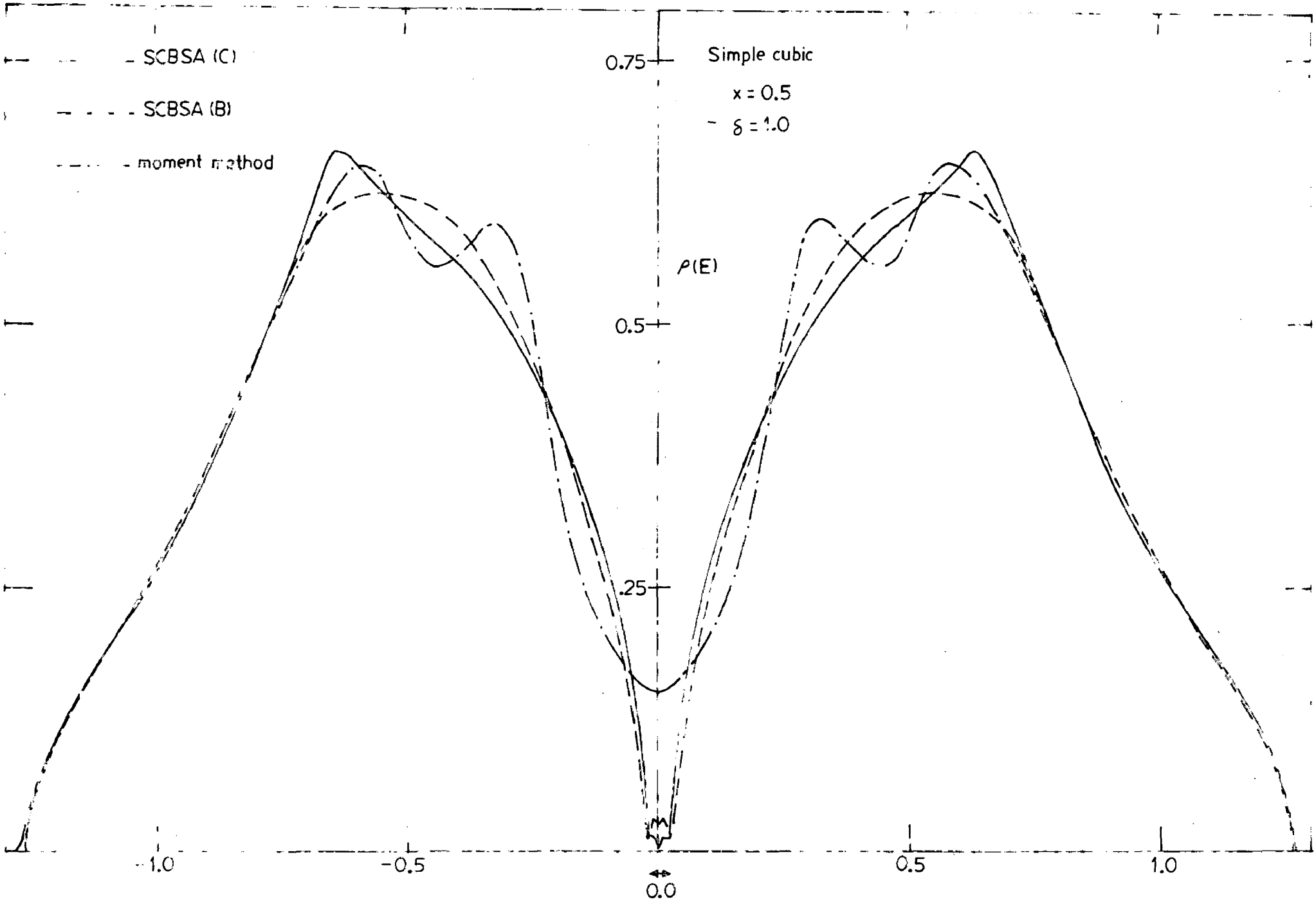
SCBSA (C)
SCBSA (B)
moment method
Simple cubic
x = 0.5
δ = 1.0
0.75
0.5
.25
ρ(E)
-1.0
-0.5
0.0
0.5
1.0
E

FIG. 3.4

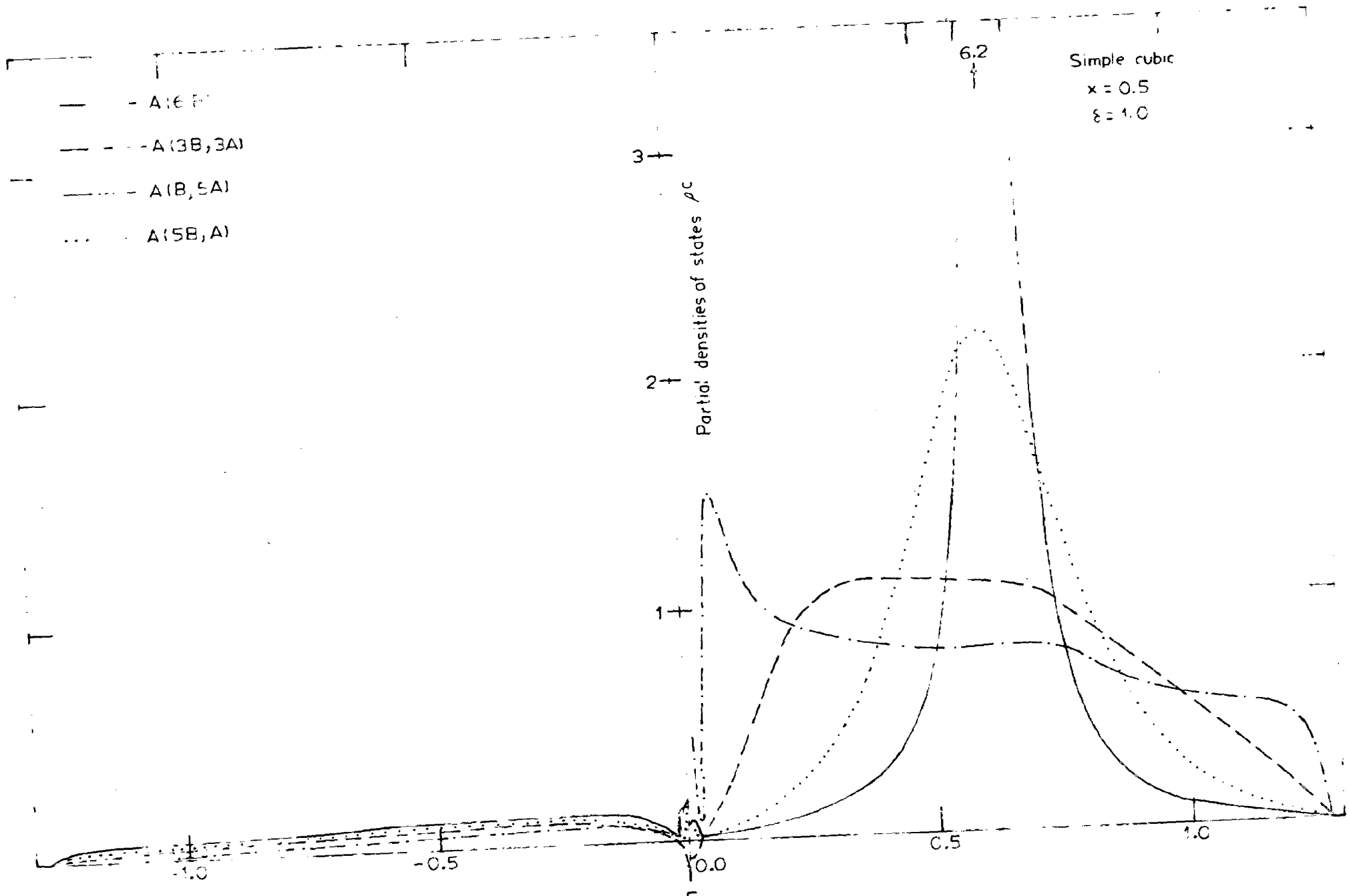
A(B,A)
A(3B,3A)
A(B,5A)
A(5B,A)
6.2
Simple cubic
x = 0.5
ε = 1.0
3
2
1
Partial densities of states ρC
-1.0
-0.5
0.0
0.5
1.0
E

FIG.3.5

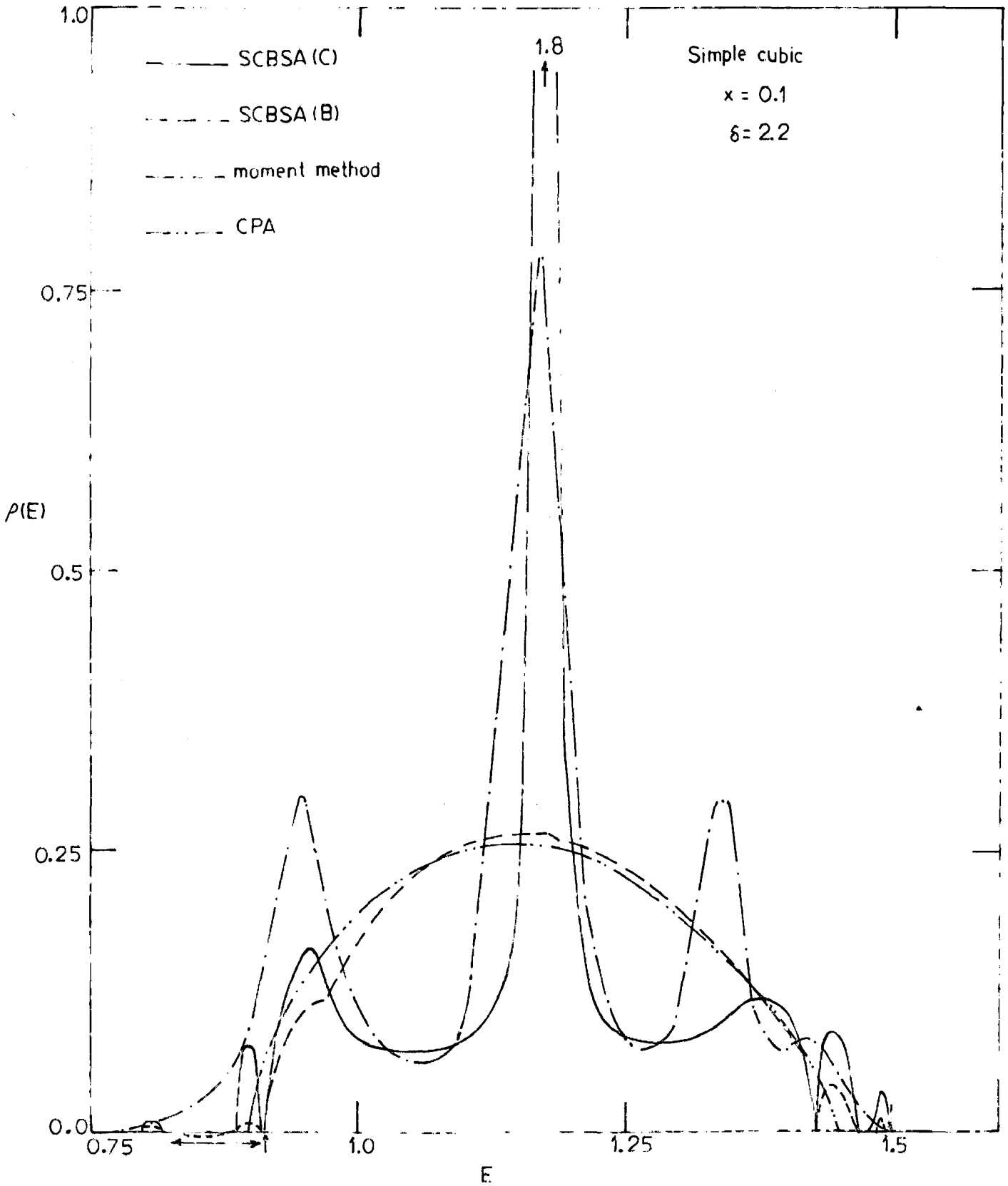
SCBSA (C)
SCBSA (B)
moment method
CPA
Simple cubic
x = 0.1
δ= 2.2
1.8
1.0
0.75
0.5
0.25
0.0
ρ(E)
0.75
1.0
1.25
1.5
E

FIG. 3.6

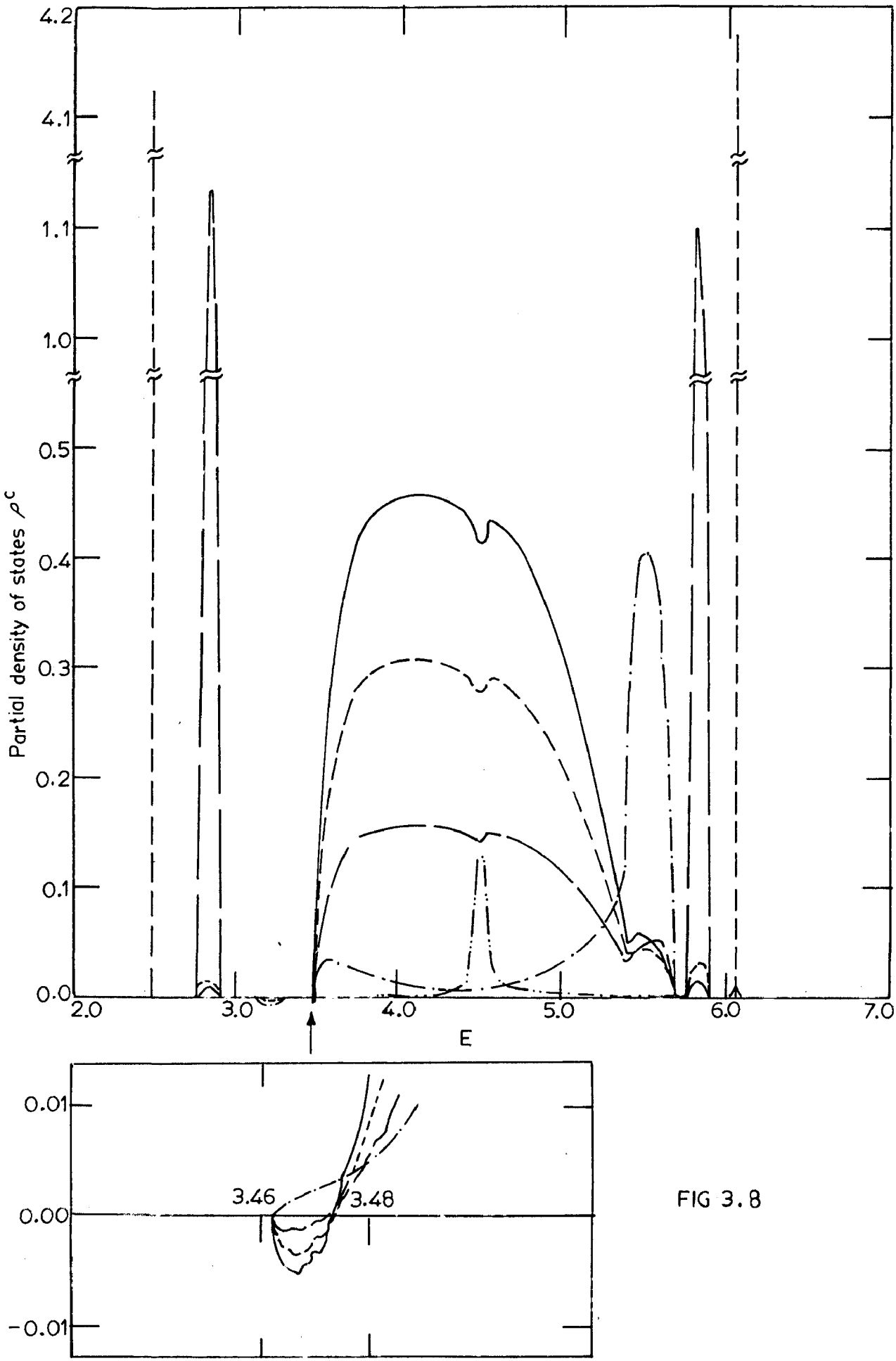
4.2
4.1
1.1
1.0
0.5
0.4
0.3
0.2
0.1
0.0
Partial density of states ρ^c
2.0
3.0
4.0
5.0
6.0
7.0
E
0.01
0.00
-0.01
3.46
3.48

FIG 3.8

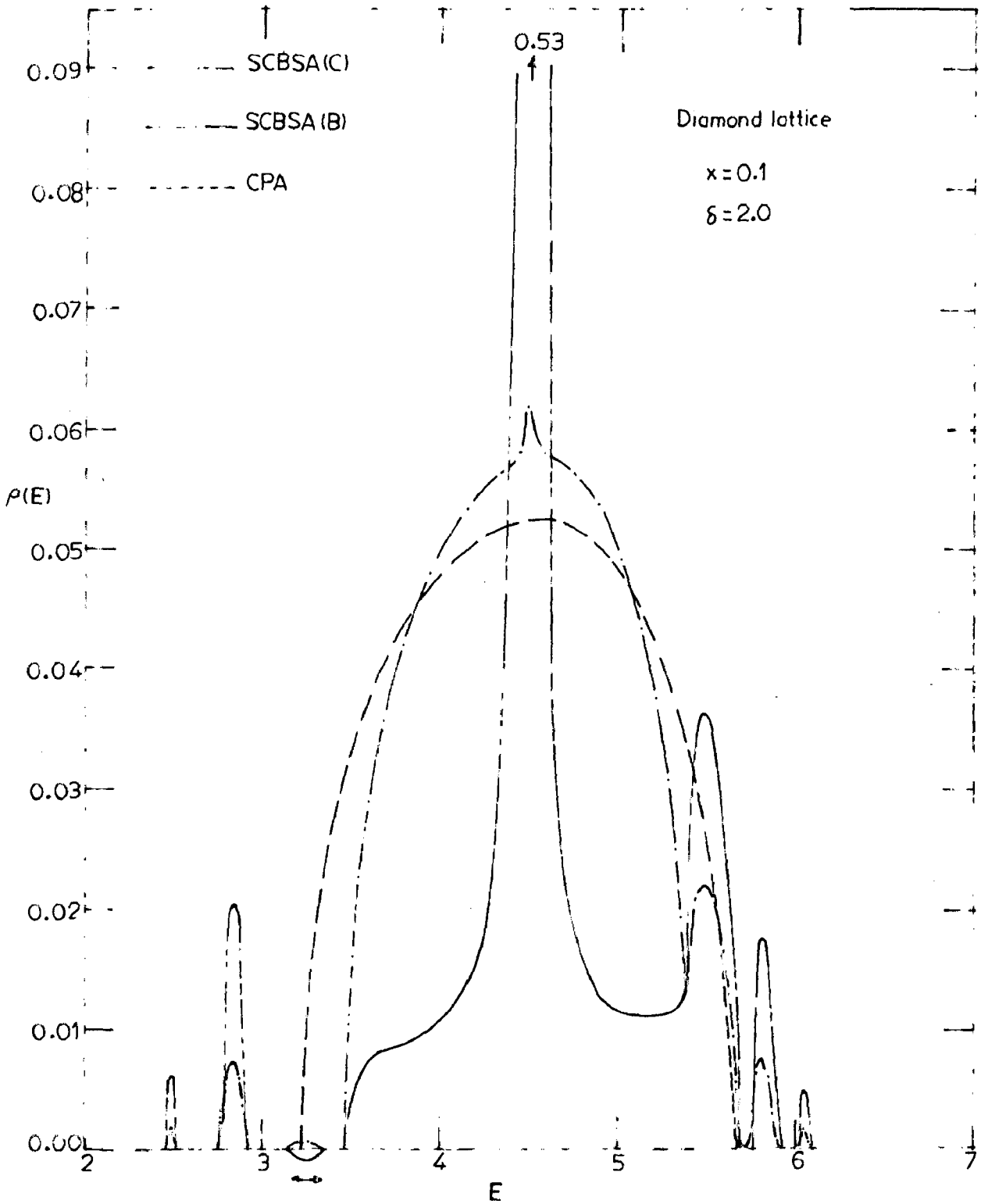
SCBSA(C)
SCBSA(B)
CPA
Diamond lattice
x = 0.1
δ = 2.0
0.53
ρ(E)
0.09
0.08
0.07
0.06
0.05
0.04
0.03
0.02
0.01
0.00
2
3
4
5
6
7
E

FIG. 3.7

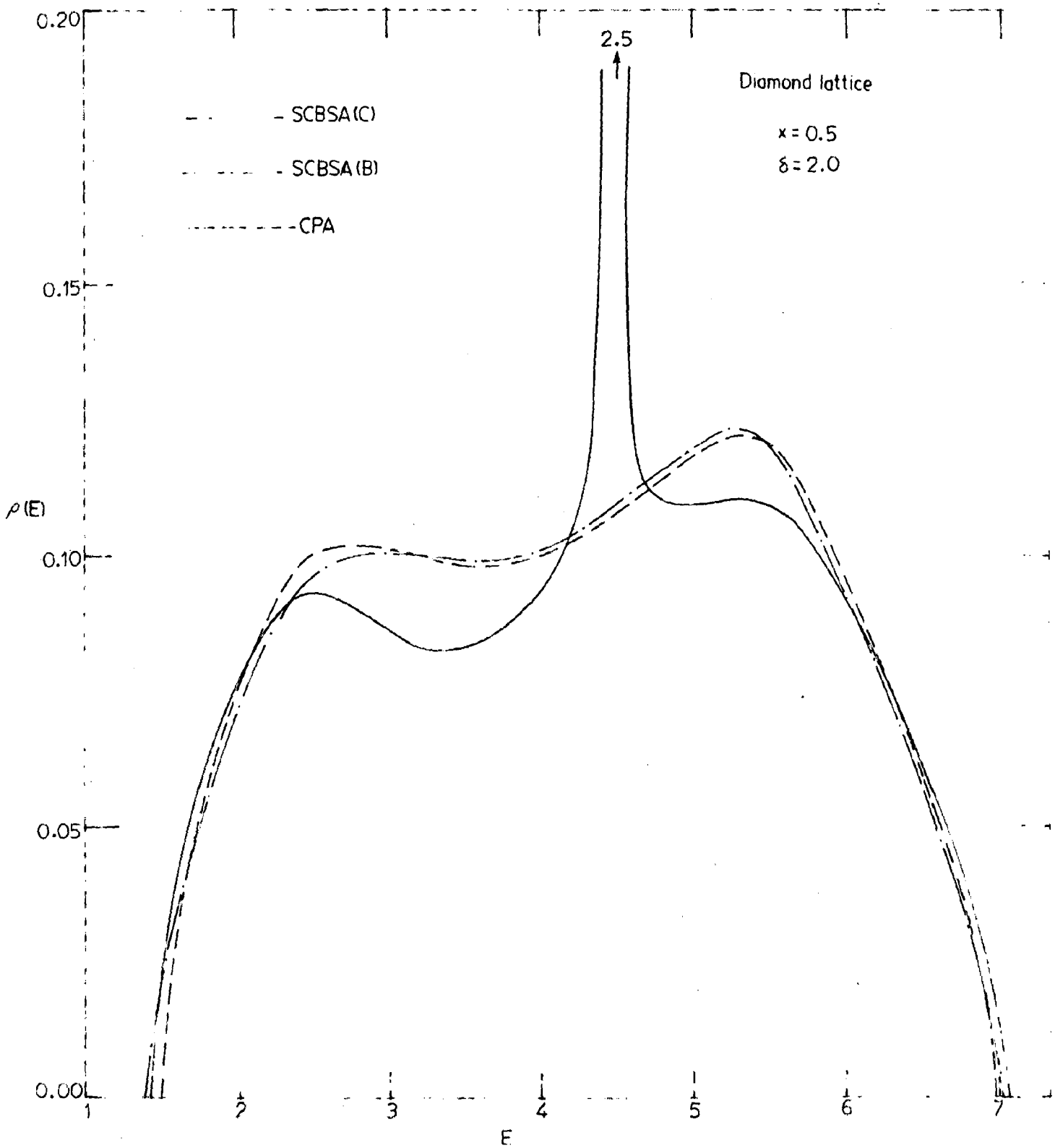
0.20
0.15
0.10
0.05
0.00
ρ(E)
2.5
Diamond lattice
x = 0.5
δ = 2.0
SCBSA(C)
SCBSA(B)
CPA
1
1/2
1/3
1/4
1/5
1/6
1/7
E

FIG. 3.9

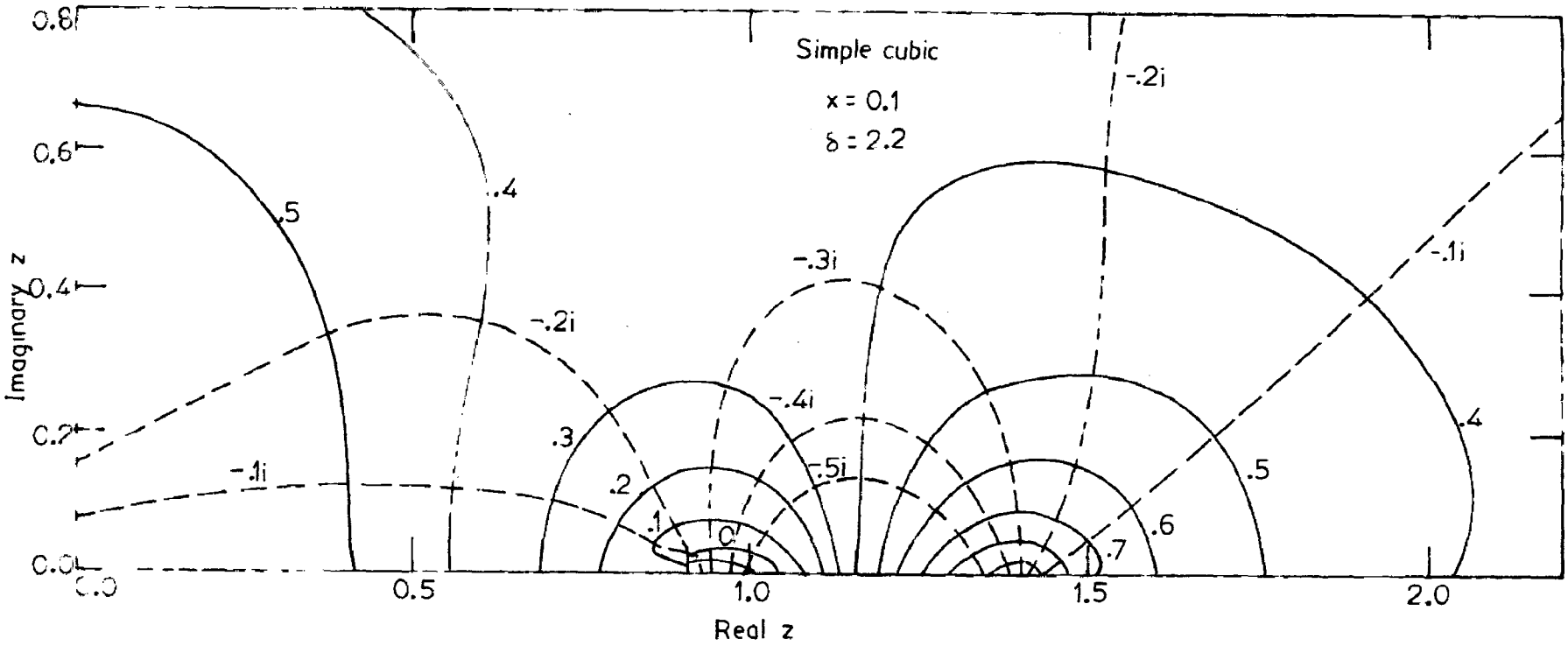
Simple cubic
x = 0.1
δ = 2.2
0.8
0.6
0.4
0.2
0.0
Imaginary z
0.0
0.5
1.0
1.5
2.0
Real z
.5
.4
-.2i
-.3i
-.2i
-.1i
-.4i
.3
-.5i
.2
.1
.4
.5
.6
.7
-.1i

FIG. 3.10

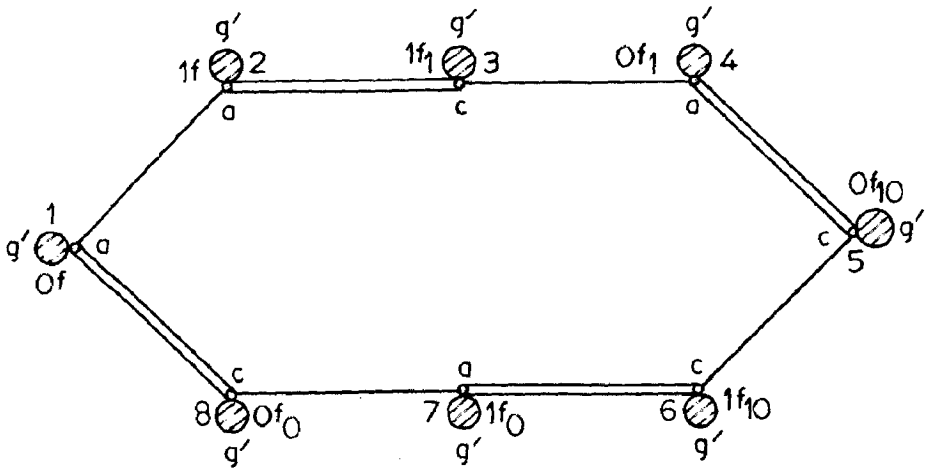

FIG. 3.11

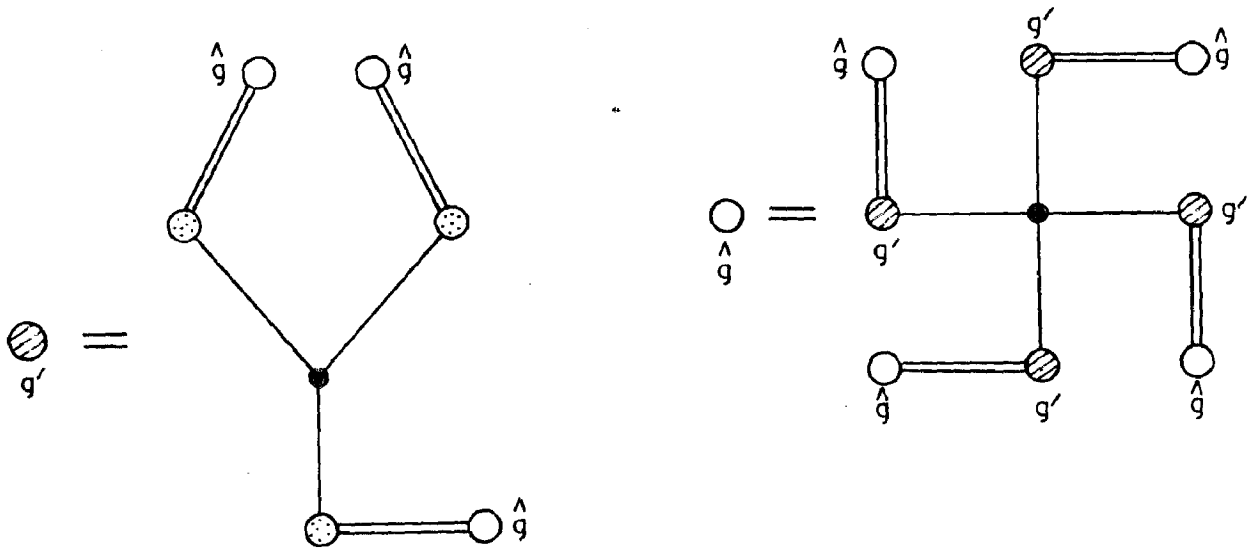

FIG. 3.12

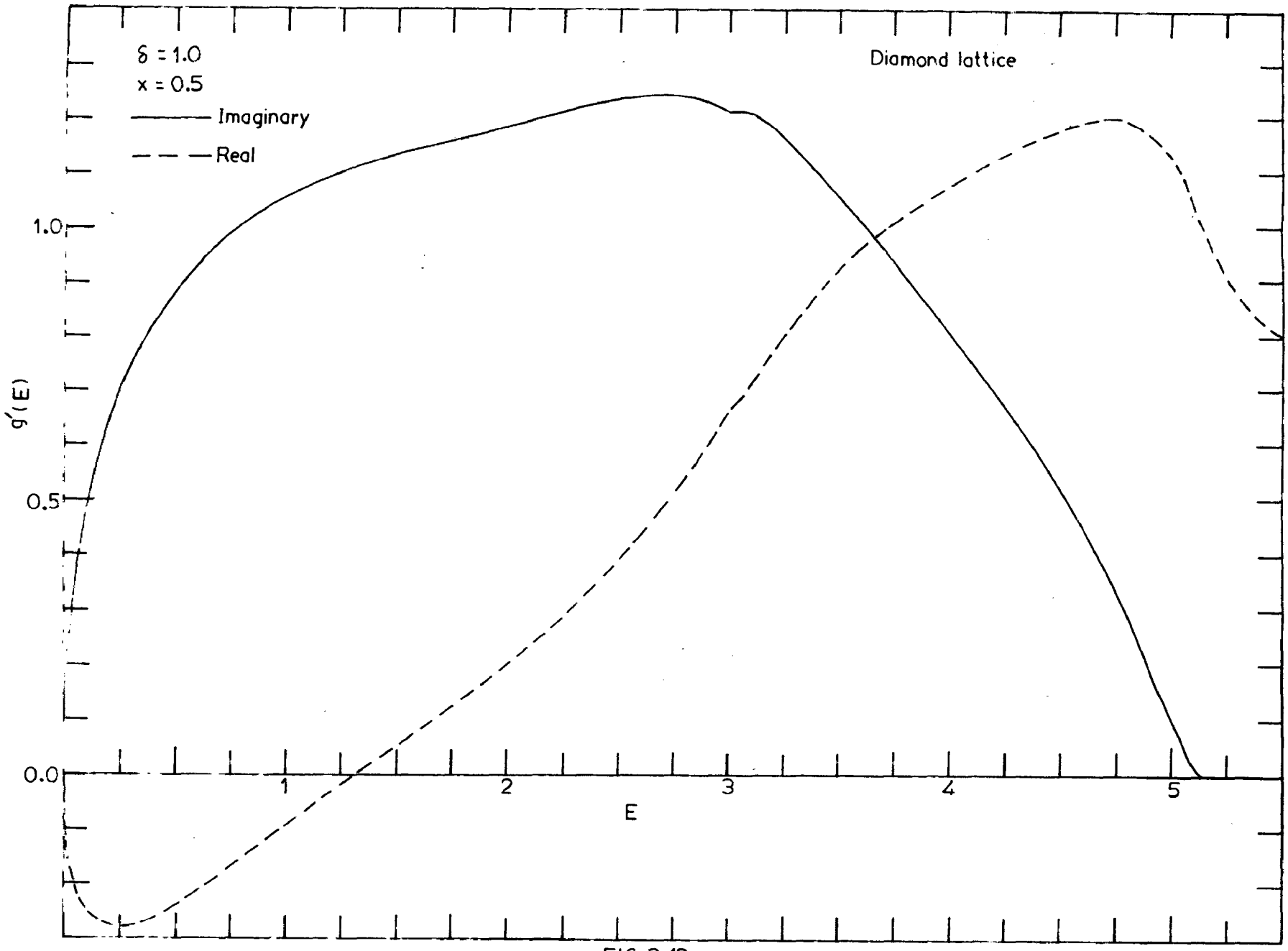

FIG. 3.13

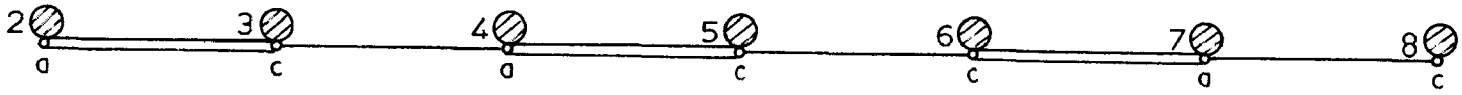

FIG. 3.14

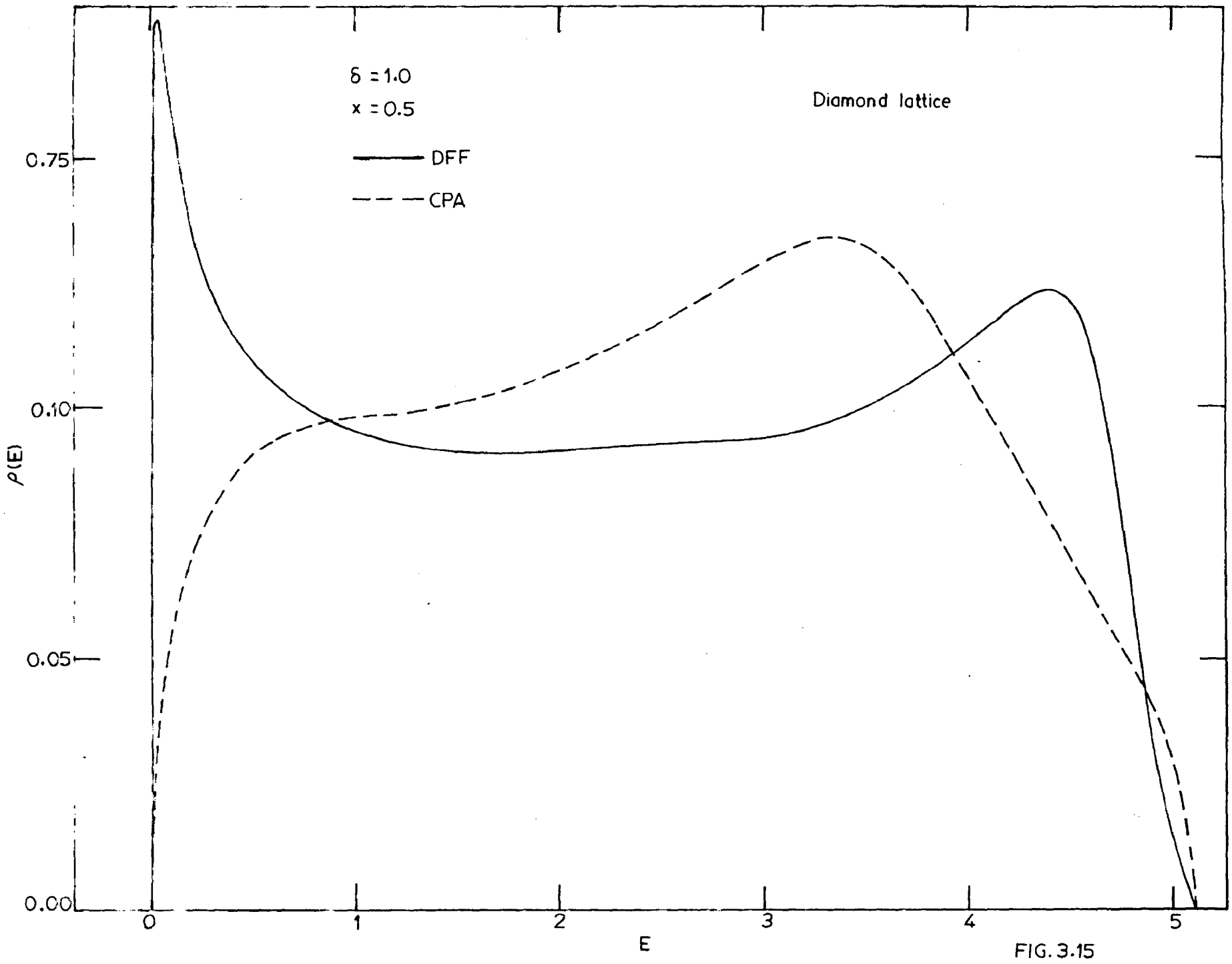

FIG. 3.15

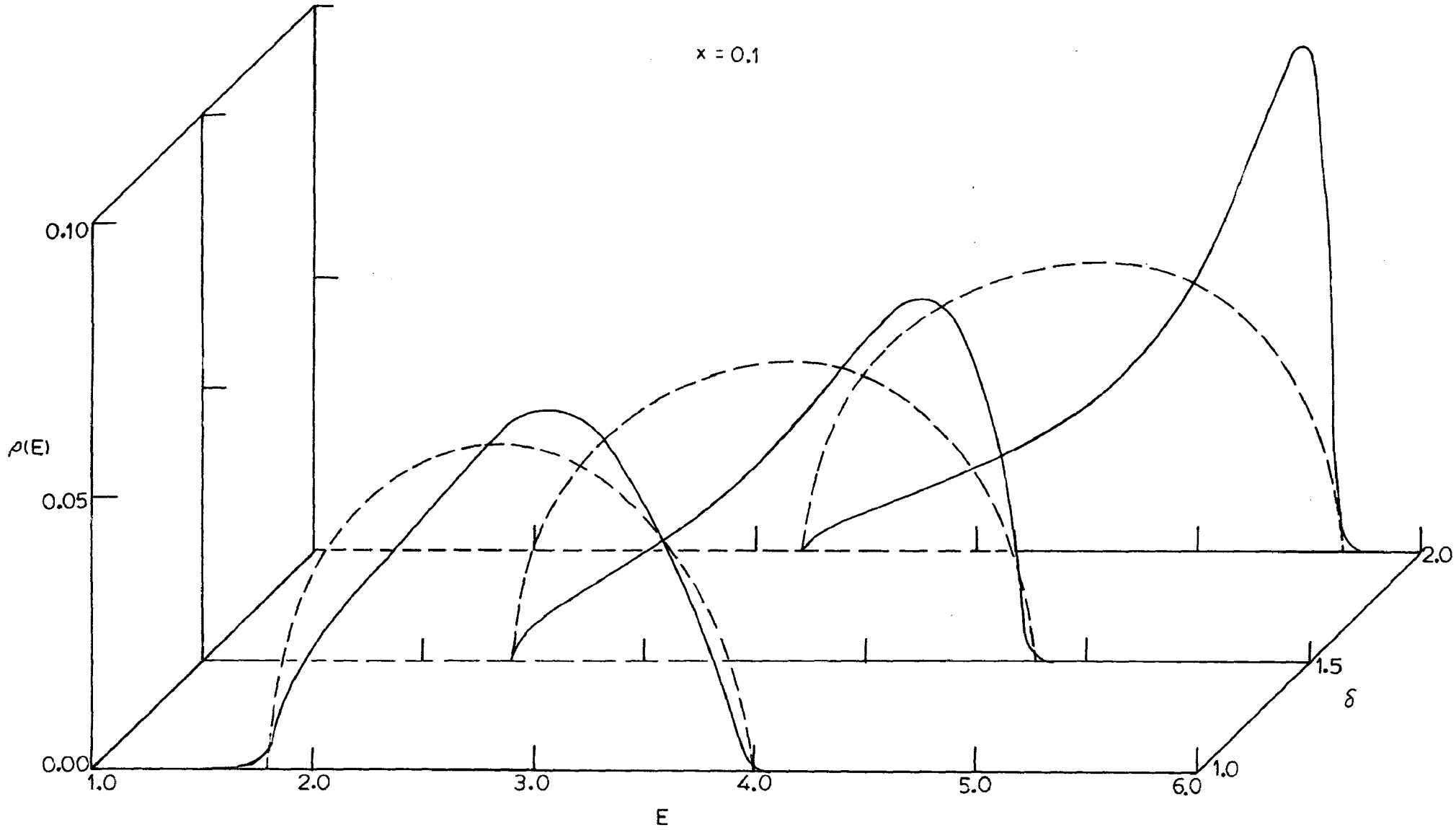

FIG. 3.16

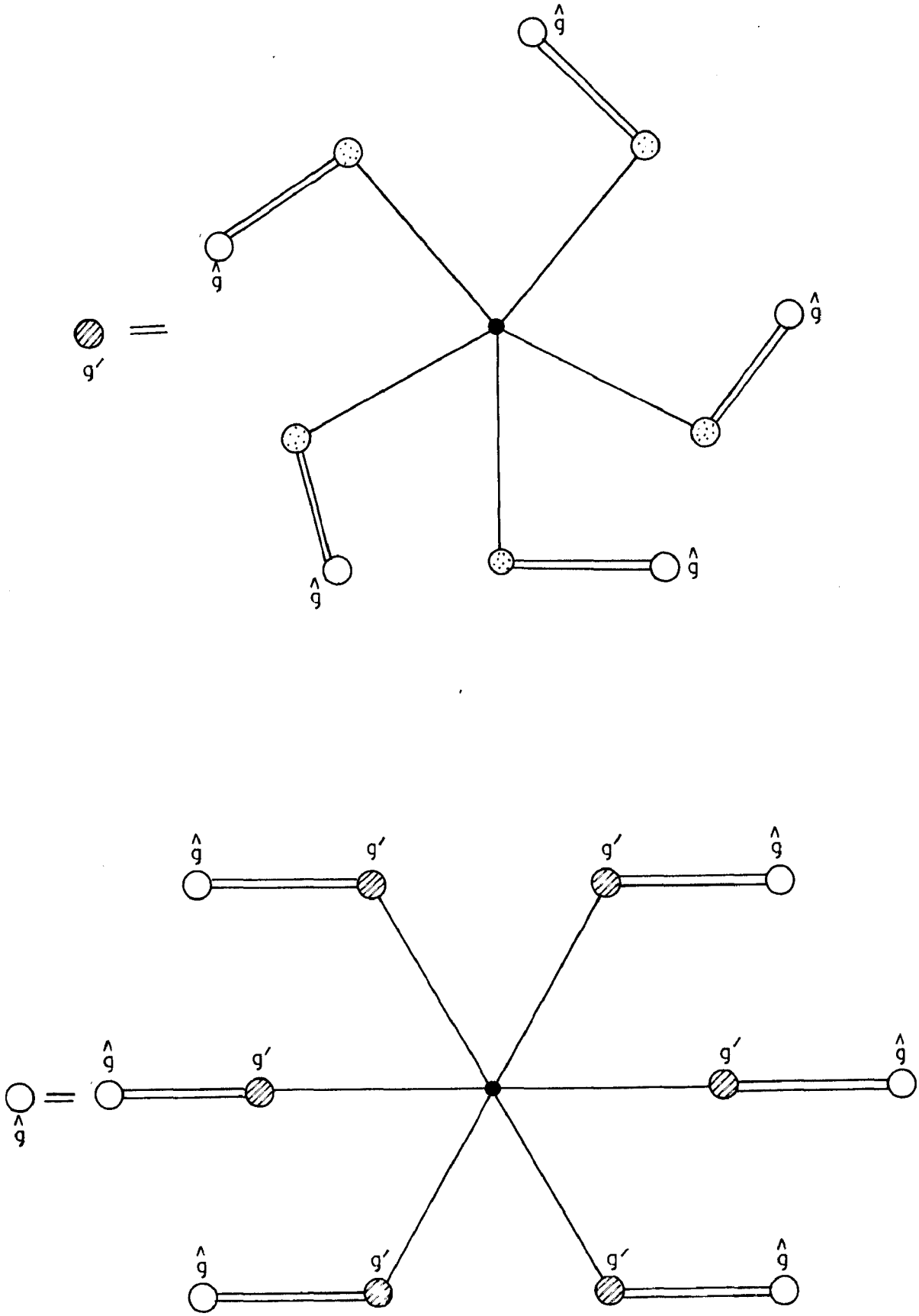

FIG. 3.17

CHAPTER IV

CLUSTER THEORIES (Extended Disorder)

So far we considered situations where only the diagonal term in the tight binding Hamiltonian (2.30) was random. While this model has played an important role in the development of the CPA, it is inadequate for real systems where addition of impurities introduces both the diagonal as well as the off-diagonal disorders. Several attempts[8] have been made to deal with the problem of the diagonal and the off-diagonal disorders but unfortunately most of these fail to produce the known results in the dilute limit (See appendix B). Another difficulty with these generalizations is that these lead to non-analytic averaged Green's functions for large δ when the hopping integrals are not too different. The standard model in these calculations has been the following. In the single band model the diagonal term ε_n is assumed to be equal to ε^A or ε^B depending on whether the site n is occupied by an A or B atom. The hopping integral h_{nm} can take three values h^{AA}, h^{AB} ($=h^{BA}$) and h^{BB} depending upon the occupancy of the sites n and m. But this model fails[159] to produce more than simply an s-wave scattering and hence does not allow[160] enough flexibility to meet the self-consistency requirement on the atomic potentials to satisfy the Friedel sum rule[161]. However, if one includes changes in the diagonal matrix elements on sites neighbouring the impurity, one can allow[162] higher phase shifts in a single s-band model. To our knowledge no

such self-consistent calculation like the CPA has been done todate.

The most successful treatment of the problem of the diagonal and the off-diagonal disorders was given by Blackman et al[163] (hereafter to be referred to as BEB) using a locator formalism. A single site approximation(Though apparently it looks impossible to develop a single site theory when the off-diagonal disorder is present), similar in nature to that used in the CPA, was employed while performing the configurational averages. In fact this simplification followed from the use of the occupation indices. For a binary alloy the use of 2x2 matrices facilitated the characterization of quantities like the Green's function $G(\vec{k},E)$ with no restriction on the hopping integrals. When the Green's function, in this formalism, is expressed in terms of an effective medium Hamiltonian, the self-energy (and hence the effective medium) requires coupling between all pairs of sites, though the hopping in the real lattice connects only the nearest neighbours. Therefore, the substitution of a single real atom into the effective medium will produce a perturbation that instead of being localized to the impurity site, as in the case of the diagonal disorder, extends to all neighbours. The BEB formalism gives the first four moments of the density of states exactly. As a special case when the hopping integral h^{AB} between A and B atoms is equal to the geometric mean of h^{AA} and h^{BB}, Shiba[57] also using a locator approach, independently, obtained results for the diagonal element of the Green's

function. It was shown by Blackman[164] that the formalism of BEB reduces to Shiba's theory when the appropriate restriction is imposed on the hopping integrals. These generalizations preserve[159] the correct dilute limit of the self-energy. Another special case, where the values of the hopping integral are additive i.e. $h^{AB} = (h^{AA} + h^{BB})/2$, was considered by Fukuyama et al[165]. In this case also the problem can be formulated within a single site approximation. Their results give the correct dilute and the split band limits and are also special cases of the BEB results. The special case considered by Shiba is interesting as in this case the problem can be reduced to that of a diagonal disorder. This particular case has been studied by us[61] using a renormalized propagator formalism[60] which gives the same results as obtained by Shiba using a locator formalism within the SSA. This has been further generalized to incorporate multisite correlations. These are discussed in Section § 4.1 whereas in section § 4.2 the general case where no restriction has been imposed on h_{ij} is studied.

§ 4.1 Renormalized Propagator Formulation (RPF)

a. CPA in RPF

When the hopping integral h^{AB} is equal to the geometric mean of h^{AA} and h^{BB}, then the hopping integrals can be factorized as[57]

$$h_{ij} = \alpha_i \hat{h} \alpha_j \qquad \ldots (4.1)$$

where $\hat{h}$ is independent of the atomic configurations and α_i

is determined from the bandwidth of the pure constituents (e.g. α_A^2 is proportional to the bandwidth of the pure A constituent.). In this approximation the Hamiltonian (2.30) can be renormalized and the problem reduces to that of the diagonal disorder. This was also noticed independently by Mertsching.[166] This method has been referred to as the renormalized propagator formalism by Niizeki[60]. In RPF one defines a diagonal, random and non-singular operator α_{op},

$$\alpha_{op} = \sum_i |i\rangle \alpha_i \langle i|. \qquad \ldots (4.2)$$

The renormalized Hamiltonian $\hat{\underline{H}}$ and the renormalized Green's function $\hat{\underline{G}}(z)$ are given by

$$\hat{\underline{H}} = \underline{\alpha}_{op}^{-1} \underline{H} \underline{\alpha}_{op}^{-1} = \sum_i |i\rangle \hat{\varepsilon}_i \langle i| + \sum_{i \neq j} \hat{h} |i\rangle\langle j| \qquad \ldots (4.3)$$

and

$$\hat{\underline{G}}(z) = \underline{\alpha}_{op} \underline{G}(z) \underline{\alpha}_{op} = (\underline{\eta}_{op} z - \hat{\underline{H}})^{-1} \qquad \ldots (4.4)$$

where $\hat{\varepsilon}_i = \alpha_i^{-2} \varepsilon_i$

$\hat{h} = \alpha_i^{-1} h_{ij} \alpha_j^{-1}$

and $\underline{\eta}_{op} = \sum_i |i\rangle \alpha_i^{-2} \langle i|. \qquad \ldots (4.5)$

Since $\hat{h}$ is configuration independent, the renormalized Hamiltonian has no off-diagonal disorder. Equations (4.3) and (4.4) can be rewritten as

$$\hat{\underline{H}} = \hat{\underline{D}} + \hat{\underline{W}}, \qquad \ldots (4.6)$$

$$\hat{\underline{G}}(z) = [\underline{M}_{op}(z) - \hat{\underline{W}}]^{-1}. \qquad \ldots (4.7)$$

Here $\hat{\underline{D}}$ is the random diagonal part in (4.3) and $\hat{\underline{W}}$ is the

non-random part and will be called the unperturbed Hamiltonian. $\underline{M}_{op}(z)$ is a random diagonal operator whose i^{th} component in the Wannier basis is

$$M_i(z) = (z-\varepsilon_i)/\alpha_i^2. \qquad \ldots (4.8)$$

We now define a quantity $\hat{\underline{\Sigma}}_{op}$ which characterizes the effective medium,

$$\langle \hat{\underline{G}}(z) \rangle = [\, \hat{\underline{\Sigma}}_{op}(z) - \hat{\underline{W}}\,]^{-1}. \qquad \ldots (4.9)$$

In order to determine $\hat{\underline{\Sigma}}_{op}(z)$ self-consistently we first use the single site approximation and see that the self-consistency equation obtained in this approximation is the same as the one obtained earlier by Shiba in the locator formalism.

In the SSA we have

$$\hat{\underline{\Sigma}}_{op}(z) = \sum_i |i\rangle \hat{\Sigma}(z) \langle i|. \qquad \ldots (4.10)$$

In order to determine $\hat{\Sigma}(z)$ we start with the reference Green's function defined as

$$\tilde{\underline{G}}(z) = [\, \tilde{\underline{\Sigma}}_{op}(z) - \hat{\underline{W}}\,] = \underline{G}^{(o)}(\tilde{\Sigma}) \qquad \ldots (4.11)$$

where $$\underline{G}^{(o)}(z) = (z\underline{I} - \hat{\underline{W}})^{-1} \qquad \ldots (4.12)$$

is the Green's function for the unperturbed crystal with Hamiltonian $\hat{\underline{W}}$. Then using the multiple scattering description of Section § 2.3 we obtain

$$\hat{\Sigma}(z) = \tilde{\Sigma}(z) - \langle \hat{t} \rangle / [\, 1 + \langle \hat{t} \rangle \tilde{F}(z)\,] \qquad \ldots (4.13)$$

where $\langle \hat{t} \rangle$ is the averaged single-site scattering matrix

$$\langle \hat{t} \rangle = \sum_{p=1}^{n} x_p \frac{\tilde{\Sigma}(z) - M_p(z)}{1 - [\tilde{\Sigma}(z) - M_p(z)]\tilde{F}(z)} \qquad \ldots (4.14)$$

and $$\tilde{F}(z) = \langle 0|\underline{\tilde{G}}(z)|0\rangle . \qquad \ldots (4.15)$$

p denotes the type of atom (say A or B...) at the site under consideration and x_p is the probability of the occurrence of a pth type of atom. Equation (4.13) is the generalization of equation (2.43) for alloys with off-diagonal disorder of Shiba type.

The density of states in this formalism is obtained in terms of the conditionally averaged renormalized Green's function $\hat{G}_o(z)$ defined as

$$\underline{\hat{G}}_o(z) = \{\underline{\hat{G}}(z)^{-1} + [\underline{M}_o(z) - \underline{\hat{\Sigma}}(z)]|0\rangle\langle 0|\}^{-1}. \qquad \ldots (4.16)$$

This is a random operator which takes the value $\hat{G}_o^p(z)$ depending on the configuration of the site 0. We define

$$\hat{F}^p(z) = \langle 0|\underline{\hat{G}}_o^p(z)|0\rangle . \qquad \ldots (4.17)$$

Then from (4.16) we obtain

$$\hat{F}^p(z) = \{F^{-1} + (M_p - \hat{\Sigma})\}^{-1}. \qquad \ldots (4.18)$$

The partial density of states is then given by

$$\rho^p(E) = -\frac{1}{\pi} \operatorname{Im} \hat{F}^p(E+i0)/\alpha_p^2. \qquad \ldots (4.19)$$

The total averaged density of states per atom is then

$$\rho(E) = \sum_{p=1}^{n} x_p \rho^p(E). \qquad \ldots (4.20)$$

It is important to note that in RPF the total averaged density of states $\rho(E)$ can not be obtained from $\hat{F}(z)$ directly. Now using a definition similar to (4.18) for $\tilde{F}^p(z)$, Eq.(4.14) can be written as

$$\hat{\Sigma} = \tilde{\Sigma} + \frac{1}{\sum_{p=1}^{n} x_p \tilde{F}^p} - \frac{1}{\tilde{F}} . \qquad \ldots (4.21)$$

The self-consistency condition for the determination of $\hat{\Sigma}$ is

$$\langle \hat{t} \rangle = 0 \qquad \ldots (4.22)$$

which means that $\hat{\Sigma} = \tilde{\Sigma}$.

Equation (4.22), when solved for a binary alloy, reduces to

$$x/(M_A - \hat{\Sigma} + \hat{F}^{-1}) + (1-x)/(M_B - \hat{\Sigma} + \hat{F}^{-1}) = \hat{F}. \qquad \ldots (4.23)$$

If the $M_i(z)$ and $\hat{\Sigma}(z)$ used here are identified with $\mathcal{L}_i$ and $\tilde{\mathcal{L}}$ used in Shiba's paper, then Eq.(4.23) is the same as the self-consistency equation derived earlier by Shiba in the locator formalism. When no restriction is imposed on the hopping integrals, Niizeki[60] showed that the RPF and the locator method of BEB are equivalent. This also shows that within the SSA, the locator and the propagator formalisms give the same results even in the case when the off-diagonal disorder is also present. Recently Gonis and Garland[167] have also shown that the formalism of BEB (and therefore of Shiba) has the correct analytic properties.

b. Cluster CPA in RPF.

We now extend the single site generalized CPA discussed in sub-section § 4.1a to include correlated scattering from

a site and its cluster of neighbors in an approximate manner and call it cluster coherent potential approximation (CCPA).

After the Hamiltonian is renormalized and the problem has been reduced to that of a diagonal disorder then the cluster formalisms (particularly MCPA, SCCSA, SCBSA etc. which are of our main interest) developed to treat the diagonal disorder problem can be carried on directly to (4.3). As already noticed, the application of the MCPA will again be cumbersome and therefore here again we shall work with simple theories like the SCCSA and the SCBSA. Here we slightly deviate from the treatment of Section § 3.2. This will facilitate our study when we later consider the general case. We consider a cluster of (Z+1) atoms (a central site and its Z nearest neighbours) immersed in an effective medium which we approximately characterize by $\underline{\hat{\Sigma}}^c = \hat{\Sigma}\, \underline{I}_c$ in the spirit of the CPA. Here $\underline{I}_c$ is the $(Z+1)\times(Z+1)$ unit matrix. The renormalized Green's function for such a system is

$$\underline{\hat{G}}^c = \langle \underline{\hat{G}} \rangle + \langle \underline{\hat{G}} \rangle \underline{\hat{V}}^c \underline{\hat{G}}^c. \qquad \ldots (4.24)$$

Proceeding parallel to our treatment of SSA we have

$$\underline{\hat{G}}^c = \underline{\alpha}_{op} \underline{G}^c \underline{\alpha}_{op} \qquad \ldots (4.25)$$

and

$$\underline{\hat{V}}^c = \sum_{i \varepsilon c} |i\rangle\langle i| (\hat{\Sigma} - M_i). \qquad \ldots (4.26)$$

c denotes a cluster and i is a site in this cluster. We can now write

$$\underline{\hat{G}}^c = \langle \underline{\hat{G}} \rangle + \langle \underline{\hat{G}} \rangle \underline{\hat{T}}^c \langle \underline{\hat{G}} \rangle, \qquad \ldots (4.27)$$

where $\underline{\hat{T}}^c = \underline{\hat{V}}^c(\underline{1} + \langle\underline{\hat{G}}\rangle\underline{\hat{T}}^c)$. ... (4.28)

$\underline{\hat{T}}^c$ is a (Z+1)x(Z+1) matrix and is difficult to solve in the present form to obtain $\underline{\hat{G}}^c$. Here we introduce an approximate scheme to simplify these equations. The physical idea behind this scheme is that for certain properties like the averaged densities of states, the magnetic response etc., environment effects depend only on the number of different kinds of atoms on the shell s of nearest neighbors and do not depend critically on their detailed configuration on the shell. So we calculate the $\hat{T}^c$ matrix with the assumption that it depends only on the total number of say A and B atoms on the shell, but is independent of their detailed configuration. This is achieved by replacing the propagators between two different sites of a shell by their averaged value. A similar approximation was also made while dealing with the problem of the diagonal disorder alone. With this approximation all the $(Z+1)^2$ matrix elements of $\hat{T}^c$ can be expressed in terms of four quantities $\hat{T}^c_{oo}$, $\hat{T}^c_{os}$, $\hat{T}^c_{so}$ and $\hat{T}^c_{ss}$. The latter three are defined as

$$\hat{T}^c_{os} = \frac{1}{Z}\sum_i{}' \hat{T}^c_{oi},$$

$$\hat{T}^c_{so} = \frac{1}{Z}\sum_i{}' \hat{T}^c_{io}, \qquad \text{... (4.29)}$$

and $$\hat{T}^c_{ss} = \frac{1}{Z^2}\sum_{ij}{}' \hat{T}^c_{ij}.$$

The prime denotes that the sum is taken over the shell sites. O denotes the central site. Here we shall not give expressions for different matrix elements of $\underline{\hat{T}}^c$ explicitly, as the relevant

expressions involved in the calculation of the density of states require expressions for $\hat{T}^c_{oo}$, $\hat{T}^c_{os}$, $\hat{T}^c_{so}$, and $\hat{T}^c_{ss}$ only. These are easily obtained from Eq.(4.28):

$$\hat{T}^c_{oo} = \hat{\tau}_{oo} + Z\,\hat{\tau}_{oo}\langle\hat{G}\rangle_R\,\hat{T}^c_{so}, \qquad \ldots (4.30a)$$

$$\hat{T}^c_{so} = \frac{1}{Z}(\langle\hat{G}\rangle_R\,\hat{T}^c_{oo} + \hat{\Gamma}\hat{T}^c_{so})\,{\sum_i}'\hat{t}_{ii}, \qquad \ldots (4.30b)$$

$$\hat{T}^c_{os} = Z\,\hat{\tau}_{oo}\langle\hat{G}\rangle_R\,\hat{T}^c_{ss}, \qquad \ldots (4.30c)$$

$$\text{and } \hat{T}^c_{ss} = \frac{1}{Z^2}(1 + Z\langle\hat{G}\rangle_R\,\hat{T}^c_{os} + Z^2\hat{\Gamma}\hat{T}^c_{ss})\,{\sum_i}'\hat{t}_{ii}\ ; \qquad \ldots (4.30d)$$

where

$$\hat{\tau}_{oo} = \hat{V}^c_{oo}/\,(1-\hat{V}^c_{oo}\langle\hat{G}\rangle_o), \qquad \ldots (4.31)$$

$$\hat{t}_{ii} = \hat{V}^c_{ii}/\,[1 - \hat{V}^c_{ii}(\langle\hat{G}\rangle_o - \hat{\Gamma})\,] \qquad \ldots (4.32)$$

(i is a site on the shell) and

$$\hat{\Gamma} = \frac{1}{(Z-1)}\,{\sum_{j\neq i}}'\langle\hat{G}\rangle_{ij}\,. \qquad \ldots (4.33)$$

Here the subscripts O and R on $\langle\hat{G}\rangle$ denote zero and nearest neighbour separations respectively. Equations (4.30) are solved to obtain

$$\hat{T}^c_{oo} = \frac{\hat{\tau}_{oo}}{D'}(1 - \hat{\Gamma}\,{\sum_i}'\hat{t}_{ii}), \qquad \ldots (4.34a)$$

$$\hat{T}^c_{so} = \hat{T}^c_{os} = \frac{\hat{\tau}_{oo}}{D'}\langle\hat{G}\rangle_R\,{\sum_i}'\hat{t}_{ii}, \qquad \ldots (4.34b)$$

$$\text{and } \hat{T}^c_{ss} = \frac{1}{Z^2 D'}\,{\sum_i}'\hat{t}_{ii} \qquad \ldots (4.34c)$$

where $D' = 1-(\hat{\Gamma} + \hat{\tau}_{oo} \langle \hat{G} \rangle_R^2) \sum_i{}' \hat{t}_{ii}$. ... (4.35)

The renormalized Green's function at the center of the cluster is obtained from Eq.(4.27),

$$\hat{G}^c_{oo} = \langle \hat{G} \rangle_o + \langle \hat{G} \rangle_o \langle \hat{G} \rangle_o \hat{T}^c_{oo} + z \langle \hat{G} \rangle_o \langle \hat{G} \rangle_R (\hat{T}^c_{os} + \hat{T}^c_{so}) + z^2 \langle \hat{G} \rangle_R \langle \hat{G} \rangle_R \hat{T}^c_{ss}. \quad \ldots (4.36)$$

This can be simplified using (4.35) to obtain

$$\hat{G}^c_{oo} = \frac{1}{D'} \frac{\hat{\tau}_{oo}}{\hat{V}^c_{oo}} (\langle \hat{G} \rangle_o + (\langle \hat{G} \rangle_R \langle \hat{G} \rangle_R - \langle \hat{G} \rangle_o \hat{\Gamma}) \sum_i{}' \hat{t}_{ii}). \quad \ldots (4.37)$$

$\hat{\Sigma}$ is then determined from the condition

$$\langle \hat{G} \rangle_o = \sum_{P_c} P_c \hat{G}^c_{oo} , \quad \ldots (4.38)$$

where again P_c is the weighted probability of the occurrence of a cluster configuration. We sum over all configurations, keeping in mind that for a fixed number of different kinds of atoms on the shell the different possible configurations are not to be distinguished in this approximation.

In the case of clusters, Eq.(4.21) can be generalized to the equation

$$\hat{\Sigma} = \tilde{\Sigma} + \frac{1}{\sum_{P_c} P_c \tilde{G}^c_{oo}} - \frac{1}{\langle \tilde{G} \rangle_o}. \quad \ldots (4.39)$$

The quantities $\langle \hat{G} \rangle_R$ and $\hat{\Gamma}$ can easily be expressed (See Section 3.2) in terms of $\hat{\Sigma}$ and $\langle \hat{G} \rangle_o$,

$$\langle \hat{G} \rangle_R = \hat{\Sigma} \langle \hat{G} \rangle_o - 1, \qquad \ldots (4.40)$$

and $$\hat{\Gamma} = [1/(Z-1)][Z \hat{\Sigma} \langle \hat{G} \rangle_R - \langle \hat{G} \rangle_o] . \qquad \ldots (4.41)$$

Here we have assumed that the unperturbed crystal half-bandwidth ($\omega_o = Z \times \hat{h}$) is unity. The averaged density of states per atom is obtained from

$$P(E) = -\frac{1}{\pi} \mathrm{Im} \sum_{P_c} P_c \hat{G}^c_{oo}/\alpha_o^2 . \qquad \ldots (4.42)$$

In the one center approximation $\hat{t}_{ii}$ is zero and Eq.(4.37) reduces to

$$\hat{G}^c_{oo} = (1/D') (\hat{\tau}_{oo}/\hat{V}^c_{oo}) \langle \hat{G} \rangle_o .$$

Taking the configurational average and using (4.38) we obtain

$$\langle \hat{\tau}_{oo} \rangle = 0$$

which is the same as Eq.(4.22) obtained in the SSA.

We have numerically evaluated the density of states for binary alloys having the simple cubic lattice structure. Equation (4.39) has been solved by an iterative procedure. The unit of energy is taken to be the half band-width of the unperturbed crystal, which is set equal to 1. The half bandwidth of pure B is also taken to be 1 which means $\alpha_B^2 = 1$. The zero of energy is chosen in such a manner that $\varepsilon_A = -\varepsilon_B = \frac{1}{2}\delta$. The alloy density of states (full curve) is shown in Figs.4.1 and 4.2 for various values of the parameters x, δ and α_A^2. The dashed curve shows the corresponding generalized CPA results calculated from Eq.(4.22). For $\delta = 1.0$, the minority band is shown completely, along with a part of the majority band.

For $\delta = 0.75$, the effects of the local environment on the density of states are not very significant and our results are in excellent agreement with the exact results[18,19]. For $\delta = 1.0$ we find a good deal of structure showing up in the impurity band. The variations with α_A^2 are best seen in the modification of the central peak of the impurity band. The central peak corresponds to the resonance level of the isolated impurity A. The peak becomes sharper when α_A^2 i.e. hopping from A atoms, is decreased. This can be understood on physical grounds as follows; since we expect that, if hopping from isolated site is reduced, an electron will spend comparatively more time at that site and the corresponding resonance level will become sharper, leading to a higher density of states in this region. We face just the reverse situation when the hopping from A atoms is increased. The central peak is reduced in height and is broadened, showing that the above mentioned life-time of the single impurity resonance level becomes smaller. Similar considerations apply to other peaks in the impurity band. These correspond to two impurity, three impurity,.... resonance levels. As α_A^2 is increased, these peaks become broad and well defined because the increased hopping among impurity atoms favours a multi-impurity resonance level at the expense of a single-impurity resonance level. Further, as α_A^2 is increased to 1.5, the impurity and the majority bands merge together, whereas the generalized CPA density of states still has a gap. Our results are in very good agreement with the results obtained from the method of moments[139] which also shows no gap in this case. For $\alpha_A^2 = 1$ our results coincide with those

of Brouers et al[130] as they should, because for this value of α_A^2 there is no off-diagonal disorder. In general for $\alpha_A^2 \neq 1$, we find extra structure in the band. The CCPA band is wider than the corresponding CPA band. In the impurity band of the CCPA there appears a gap which is not present in the exact results.[18,19] The majority band in the CPA and the CCPA are almost similar.

Recently Gonis and Garland[168] have generalized the MCPA formalism for alloys having the diagonal as well as the off-diagonal disorders. This is based on a reformulation of the renormalized interactor formalism of BEB which is the best treatment of the off-diagonal disorder (ODD) problem within the SSA. It has been further shown that the MCPA with ODD always yields analytic Green's functions like the ordinary MCPA. However, it is computationally quite difficult. Therefore they studied two simple approximations namely the SCCSA and the SCBSA in the presence of ODD treated in the BEB manner. It was found that the SCCSA yielded severely non-analytic results whereas the SCBSA was equivalent to the MCPA even in the presence of ODD for a linear chain and therefore for a linear chain it would always yield analytic results. This will also be true if ODD is treated in Shiba's manner. The calculations of this section can easily be carried onto the SCBSA following the treatment of Sections § 4.1a and 3.2. As noticed in the case of the diagonal disorder, for small values of δ, the general features of the results in presence of ODD in the SCBSA will be quite similar to the one obtained in the

SCCSA. But for large δ, in two and three dimensions, the analyticity of the SCBSA with ODD is still questionable as we found the SCBSA to be non-analytic for three dimensional systems in the absence of ODD. However, it may turnout that in some cases the difficulties of non-analyticity get eliminated in the presence of ODD. In the next section we present a generalization of the CPA where no restrictions have been imposed on the hopping integrals.

§ 4.2 Self-Consistent T-matrix Formulation

In this section we consider the case of extended disorder where no restriction is placed on the hopping integrals. This problem has been tackled within a cluster formulation which is a generalization[169] of our treatment given in sub-section 4.1b. In this case we do not renormalize the alloy Hamiltonian, but start with the following most general form of the effective medium Hamiltonian

$$\underline{H}_{eff} = \sum_{n} |n\rangle \underline{\Sigma}_{nn} \langle n| + \sum_{m \neq n} \underline{\Sigma}_{nm} |n\rangle\langle m| \qquad \ldots (4.43)$$

where $\underline{\Sigma}_{nn}$ and $\underline{\Sigma}_{nm}$ are the diagonal and the off-diagonal parts of the effective Hamiltonian respectively. Here the summations over n and m in the second term run over all the lattice sites. The Green's function corresponding to this effective medium is

$$\underline{\bar{G}}(z) = (z\underline{I} - \underline{H}_{eff})^{-1}. \qquad \ldots (4.44)$$

Here it is important to notice that the effective Hamiltonian has the translational symmetry of the empty lattice in

contrast to the MCPA formalism where this translational symmetry is not preserved.

The alloy Green's function $\underline{G}$ can now be written as

$$\underline{G} = \overline{\underline{G}} + \overline{\underline{G}}\,\underline{T}\,\overline{\underline{G}} \qquad \ldots (4.45)$$

where $$\underline{T} = \underline{V}(\underline{1} + \overline{\underline{G}}\,\underline{T}) \qquad \ldots (4.46)$$

and $$\underline{V} = \underline{H} - \underline{H}_{eff}. \qquad \ldots (4.47)$$

Taking the configurational average of Eq.(4.45) we obtain

$$\langle \underline{G} \rangle = \overline{\underline{G}} + \overline{\underline{G}} \langle \underline{T} \rangle \overline{\underline{G}}. \qquad \ldots (4.48)$$

The self-consistency requirement for the determination of the effective medium gives the following condition

$$\langle \underline{T} \rangle = 0 \qquad \ldots (4.49)$$

or equivalently $$\langle \underline{G} \rangle = \overline{\underline{G}}. \qquad \ldots (4.50)$$

Equation (4.49) implies that on the average there is no scattering from the crystal and Eq.(4.50) means that the configurational average of any matrix element of the alloy Green's function should be equal to the corresponding matrix element of the effective medium Green's function. One can in principle utilize the set of equations (4.49) or (4.50) to determine all Σ_{nm}'s. No approximations have so far been made. But it will be impossible to solve these extremely large number of coupled equations in a self-consistent manner without making any approximation. Therefore, one considers scattering from a small cluster of say $\underline{n}$ atoms and introduces some physical

simplifications which allow one to keep only a few parameters in the effective Hamiltonian. For the problem involving only the diagonal disorder Butler and others put forth models with only one parameter for the effective potential matrix. In the same spirit here, where we are having the off diagonal disorder also, we choose two parameters to represent the effective potential matrix. Σ_1 corresponding to an effective site energy and Σ_2 representing an effective hopping integral between the nearest neighbours. As done in the case of the diagonal disorder, here also we shall consider clusters made up of a central atom and its Z nearest neighbours. One such cluster is thought to be immersed in the effective medium. Then there is problem to introduce parameters for hopping between a real and a effective medium atom. Stern and Zin[170] have emphasized that to treat the problem of such nearest neighbour clusters properly one should consider clusters upto the second nearest neighbours. But here we shall make use of our earlier hypothesis that for a fixed number of different kinds of atoms on the shell of nearest neighbours, the different configurations will not be distinguished. Consistent with this we shall assume that the hopping matrix element from a shell atom to the nearest neighbour effective medium site is equal to Σ_2. Therefore, the potential fluctuation matrix due to this cluster can be written as

$$\underline{V}^c = V_{oo}|0\rangle\langle 0| + \sum_n{}' \{V_{nn}|n\rangle\langle n| + V_{on}|0\rangle\langle n| + V_{no}|n\rangle\langle 0|\} \quad \ldots\ (4.51)$$

Also $V_{oo} = \varepsilon_o - \Sigma_1$, $V_{nn} = \varepsilon_n - \Sigma_1$ and $V_{on} = V_{no} = h_{on} - \Sigma_2$.

The Green's function for such a system with the medium every where except the cluster c is

$$\underline{G}^c = \underline{\bar{G}} + \underline{\bar{G}}\,\underline{T}^c\underline{\bar{G}} \qquad \ldots (4.52)$$

with $$\underline{T}^c = \underline{V}^c(\underline{1} + \underline{\bar{G}}\,\underline{T}^c). \qquad \ldots (4.53)$$

Performing the configurational average in (4.52) one obtains

$$\langle \underline{G}^c \rangle = \underline{\bar{G}} + \underline{\bar{G}} \langle \underline{T}^c \rangle \underline{\bar{G}} \,. \qquad \ldots (4.54)$$

The effective medium is now determined self-consistently by imposing the condition

$$\langle \underline{T}^c \rangle = \underline{0} \qquad \ldots (4.55)$$

or equivalently $$\langle \underline{G}^c \rangle = \underline{\bar{G}} \,. \qquad \ldots (4.56)$$

As noticed earlier, in our formulation, the various matrix elements of $\underline{T}^c$ can be expressed in terms of T^c_{oo}, T^c_{os}, T^c_{so} and T^c_{ss} defined in (4.29). Now using only two parameters Σ_1 and Σ_2 in $\underline{H}_{eff}$, it is impossible to satisfy Eq.(4.55) or (4.56). Then to determine the effective medium self-consistently one can choose a variety of different self-consistency conditions. Here we replace (4.55) or (4.56) by two sets of alternate conditions. These are:

1. Adopting the philosophy of Butler and others we require that the total averaged density of states at the center of the cluster is consistent with the external medium i.e.

$$\langle\langle o|\underline{G}^c|o\rangle\rangle = \langle o|\underline{\bar{G}}|o\rangle \qquad \ldots (4.57a)$$

and the average matrix element of the cluster Green's function

between the central site and a shell site is equal to the corresponding matrix element of the effective medium Green's function i.e.

$$\left\langle \frac{1}{Z} \sum_{n}{}' \langle o|\underline{G}^{c}|n\rangle \right\rangle = \langle o|\underline{\bar{G}}|n\rangle = \bar{G}(R) \quad . \qquad \ldots (4.57b)$$

Here R denotes nearest neighbour separation. As the shell is not treated exactly, here, we have summed over all the shell sites and divided by Z to obtain an average matrix element between the site O and a shell site.

2. $$\langle T^{c}_{oo} \rangle = 0 \qquad \ldots (4.58a)$$

and $$\langle T^{c}_{os} \rangle = 0 \; . \qquad \ldots (4.58b)$$

Expressions for the matrix elements of the Green's function $\underline{G}^{c}$ are obtained from (4.52) and are given by

$$G^{c}_{oo} = \bar{G}(o) + \bar{G}(o)^{2} T^{c}_{oo} + Z\bar{G}(o)\bar{G}(R)\left[T^{c}_{os} + T^{c}_{so}\right] + Z^{2}\bar{G}(R)^{2} T^{c}_{ss} \qquad \ldots (4.59)$$

and $$\frac{1}{Z}\sum_{n}{}' G^{c}_{on} = \bar{G}(R) + \bar{G}(o)\bar{G}(R)T^{c}_{oo} + \bar{G}(o)\left[\bar{G}(o) + (Z-1)\bar{\Gamma}\right] T^{c}_{os} + Z\bar{G}(R)^{2} T^{c}_{so} + Z\bar{G}(R)\left\{\bar{G}(o) + (Z-1)\bar{\Gamma}\right\} T^{c}_{ss} . \qquad \ldots (4.60)$$

The quantities $\bar{G}(R)$ and $\bar{\Gamma}$ (defined in 3.42) can be easily expressed in terms of $\bar{G}(o)$ to obtain

$$\bar{G}(R) = \left[(z - \Sigma_{1})\bar{G}(o) - 1\right]/Z\,\Sigma_{2} \qquad \ldots (4.61)$$

and $$\bar{\Gamma} = \left[\left(\frac{z-\Sigma_{1}}{\Sigma_{2}}\right)\bar{G}(R) - \bar{G}(o)\right]/(Z-1) \; . \qquad \ldots (4.62)$$

Expressions for T^{c}_{oo}, T^{c}_{os}, T^{c}_{so} and T^{c}_{ss} are obtained from

Eq.(4.53) and are given by

$$T^c_{oo} = \tau_{oo} + Z(\tau_{oo}\bar{G}(R) + Z\bar{\Gamma}\tau_{os})T^c_{so} + (\bar{G}(o) - \bar{\Gamma}) \sum_n{}' \tau_{on}T^c_{no} \quad \ldots (4.63a)$$

$$T^c_{os} = \tau_{os} + Z(\tau_{oo}\bar{G}(R) + Z\bar{\Gamma}\tau_{os})T^c_{ss} + \frac{1}{Z}(\bar{G}(o) - \bar{\Gamma}) \sum_{nm}{}' \tau_{om}T^c_{mn} \quad \ldots (4.63b)$$

$$T^c_{so} = \{t_{so} + (t_s\bar{G}(R) + t_{so}\bar{G}(o))T^c_{oo}\}/\{1 - Z(t_s\bar{\Gamma} + t_{so}\bar{G}(R))\} \quad \ldots (4.63c)$$

and

$$T^c_{ss} = (\frac{1}{Z}t_s + (t_s\bar{G}(R) + t_{so}\bar{G}(o))T^c_{os})/\{1 - Z(t_s\bar{\Gamma} + t_{so}\bar{G}(R))\} \quad \ldots (4.63d)$$

where

$$\tau_{oo} = V^c_{oo}/D_o \quad ; \quad D_o = 1 - V^c_{oo}\bar{G}(o) - \bar{G}(R) \sum_n{}' V^c_{on}$$

$$\tau_{os} = \frac{1}{Z} \sum_n{}' \tau_{on} \quad ; \quad \tau_{on} = V^c_{on}/D_o$$

$$t_s = \frac{1}{Z} \sum_n{}' t_{nn} \quad ; \quad t_{nn} = V^c_{nn}/D_n \quad \ldots (4.64)$$

$$t_{so} = \frac{1}{Z} \sum_n{}' t_{no} \quad ; \quad t_{no} = V^c_{no}/D_n$$

and

$$D_n = 1 - V^c_{nn}(\bar{G}(o) - \bar{\Gamma}).$$

In equations (4.63a) and (4.63b) the quantities $\sum_n{}' \tau_{on}T^c_{no}$ and $\sum_{nm}{}' \tau_{om}T^c_{mn}$ were again calculated from (4.53). We find

$$\sum_n{}' \tau_{on}T^c_{no} = 1 + Z(\bar{G}(R)T^c_{os} + \bar{G}(o)T^c_{oo}) \sum_n{}' \tau_{on}t_{no} \quad \ldots (4.65)$$

$$+ Z(\bar{\Gamma}T^c_{os} + \bar{G}(R)T^c_{oo}) \sum_n{}' \tau_{on}t_{nn} \quad \ldots (4.65)$$

and

$$\sum_{nm}' \tau_{om} T^c_{mn} = 1 + Z(\bar{G}(R) T^c_{os} + Z\bar{\Gamma} T^c_{ss}) \sum_n' \tau_{on} t_{nn} + Z(\bar{G}(o) T^c_{os} + Z\bar{G}(R) T^c_{ss}) \sum_n' \tau_{on} t_{no}. \quad \ldots (4.66)$$

Equations (4.65) and (4.66) are substituted in equations (4.63a,b) and ultimately the set of equations (4.63a,b,c,d) is solved for T^c_{oo}, T^c_{os}, T^c_{so} and T^c_{ss}. The final expressions are:

$$T^c_{oo} = \{\tau_{oo} - Z\tau_{oo} t_s \bar{\Gamma} + (\bar{G}(o) - \bar{\Gamma}) \sum_n' \tau_{on} t_{no} + Z^2 \bar{\Gamma} \tau_{os} t_{so} + Z\bar{\Gamma} (\bar{G}(o) - \bar{\Gamma}) [t_{so} \sum_n' \tau_{on} t_{nn} - t_s \sum_n \tau_{on} t_{no}]\} / D \quad \ldots (4.67a)$$

$$T^c_{os} = \{\tau_{os} + \tfrac{1}{Z}(\bar{G}(o) - \bar{\Gamma}) \sum_n' \tau_{on} t_{nn} - Z\bar{G}(R) \tau_{os} t_{so} + \bar{G}(R) \tau_{oo} t_s + \bar{G}(R) (\bar{G}(o) - \bar{\Gamma}) [t_s \sum_n' \tau_{on} t_{no} - t_{so} \sum_n' \tau_{on} t_{nn}]\}/D \quad \ldots (4.67b)$$

$$T^c_{so} = \{t_{so} + \tau_{oo}(\bar{G}(R) t_s + \bar{G}(o) t_{so}) + \bar{G}(R) (\bar{G}(o) - \bar{\Gamma}) [t_s \sum_n' \tau_{on} t_{no} - t_{so} \sum_n' \tau_{on} t_{nn}]\} / D \quad \ldots (4.67c)$$

and

$$T^c_{ss} = [\tfrac{1}{Z} t_s + \tau_{os}(\bar{G}(R) t_s + \bar{G}(o) t_{so}) + \tfrac{1}{Z}\bar{G}(o) (\bar{G}(o) - \bar{\Gamma}) [t_{so} \sum_n' \tau_{on} t_{nn} - t_s \sum_n' \tau_{on} t_{no}]\} / D \quad \ldots (4.67d)$$

where

$$D = \{1 - Z(\bar{\Gamma} t_s + \bar{G}(R) t_{so})\}\{1 - (\bar{G}(o) - \bar{\Gamma})(\bar{G}(R) \sum_n' \tau_{on} t_{nn} + \bar{G}(o) \sum_n' \tau_{on} t_{no})\} - Z\{t_s \bar{G}(R) + t_{so} \bar{G}(o)\}\{\tau_{oo} \bar{G}(R) + Z\bar{\Gamma} \tau_{os} + (\bar{G}(o) - \bar{\Gamma})(\bar{\Gamma} \sum_n' \tau_{on} t_{nn} + \bar{G}(R) \sum_n' \tau_{on} t_{no})\}. \quad \ldots (4.68)$$

Here it is noticed that the expressions for T^c_{os} and T^c_{so} are different as the central site and the shell sites are not treated on the same footing. But as we shall see numerically, the difference is negligible.

The averaged density of states per site is obtained from the imaginary part of $\bar{G}(o)$ which is defined as

$$\bar{G}(o) = \frac{1}{N} \sum_{\vec{k}} \bar{G}(\vec{k},z) \qquad \ldots (4.69)$$

where $$\bar{G}(\vec{k},z) = \frac{1}{z - \Sigma_1 - z\,\Sigma_2 s(\vec{k})} \qquad \ldots (4.70)$$

Since values of k are quasi-continuously distributed, we can convert the summation in (4.70) into an integral to obtain

$$\bar{G}(o) = \frac{\Omega}{8\pi^3} \int \frac{d^3k}{z - \Sigma_1 - z\,\Sigma_2 s(\vec{k})}, \qquad \ldots (4.71)$$

where Ω is the volume of a unit cell.

Eqn. (4.71) can be further written as

$$\bar{G}(o) = \frac{\Omega}{8\pi^3} \int \frac{d^3k\; dE' \delta(E' - \omega_B s(\vec{k}))}{z - \Sigma_1 - \Sigma_2 E'/h^{BB}}. \qquad \ldots (4.72)$$

Now using the definition

$$\frac{\Omega}{8\pi^3} \int d^3k \delta(E' - \omega_B s(\vec{k})) = \rho^{(o)}(E') \qquad \ldots (4.73)$$

for the density of states of pure B constituent and the fact that $\omega_B = Zh^{BB}$; equation (4.72) can be written as

$$\bar{G}(o) = \int \frac{dE' \rho^{(o)}(E')}{z - \Sigma_1 - \Sigma_2 E'/h^{BB}}. \qquad \ldots (4.74)$$

This can now be written in the following form

$$\bar{G}(o) = \frac{1}{z\,\Sigma_2/\omega_B} \int \frac{dE'\rho^{(o)}(E')}{\frac{z-\Sigma_1}{z\,\Sigma_2/\omega_B} - E'}$$

$$\equiv \left(\frac{1}{z\,\Sigma_2/\omega_B}\right) F^{(o)}\left(\frac{z-\Sigma_1}{z\,\Sigma_2/\omega_B}\right), \qquad \ldots (4.75)$$

where $$F^{(o)}(z) = \int_{-\infty}^{\infty} \frac{dE'\rho^{(o)}(E')}{z - E'} . \qquad \ldots (4.76)$$

We introduce two dimensionless variables β and η such that $h^{AA} = \beta h^{BB}$ and $h^{AB} = \eta h^{BB}$. Our results for the density of states are shown in Figs.4.3-4.6. In figure 4.3 we have shown the density of states for a binary alloy having the diamond lattice structure with $\delta = 1.0$ and $x = 0.5$. ω_B is taken to be 4. The hopping integrals are taken to be non-random in this case. It is seen that the results obtained using the conditions (4.57) and (4.58) are very similar. When the condition (4.57) on the Green's function matrix elements was applied, the averaged T-matrix elements $\langle T^c_{oo} \rangle$, $\langle T^c_{os} \rangle$, $\langle T^c_{so} \rangle$, and $\langle T^c_{ss} \rangle$ are found to be small and showed an oscillatory behaviour with respect to energy. When the condition (4.58) was applied, $\langle T^c_{so} \rangle$ was also equal to zero (within the desired accuracy) and $\langle T^c_{ss} \rangle$ had a very small value. The variation of $\langle T^c_{ss} \rangle$ as a function of energy was again oscillatory. The non-analytic difficulties encountered in this case in the SCCSA are not there in the present formulation. The results of this calculation are in close agreement with those obtained in the SCBSA(c).

In Figs.4.4-4.6, we have shown the density of states

for alloys having the simple cubic lattice structure with $\delta = 0.75$ and $x = 0.30$. ω_B is taken to be 1. In this case the densities of states obtained from the two conditions are almost similar. Here we have shown the results obtained from the condition (4.57). In figure 4.4 we have shown the density of states for a case where the hopping integrals are non-random. If this result is compared with the one obtained in the CCPA (Section 4.1) then it is found that the density of states curves are smoother in the present formalism. The variation of the density of states with respect to β and η is shown in Figs. 4.5 and 4.6. For $\beta = 1.5$ and $\eta = 1.25$, the band becomes wider whereas in the case of $\beta = 0.5$ and $\eta = 0.75$, the band has narrowed down. It is noticed that for $\delta = 0.75$ the effects of local environment on the density of states are not very significant (see also Fig.4.1) but for $\delta = 1$, these effects show up in figure 4.4. For large values of δ this formalism gives some non-analytic results such as non-unique density of states at some energies in the minority band. This problem was also encountered by Bose and Foo[171] in their calculation for a linear chain. They also used the same effective medium Hamiltonian as used by us in this calculation. However, it is observed that if the hopping integrals are significantly different then the problem of non-analyticities may be overcome in some cases.

In Figs.4.7-4.9 we have shown the spectral densities of states for three values of structure factor $s(\vec{k})$ (Eqn. 2.34) (a) $s(\vec{k}) = 1.0$, (b) $s(\vec{k}) = 0.0$ and (c) $s(\vec{k}) = -1.0$. The values

of other parameters are the same as in Figs.4.4-4.6. As expected the spectral functions become sharper when the values of β and η are increased. There is some structure in the spectral functions in the energy region $E \approx 0.0$ to $E \approx 1.0$. This structure becomes prominent as the values of β and η are reduced. It can be understood as follows. When the values of β and η are reduced i.e. the hopping from the impurity is reduced, then the electronic wave function will have larger amplitude on impurity sites, giving rise to a peak in the spectral density of states.

From the foregoing discussion it can be said that our formalism takes into account the cluster effects and the hopping disorder in a fairly satisfactory manner, but it is not the complete solution of the problem. The merit of our formalism is that the computation of density of states is tractible. Our formalism suffers from two drawbacks. (i) It does not give the correct dilute limit and (ii) in the strong scattering regime it suffers from the difficulty of non-analyticity of $\langle \underline{G} \rangle$. However, our formalism can be easily improved to get rid off these difficulties. It was noticed by Schwartz et al[172] that the self-energy should at least have a factor of $s(\vec{k})^2$ in order to give the correct dilute limit. In our formalism we can attain the proper dilute limit if we take the matrix elements of the effective medium Hamiltonian between two different sites of the shell to be non-zero. These matrix elements are expected to be small as compared to Σ_1 and Σ_2 and may be approximately taken to be equal to Σ_3 for all pairs of sites on the shell in our

formalism. With this, the self-energy in the $\vec{k}$-representation can be written as

$$\sum(\vec{k},z) = \frac{1}{N}\sum_{ij} e^{i\vec{k}.(\vec{R}_i-\vec{R}_j)} \sum_{ij}. \qquad \ldots (4.77)$$

For the simple cubic lattice it can be simplified to obtain

$$\sum(\vec{k},z) = \sum_1 + 6\sum_2 s(\vec{k}) + 6\sum_3 s(2\vec{k}) + 12\sum_3 \gamma(\vec{k}) \qquad \ldots (4.78)$$

where $$\gamma(\vec{k}) = \frac{1}{12}\sum_{\vec{\delta}_2} e^{i\vec{k}.\vec{\delta}_2} \qquad \ldots (4.79)$$

$\vec{\delta}_2$ is the second nearest neighbour lattice vector. $\gamma(\vec{k})$ can be alternatively written as

$$\gamma(\vec{k}) = \frac{1}{4}\left[6\, s(\vec{k})^2 - 1 - s(2\vec{k})\right]. \qquad \ldots (4.80)$$

It is now noticed from (4.78) and (4.80) that the self-energy contains a factor $s(\vec{k})^2$. This ensures us that with this modification our formalism will give the proper dilute limit. We also expect that the problem of non-analytic behaviour of the averaged Green's function will no longer be there after the introduction of $\sum_3$ in H_{eff}. The three quantities $\sum_1$, $\sum_2$ and $\sum_3$ can then be determined self-consistently from the following conditions:

$$\begin{aligned} \langle T^c_{oo} \rangle &= 0 \\ \langle T^c_{os} \rangle &= 0 \\ \langle T^c_{ss} \rangle &= 0 . \end{aligned} \qquad \ldots (4.81)$$

The formalisms presented in this chapter (and also of sections 3.1 and 3.2) can be used to study alloys having some short-range-order. The only change will be in the probability factor P_c in performing the configurational averages. We can define a short-range-order parameter α so that the probability P_{AB} of finding a B atom near an A atom is $x\alpha(1-x)$. Then the probabilities of pairs AA, BA and BB are $P_{AA} = x(1-\alpha(1-x))$, $P_{BA} = (1-x)\alpha x$ and $P_{BB} = (1-x)(1-\alpha x)$ respectively. If $\alpha = 1$, the system is perfectly random. If α is larger (smaller) than 1, the system favours the amalgamation of different (same) atoms in the nearest neighbour sites. The probabilities of different cluster configurations can then be easily calculated.

FIGURE CAPTIONS

Fig.4.1 Density of states curves for a simple cubic binary alloy with $x = 0.3$ and $\delta = 0.75$, (a) $\alpha_A^2 = 0.5$, (b) $\alpha_A^2 = 1.0$ and (c) $\alpha_A^2 = 1.5$.

Fig.4.2 Impurity band of the density of states curves for $x = 0.1$ and $\delta = 1.0$. (a) $\alpha_A^2 = 0.5$, (b) $\alpha_A^2 = 1.0$ and (c) $\alpha_A^2 = 1.5$.

Fig.4.3 Density of states curves for a binary alloy $A_{0.5}B_{0.5}$ having the diamond lattice structure. (——) and (— · · · —) correspond to conditions (4.57) and (4.58) respectively. (- - -) and (— · —) show the corresponding CPA and DFF results. The curves are symmetric about $E = 0$.

Fig.4.4 Density of states for a simple cubic alloy with $\delta = 0.75$ and $x = 0.3$. $\beta = 1.0$ and $\eta = 1.0$.

Fig.4.5 Density of states for a simple cubic binary alloy with $\delta = 0.75$, $x = 0.3$, $\beta = 1.5$ and $\eta = 1.25$.

Fig.4.6 Density of states for a simple cubic binary alloy with $\delta = 0.75$, $x = 0.3$, $\beta = 0.5$ and $\eta = 0.75$.

Fig.4.7 Plots of the spectral densities of states (a) $s(\vec{k}) = 1.0$, (b) $s(\vec{k}) = 0.0$ and (c) $s(\vec{k}) = -1.0$. Other parameters are the same as in Fig.4.4.

Fig.4.8 Plots of spectral densities of states, (a) $s(\vec{k}) = 1.0$, (b) $s(\vec{k}) = 0.0$ and (c) $s(\vec{k}) = -1.0$. Other parameters are the same as in Fig.4.5.

Fig.4.9 Plots of spectral densities of states, (a) $s(\vec{k}) = 1.0$, (b) $s(\vec{k}) = 0.0$ and (c) $s(\vec{k}) = -1.0$. Other parameters are the same as in Fig.4.6.

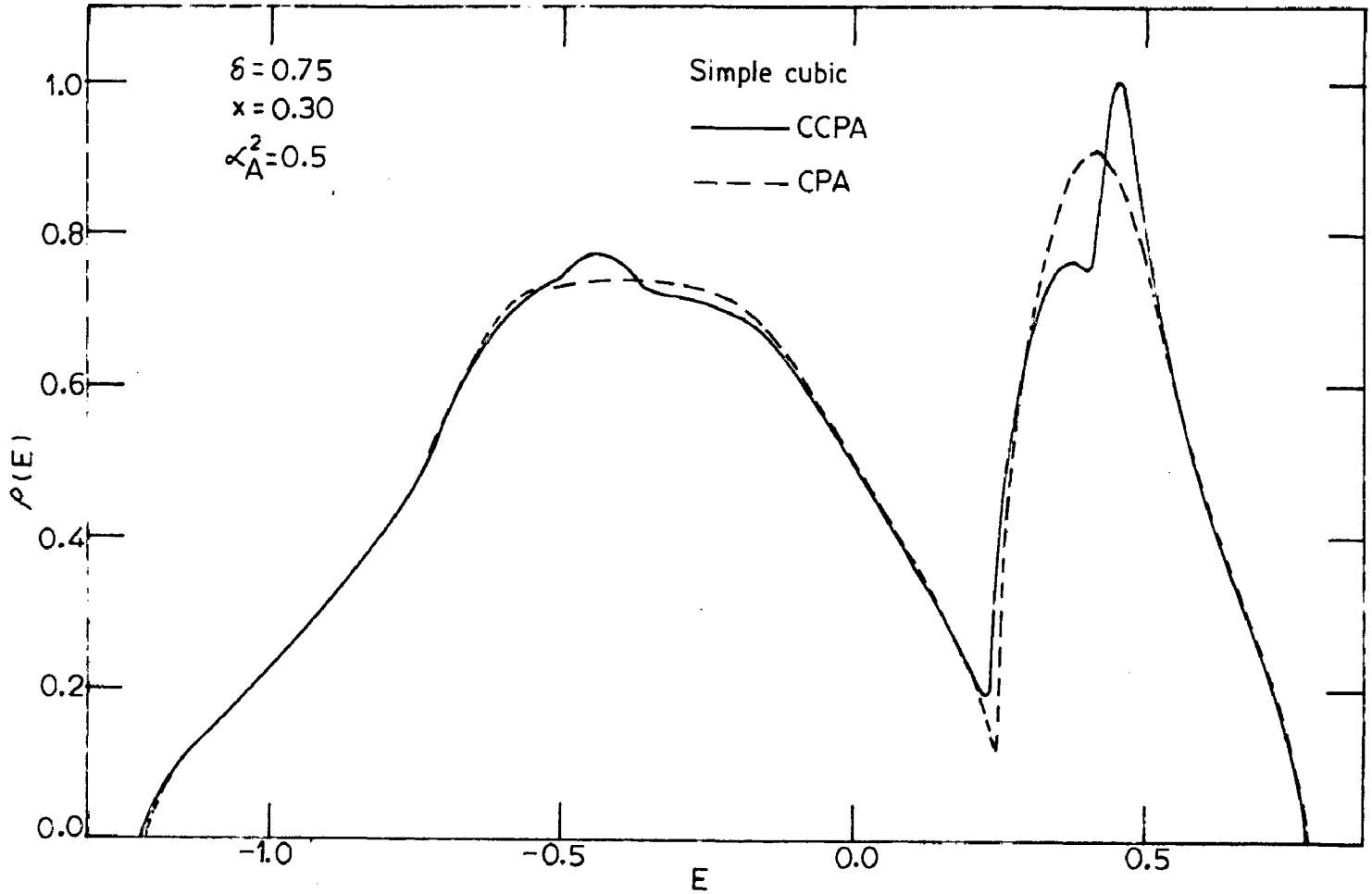
δ = 0.75
x = 0.30
α_A^2=0.5
Simple cubic
CCPA
CPA
1.0
0.8
0.6
0.4
0.2
0.0
ρ(E)
-1.0
-0.5
0.0
0.5
E

FIG. 4.1 (a)

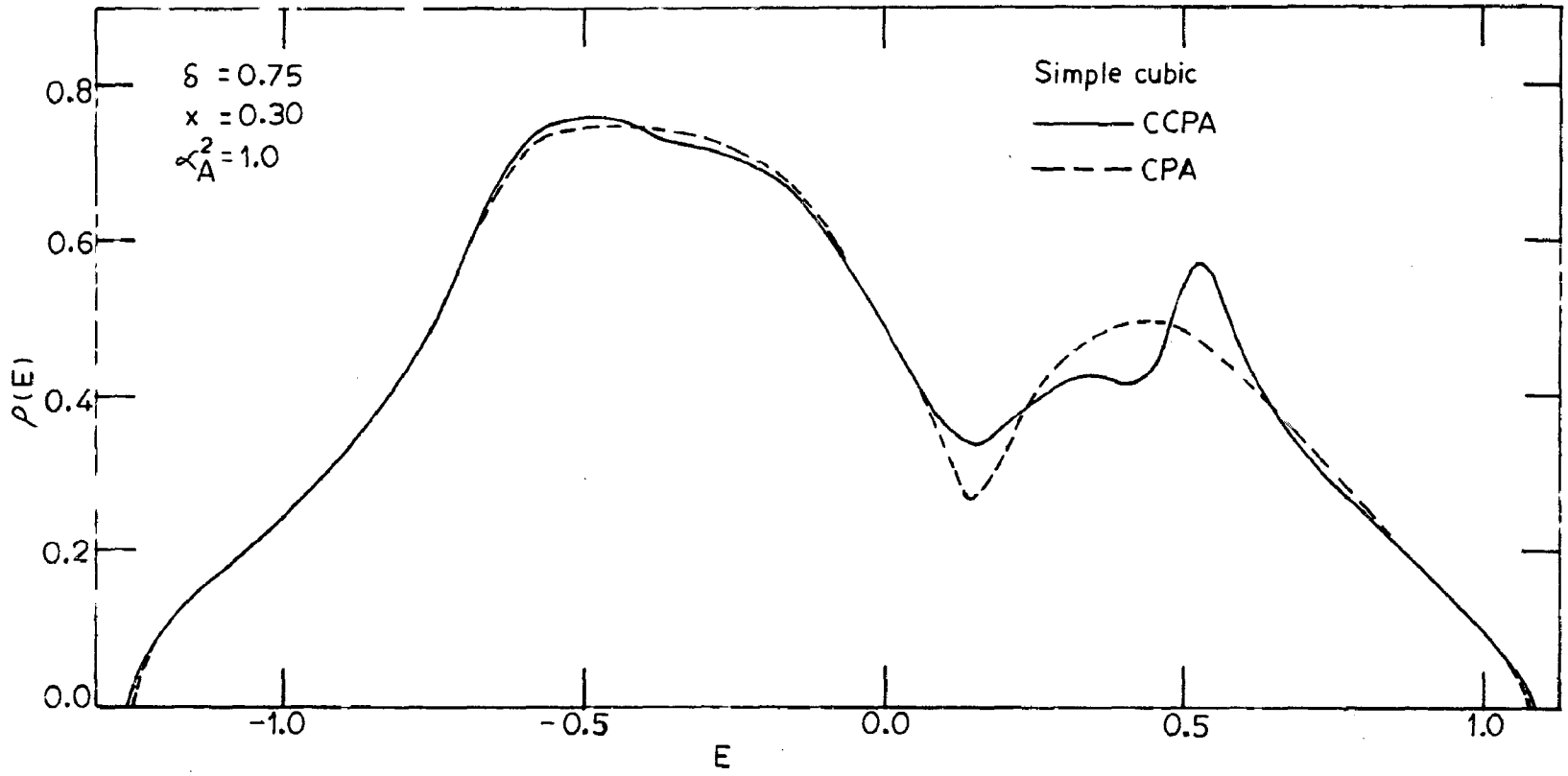
δ = 0.75
x = 0.30
α_A^2 = 1.0
Simple cubic
CCPA
CPA
0.8
0.6
0.4
0.2
0.0
ρ(E)
-1.0
-0.5
0.0
0.5
1.0
E

FIG. 4.1 (b)

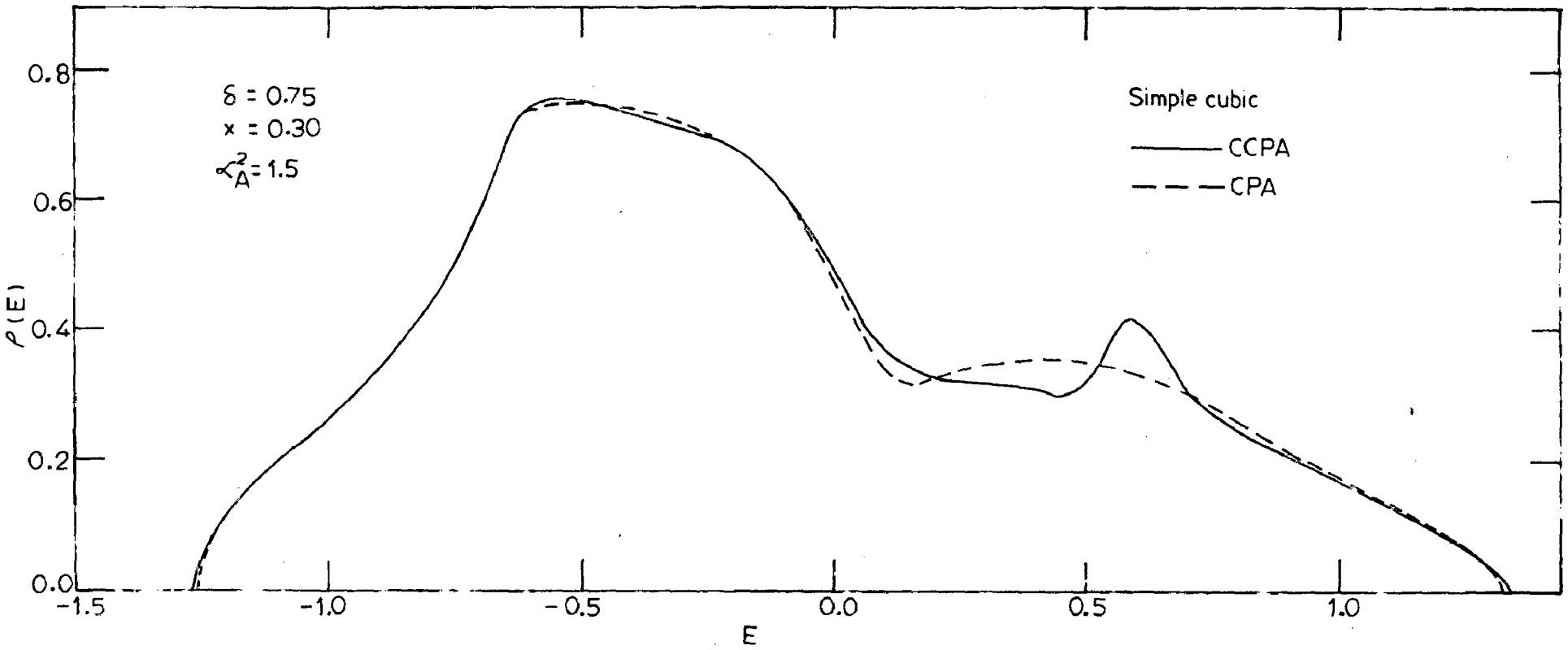
δ = 0.75
x = 0.30
α_A^2 = 1.5
Simple cubic
CCPA
CPA
ρ(E)
E
0.0
0.2
0.4
0.6
0.8
-1.5
-1.0
-0.5
0.0
0.5
1.0

FIG. 4.1 (c)

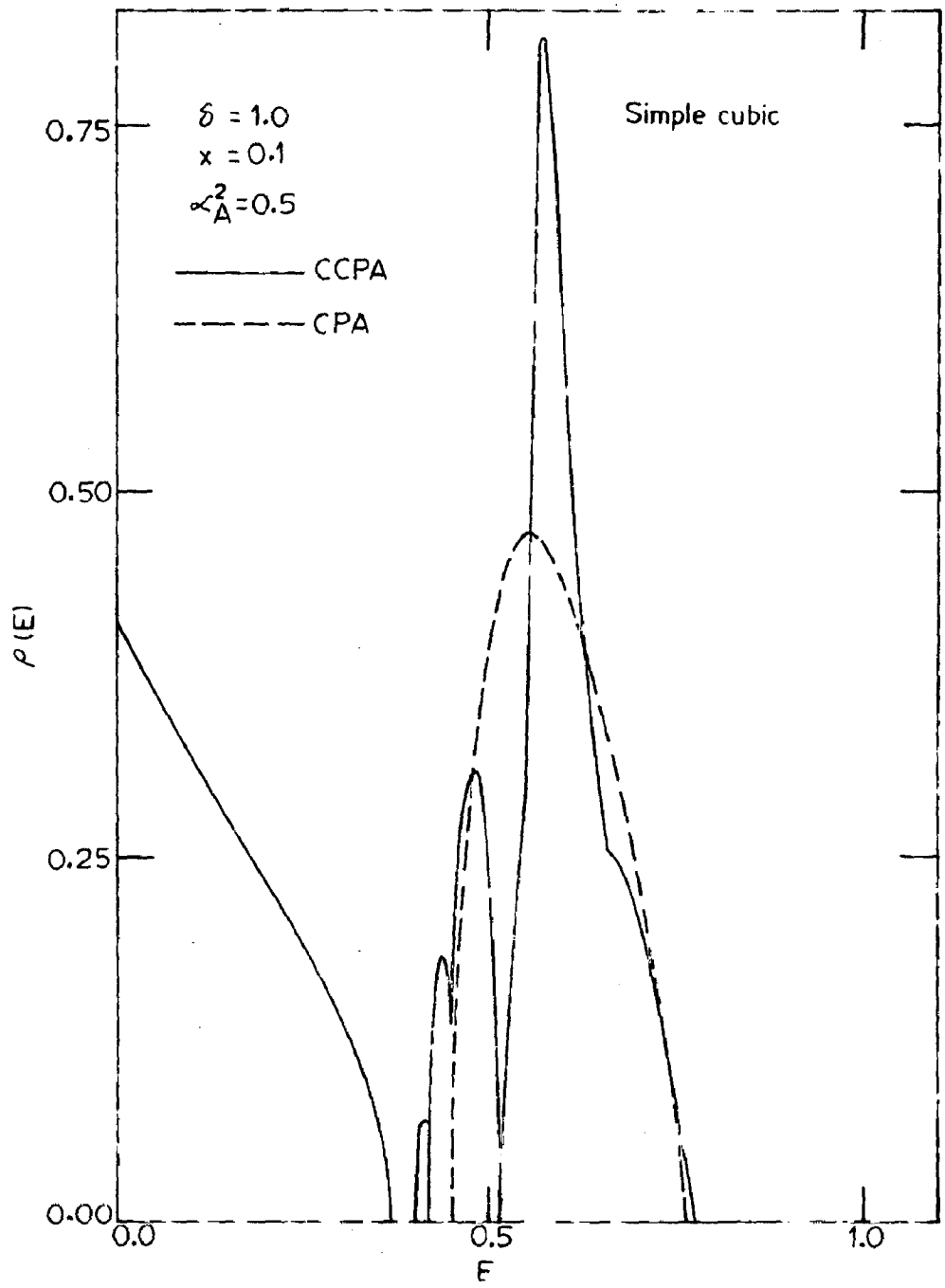
δ = 1.0
x = 0.1
α_A^2=0.5
CCPA
CPA
Simple cubic
0.75
0.50
0.25
0.00
ρ(E)
0.0
0.5
1.0
E

FIG.4.2 (a)

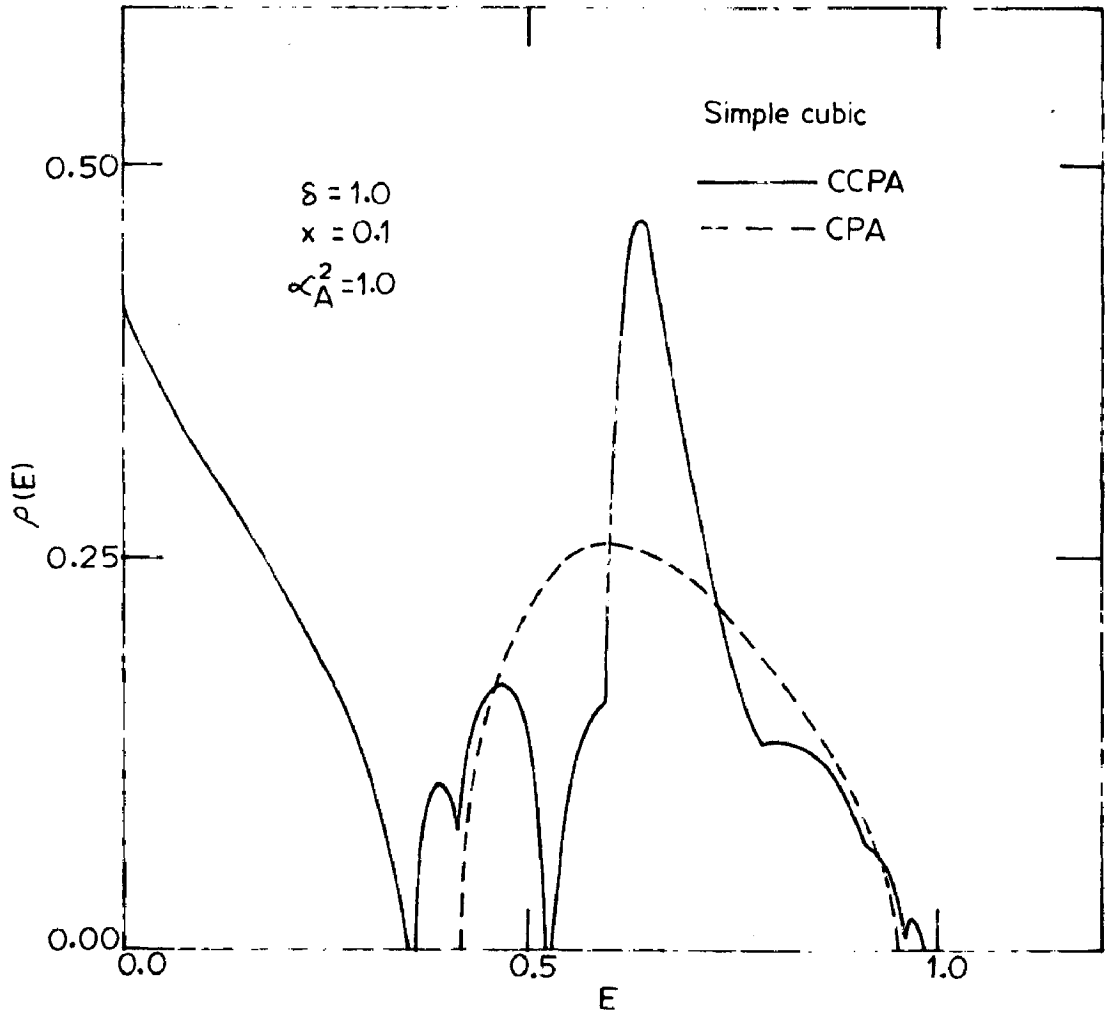
Simple cubic
CCPA
CPA
δ = 1.0
x = 0.1
α_A^2 = 1.0
0.50
0.25
0.00
ρ(E)
0.0
0.5
1.0
E

FIG. 4.2(b)

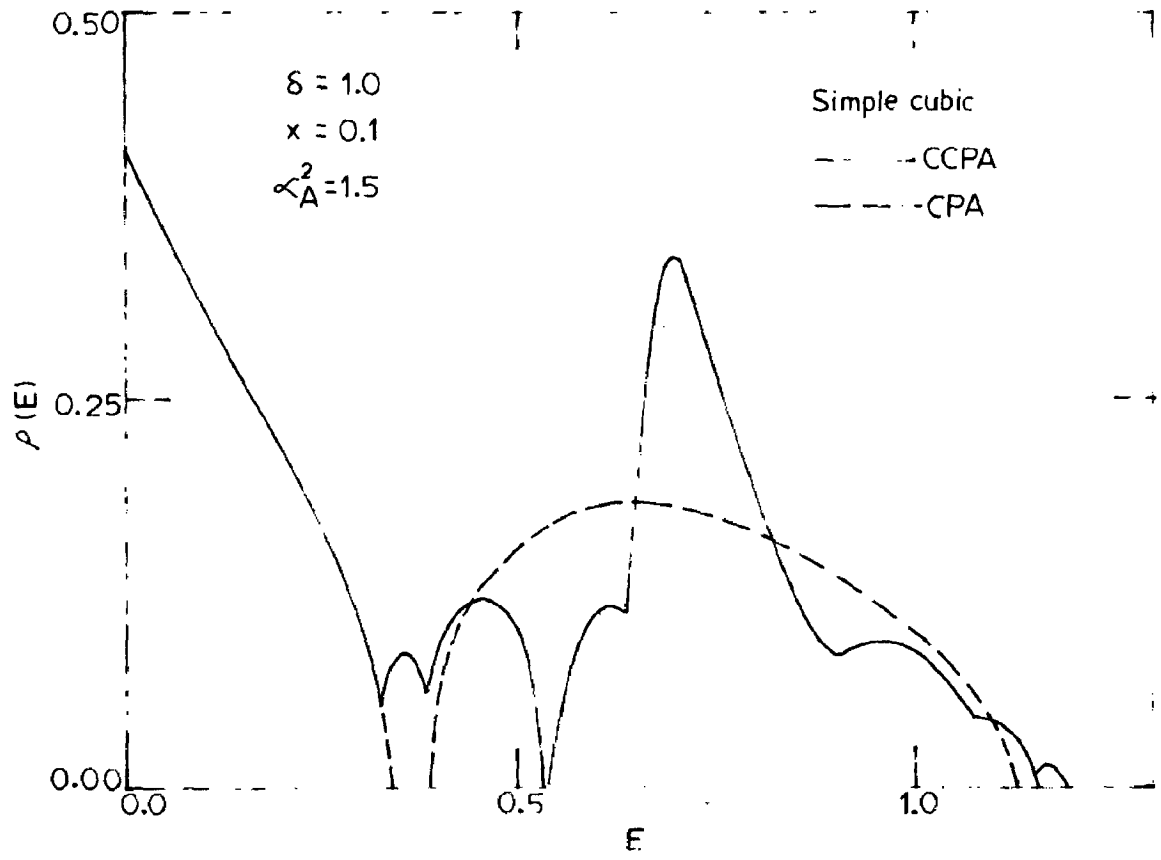
0.50
0.25
0.00
ρ(E)
δ = 1.0
x = 0.1
α_A^2=1.5
Simple cubic
CCPA
CPA
0.0
0.5
1.0
E

FIG. 4.2(c)

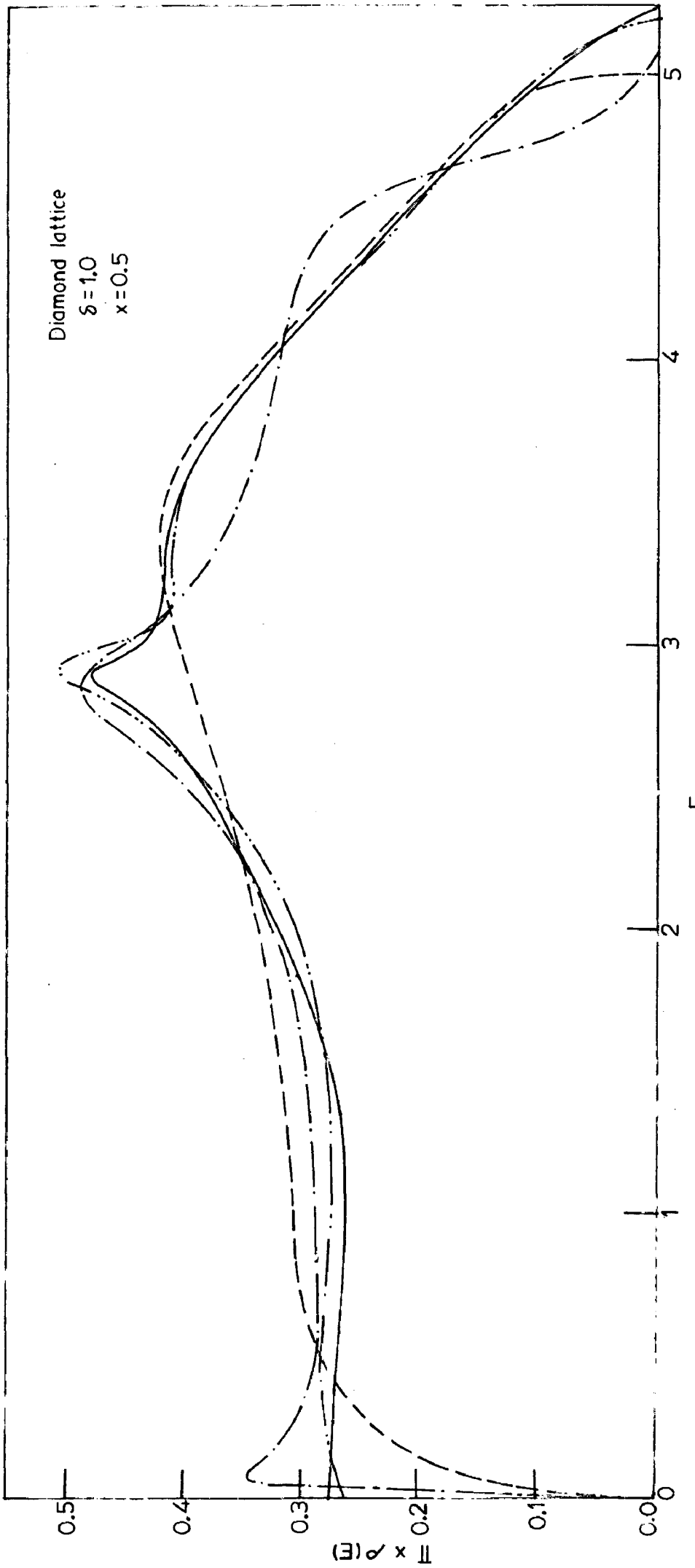

FIG. 4.3

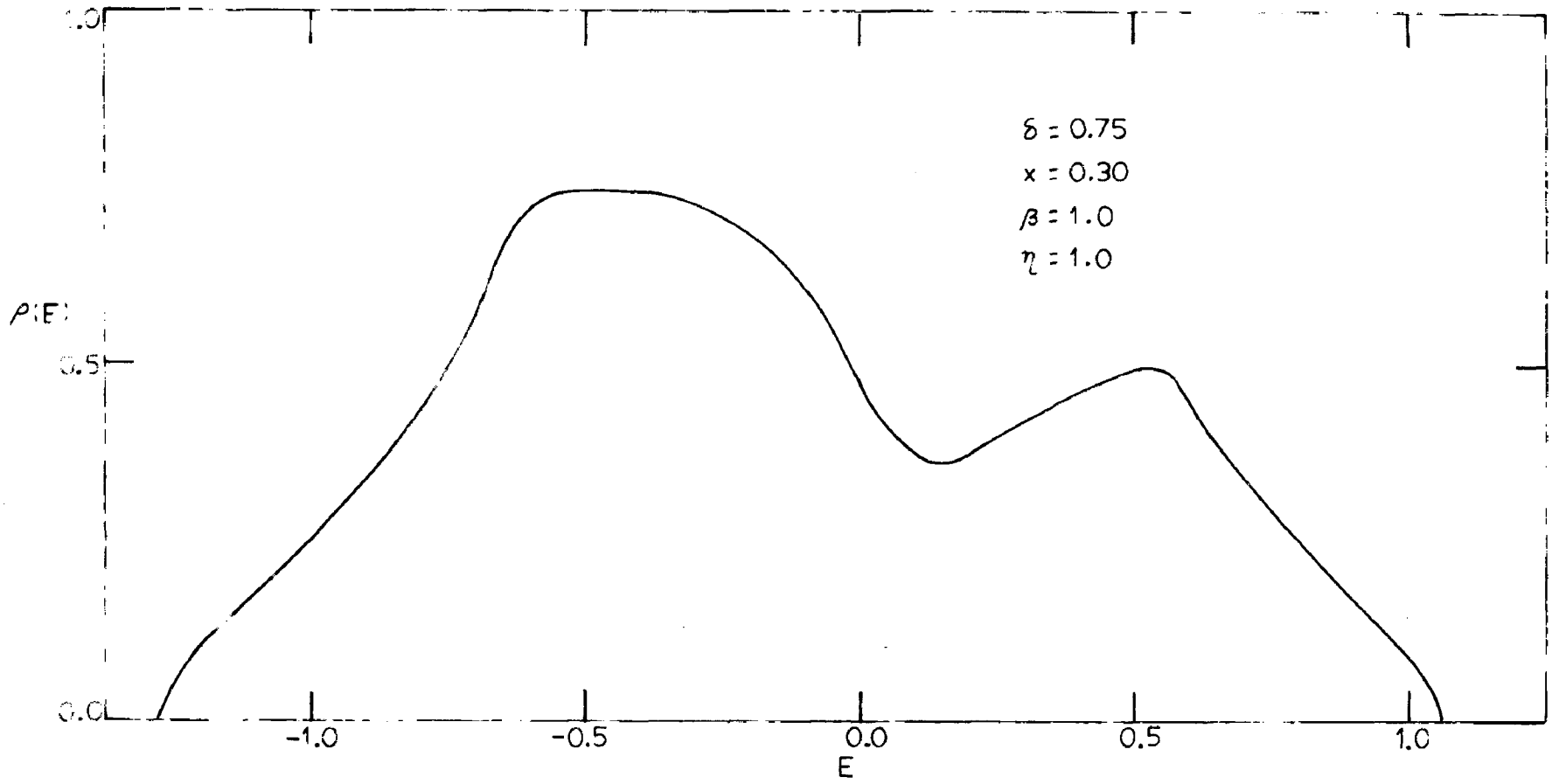

FIG. 4.4

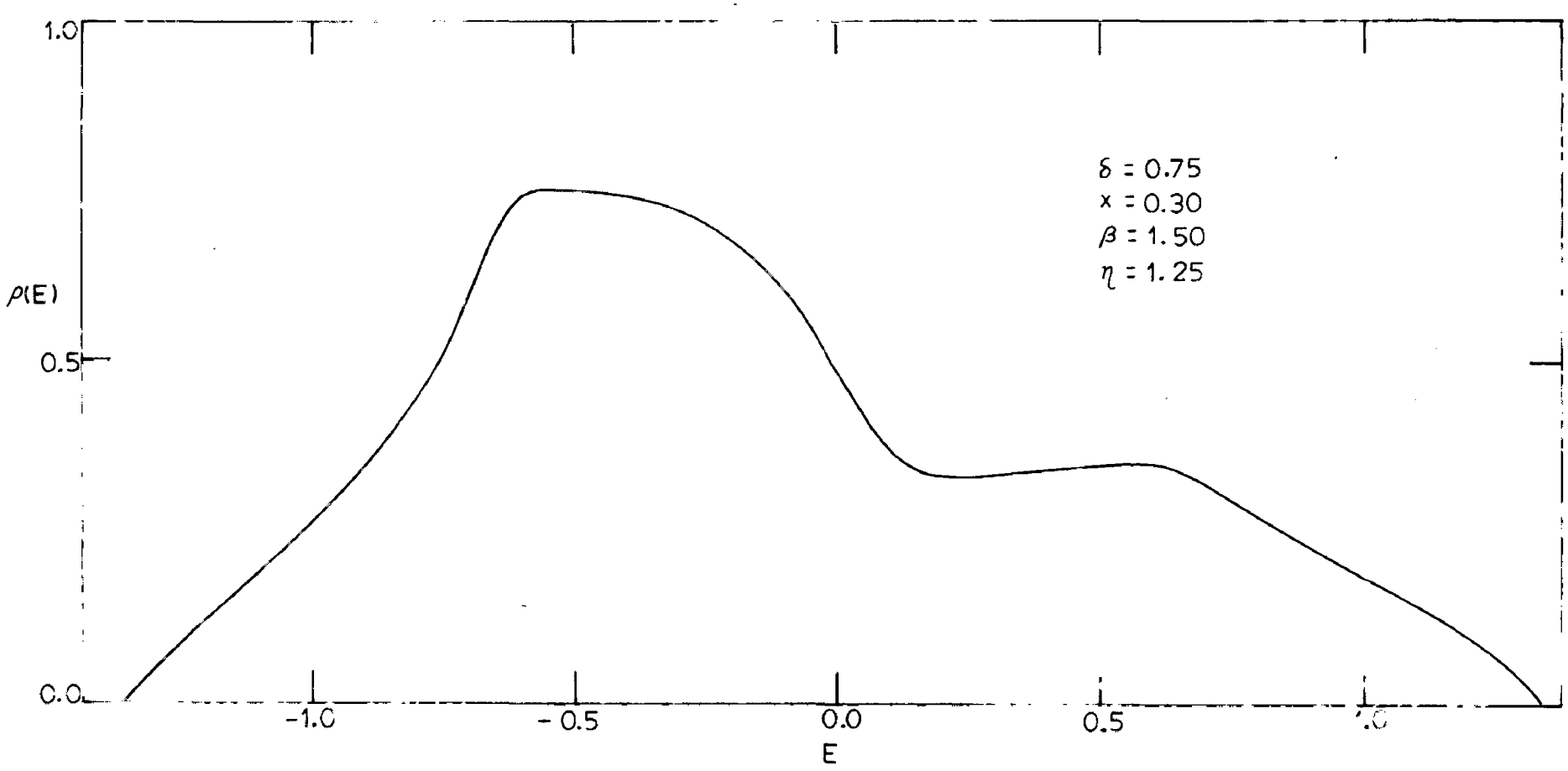

FIG. 4.5

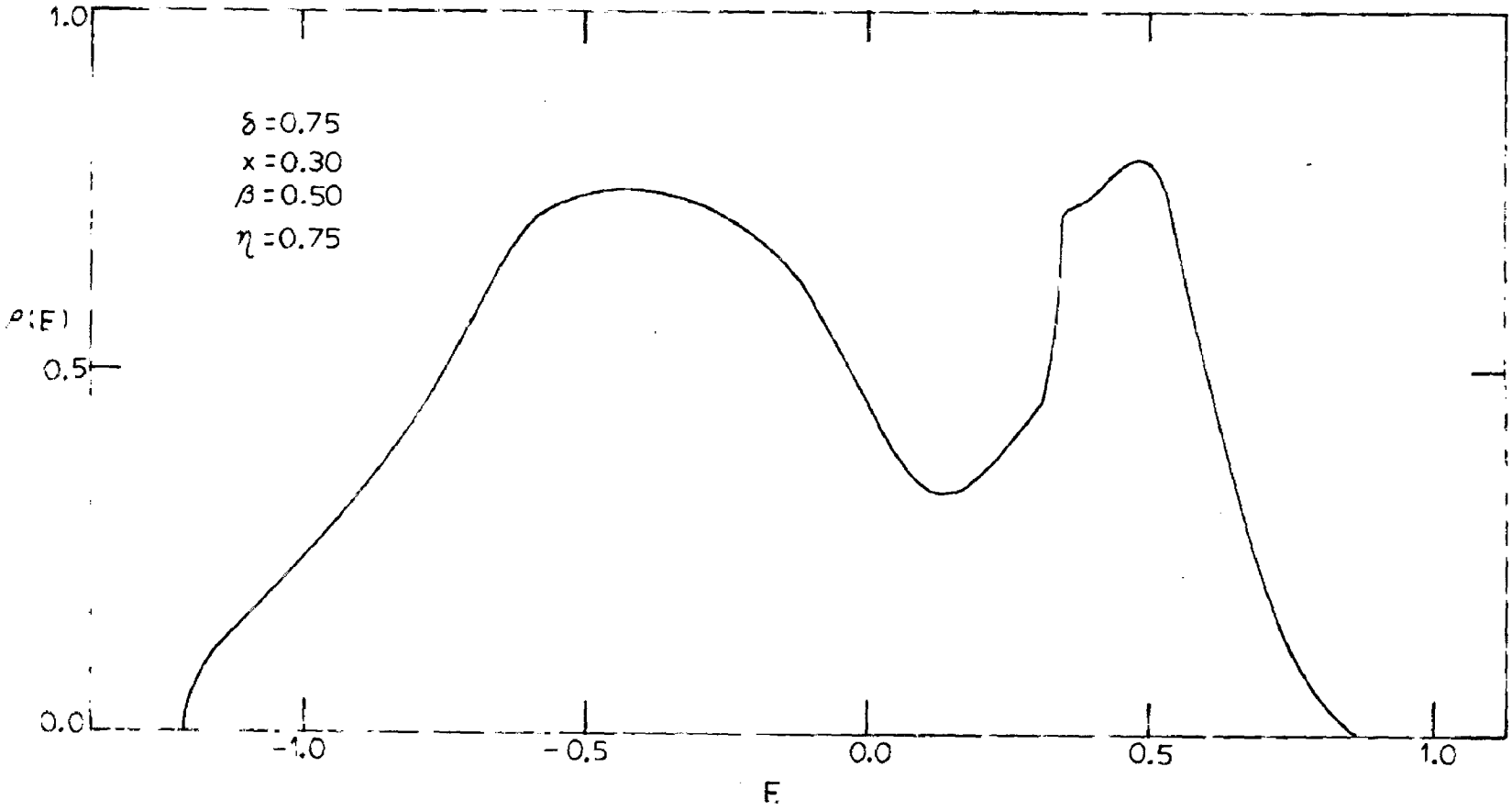

FIG. 4.6

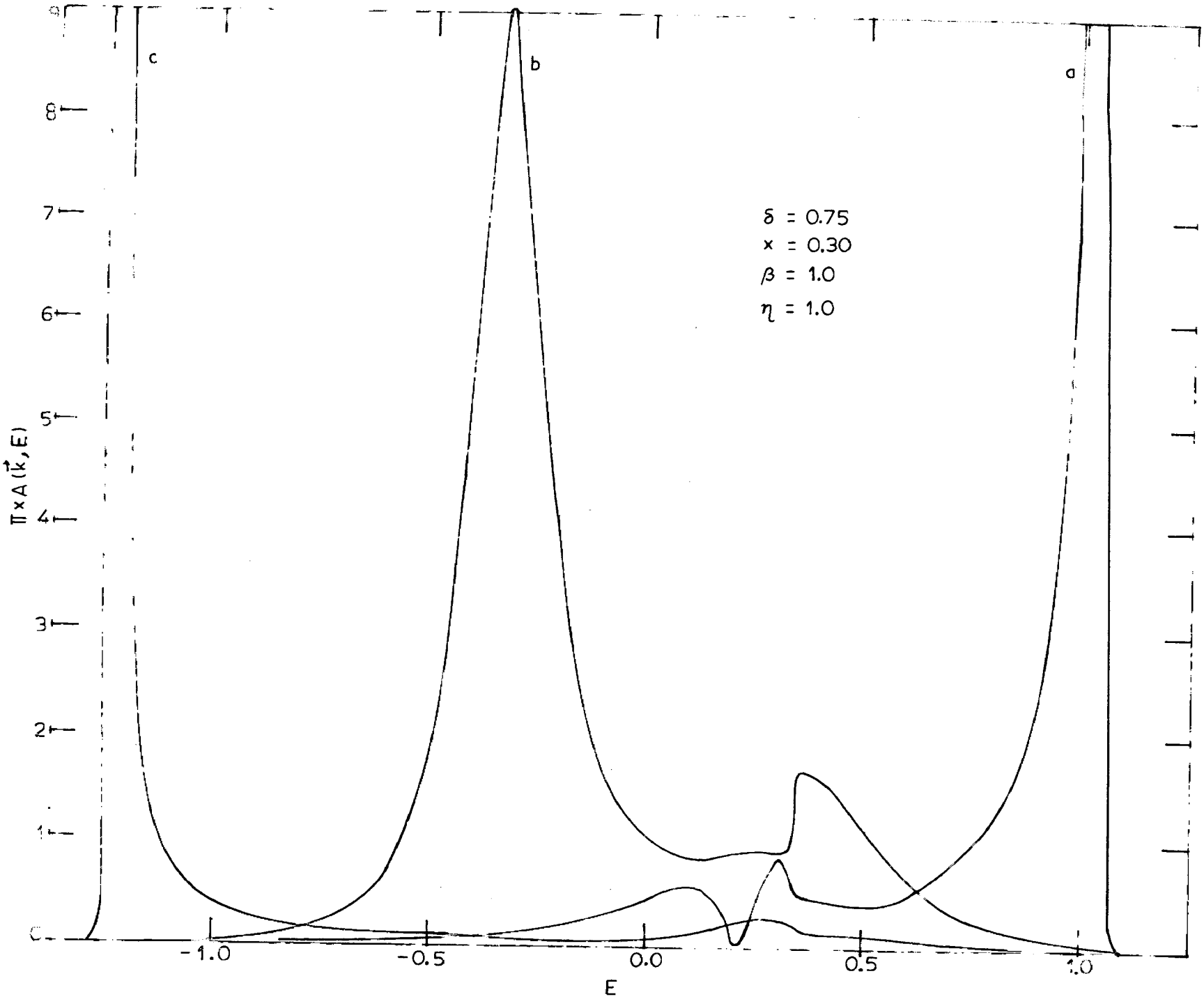

FIG. 4.7

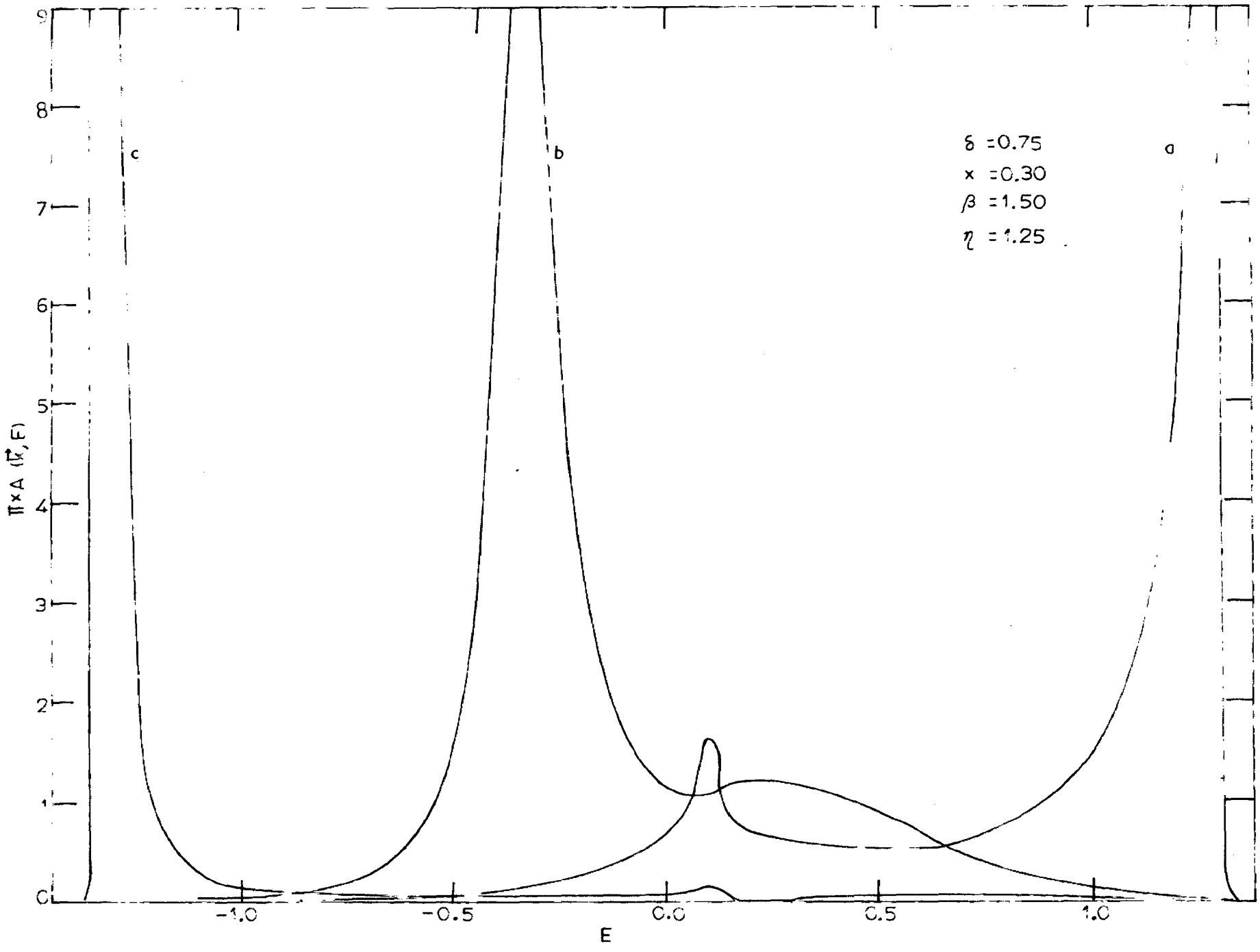

FIG. 4.8

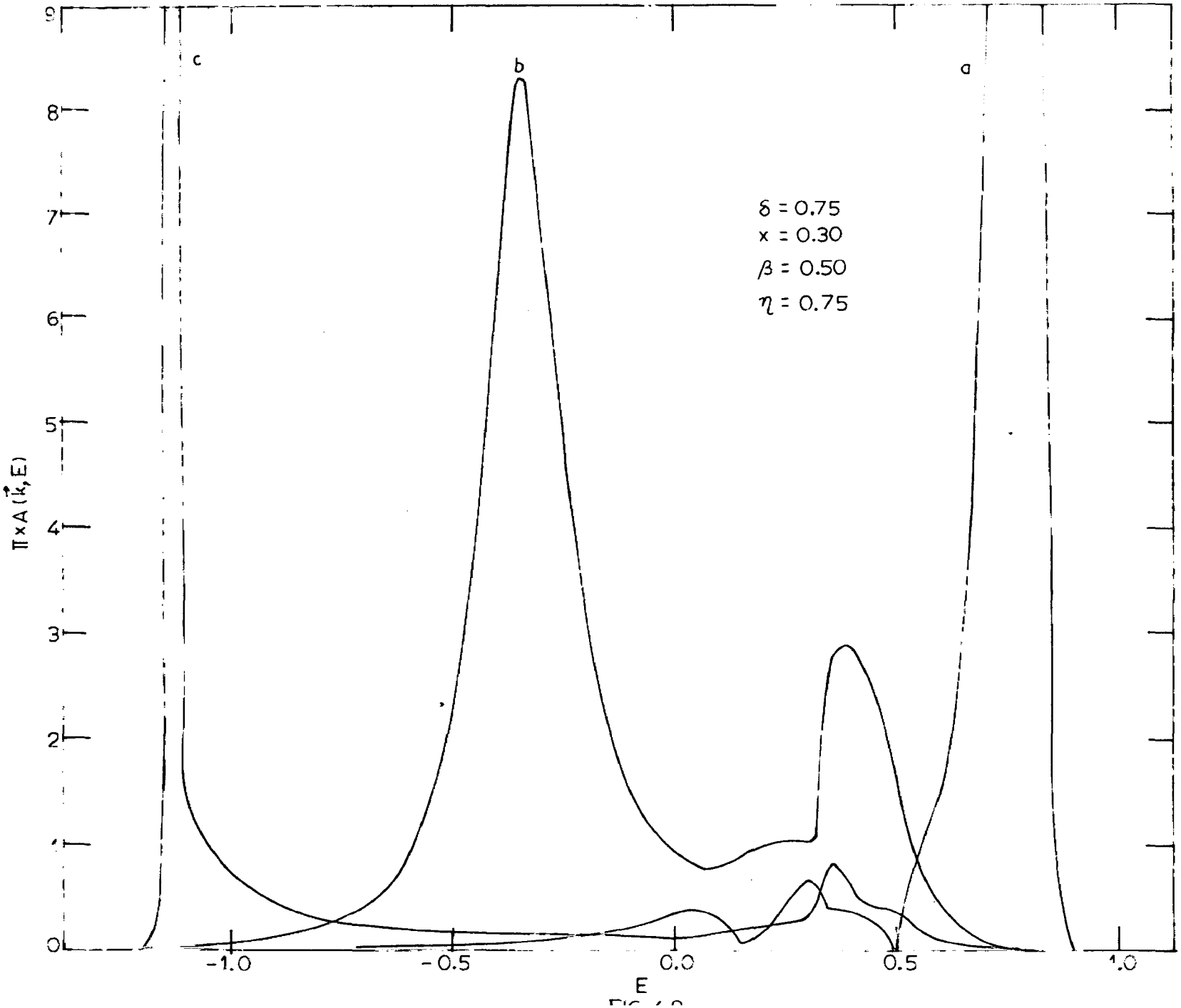
c
b
a
δ = 0.75
x = 0.30
β = 0.50
η = 0.75
π x A (k, E)
0
1
2
3
4
5
6
7
8
9
-1.0
-0.5
0.0
0.5
1.0
E

CHAPTER V

THEORY OF DISORDERED HEISENBERG FERROMAGNETS

§5.1 Brief Survey of Early Work

So far our efforts were confined to the study of a simple single band model for electrons in disordered systems. Attempts were made to get a reasonable fit with the exact results. No attempt was made to apply the models developed to realistic systems and to get experimental agreements. Considerable experimental work on lattice vibration spectra[173] and spin wave spectra[5] of alloys using neutron scattering has appeared in past few years. Cowley and Buyers[5] and others have pointed out that the magnetic excitations are the best candidates for quantitative comparison between the theory and the experiments. The reason is that the magnetic excitations in several cases are well described by simple Heisenberg exchange Hamiltonian along with suitable single ion anisotropics. On the other hand the realistic models for phonons and electronic states tend to be rather complicated.

As we mentioned in the introduction, all the above mentioned excitations in several cases may be well described by the Hamiltonian (2.30) with proper interpretation to the states $|n\rangle$. The spin wave problem based on the Heisenberg exchange Hamiltonian involves both the diagonal and the off-diagonal disorders in a correlated manner. In fact the site energy (diagonal term) is determined by the composition of

the neighbours of the given site and the hopping integrals (off-diagonal terms) connected to a given site are all correlated. The correlation in the matrix elements is related to the isotropy of the Hamiltonian in the spin-space and gives rise to the Goldstone theorem. The simplest theory that would preserve the relationship between the site energies and the hopping energies, would have to treat scattering from a cluster of (Z+1) sites i.e. a cluster consisting of a central site and its Z nearest neighbours coherently.

There exist several treatments of this problem. The earlier treatments of Foo and Wu[174], Tahir-Kheli[175], and Elliott and Pepper[176] can be classed as effective bond theories. These theories are simplest extensions of the CPA in which one calculates the scattering from one bond at a time with respect to an effective medium. The effective medium is then determined by requiring that scattering from a single bond vanishes on the average. The requirement of the Goldstone theorem is built into the theory by properly choosing the diagonal and the off-diagonal parts of the self-energy characterizing the effective medium. Tsukada[177] has extended this sort of calculation by considering a cluster scattering from four bonds for an fcc lattice. His treatment, however, makes use of a spatial simplification that occurs for a four bond cluster on an fcc lattice. The theories of Kaneyoshi[178], Edwards and Jones[179] and Jones and Yates[180] are based on diagrammatic expansions of the Green's function. These theories are not

self-consistent and the approximations made in them are really valid in low impurity concentration limit. The first attempt to take into account the disorder in site energies as it arises from the configurations of the neighbours of a given site, was by Buyers et al[33,34] for the case of anti-ferromagnets. These authors obtained reasonable agreement with experimental results, but their theory had the drawback that it did not treat the off-diagonal disorder at the same footing. On the other hand Theumann[181] proposed a theory in which the off-diagonal disorder was treated quite adequately using the method of BEB, but the diagonal disorder was treated in the virtual-crystal approximation.

Another point that has not been realised explicitly in the earlier work is that for a problem in which two types of atoms, being alloyed, have different spins, the normalized spin deviation operators $a_i = \frac{1}{\sqrt{2S_i}} S_i^+$ have been conventionally employed. However, the operator $A^\dagger = \sum_i a_i^\dagger$ does not commute with the Hamiltonian and thus the spectrum of excitations given by the operators $\{a_i\}$ does not start with zero energy as required by the Goldstone theorem. On the other hand if one makes use of the true spin-deviation operators, one obtains a Green's function equation of motion in which the inhomogeneous term is also random. Murray[182] has handled this difficulty in a variational method, but her method is suitable only in the long wave-length limit. Edwards and Jones[179] have also employed the operators S_i^+, but it is difficult to see how one can construct a CPA type self-consistent theory in

The ground state of the Heisenberg ferromagnet is assumed to be the one in which all the spins are alligned in the z-direction. The spin excitations are then described through the equations of motion of the operators $S_i^{\pm} = S_{ix} \pm iS_{iy}$, which increase or decrease the spin component along the z-direction. For the discussion of the spin wave spectra it is convenient to write the Hamiltonian (5.1) in terms of Boson operators $\{a_i\}$ related to spin operators $S_i^{\pm}$ through the Holstein-Primakoff transformation

$$S_i^- = (2S_i)^{1/2} a_i^\dagger$$

$$S_i^+ = (2S_i)^{1/2} a_i \qquad \ldots (5.2)$$

and $$S_{iz} = S_i - a_i^\dagger a_i.$$

Here we have considered the first order approximation and neglected the higher order terms. Thus we obtain for the Hamiltonian of Eq.(5.1)

$$\underline{H} = 2 \sum_{ij} J_{ij} S_j a_i^\dagger a_i - 2 \sum_{ij} J_{ij} (S_i S_j)^{1/2} a_i^\dagger a_j \ldots . (5.3)$$

Here again we have neglected the higher order terms since we are interested only in the spin wave spectra.

If we now define

$$\varepsilon_i = 2 \sum_j J_{ij} S_j$$

and $$h_{ij} = -2(S_i S_j)^{1/2} J_{ij}, \qquad \ldots (5.4)$$

then Eq.(5.3) can be rewritten as

this approach. In some of the earlier work employing normalized operators, the requirement of the Goldstone theorem is artificially achieved by imposing it on the self-energy. However, this does not make the procedure strictly self-consistent. Here we have employed the formalism of Section § 4.2 which treats the diagonal and the off-diagonal disorders on an equal footing. In this method both the diagonal and the off-diagonal parts of the self-energy are determined self-consistently from the T-matrix equation. So there are slight deviations from the Goldstone symmetry. Thus we do not expect our results to be good at low energies.

§ 5.2 The Model

We consider a substitutionally disordered ferromagnetic binary alloy $A_{1-x}B_x$ where the magnetic atoms of the constituents A and B have spins S_A and S_B respectively. The interaction among the spins is represented by the Heisenberg Hamiltonian

$$H = - \sum_{ij} J_{ij} \vec{S}_i \cdot \vec{S}_j \qquad \ldots (5.1)$$

where the summation is taken over the nearest neighbour pairs. J_{ij}, the exchange integral is nonzero only for the nearest neighbour pair $(\vec{R}_i, \vec{R}_j)$ and its value depends upon the species of spins which are being connected by it. For a binary alloy it can, therefore, take three values J_{AA}, $J_{AB} (= J_{BA})$ and J_{BB}. $\vec{S}_i$ is the atomic spin operator for the atom located at the lattice position $\vec{R}_i$.

$$H = \sum_i \varepsilon_i a_i^\dagger a_i + \sum_{ij} h_{ij} a_i^\dagger a_j . \qquad \ldots (5.5)$$

Clearly we have reduced the Hamiltonian (5.1) to a form (5.5) which we have already dealt with. From Eq.(5.4) it is seen that the diagonal matrix element ε_i depends on the occupancy of the site at $\vec{R}_i$ as well as on the occupancies of sites which are nearest neighbours to the site at $\vec{R}_i$. Moreover, the diagonal and the off-diagonal disorders are both equally important as they arise from the same terms. The Goldstone theorem is obeyed when

$$\langle \varepsilon_i \rangle = - \sum_j \langle h_{ij} \rangle . \qquad \ldots (5.6)$$

However, this condition is not obeyed for Eq.(5.5).

The dynamics of the spin disordered system is best described by the double time retarded Green's function which is defined as

$$G_{ij}(t) = -2\pi i \theta(t) \langle [S_i^+(t), S_j^-(o)] \rangle / \{ 2(S_i S_j)^{1/2} \}$$
$$\equiv \ll a_i(t), a_j^\dagger(o) \gg . \qquad \ldots (5.7)$$

The Fourier transform of $G_{ij}(t)$ is defined as

$$G_{ij}(\omega) = \frac{1}{2\pi} \int_{-\infty}^{\infty} e^{i\omega t} G_{ij}(t) dt. \qquad \ldots (5.8)$$

We shall be interested in obtaining the averaged density of states $\rho(\omega)$ for the spin waves and the spectral functions $A(\vec{k},\omega)$ which are given by

$$\rho(\omega) = - \frac{1}{\pi} \mathrm{Im} \langle G_{ii}(\omega) \rangle \qquad \ldots (5.9a)$$

and $A(\vec{k},\omega) = -\frac{1}{\pi}\mathrm{Im}\langle G(\vec{k},\omega)\rangle$ ... (5.9b)

where $\langle G(\vec{k},\omega)\rangle$ is the momentum transform of $\langle G_{ij}(\omega)\rangle$.

The equation of motion for the Green's function $G_{ij}(t)$ follows from (5.7),

$$\omega\, G_{ij}(\omega) = \delta_{ij} + \varepsilon_i G_{ij}(\omega) + \sum_{\ell} h_{i\ell} G_{\ell j}(\omega). \qquad \ldots (5.10)$$

In matrix notation it can be written as

$$(\omega \underline{I} - \underline{H})\underline{G} = \underline{I}. \qquad \ldots (5.11)$$

We now define an effective medium Green's function $\underline{\tilde{G}}$ such that

$$(\omega \underline{I} - \underline{H}_{\mathrm{eff}})\underline{\tilde{G}} = \underline{I}. \qquad \ldots (5.12)$$

$\underline{H}_{\mathrm{eff}}$ is the corresponding effective medium Hamiltonian (so far undetermined) and we choose it to have the following form:

$$\underline{H}_{\mathrm{eff}} = \sum_i \tilde{\sigma_1}\, a_i^{\dagger} a_i + \sum_{ij} \tilde{\sigma_2}\, a_i^{\dagger} a_j. \qquad \ldots (5.13)$$

Here the summation in the second term is over the nearest neighbour pairs. As already noticed this choice of effective medium is not consistent with cluster T-matrix equations, as we have ignored the self-energy matrix elements between the shell sites. For this reason the results obtained do not reduce correctly to the single impurity result of Izyumov[183].

Further treatment runs parallel to what we have already done in Section § 4.2. Here again we consider a cluster $\underline{c}$ made up of a central site and its Z nearest neighbours, immersed in an otherwise effective medium. The Green's

function $\underline{G}^c$ for such a system is written as

$$\underline{G}^c = \underline{\bar{G}} + \underline{\bar{G}}\ \underline{V}^c\ \underline{G}^c \qquad \ldots (5.14)$$

where

$$\underline{V}^c = \sum_{i\varepsilon c} (\varepsilon_i - \bar{\sigma}_1) a_i^\dagger a_i + \sum_{j\varepsilon s} (h_{ij} - \bar{\sigma}_2)(a_i^\dagger a_j + a_j^\dagger a_i) \ldots . \quad (5.15)$$

s denotes the shell of nearest neighbours. Just like the electronic case, an approximation has been made in writing Eq.(5.15). There is a problem of how to write interaction between a spin on the shell $\underline{s}$ and a spin in the effective medium. To simplify the algebra as well as the numerical computation we assume it to be the same as in the effective medium and similarly for a shell site $\varepsilon_i - \bar{\sigma}_1 = 2J_{io}S_o - \frac{1}{Z}\bar{\sigma}_1$, where o denotes the central site.

Equation (5.14) can now be written as

$$\underline{G}^c = \underline{\bar{G}} + \underline{\bar{G}}\ \underline{T}^c\ \underline{\bar{G}} \qquad \ldots (5.16)$$

where $$\underline{T}^c = \underline{V}^c(\underline{I} + \underline{\bar{G}}\ \underline{T}^c) \qquad \ldots (5.17)$$

is the T-matrix corresponding to the cluster $\underline{c}$ imbedded in the effective medium. The T-matrix equations are simplified in terms of T^c_{oo}, T^c_{os}, T^c_{so} and T^c_{ss} as we did in the case of electrons. The expressions for these have already been derived in Section § 4.2. The effective medium is then determined by solving the following conditions self-consistently,

$$\langle T^c_{oo} \rangle = 0, \qquad \langle T^c_{os} \rangle = 0 . \qquad \ldots (5.18)$$

These conditions have been solved for various values of concentration and exchange integrals. It has been found that

$\langle T^c_{so} \rangle$ is also vanishingly small and $\langle T^c_{ss} \rangle$ has a very small value which oscillates about zero as energy is varied.

§ 5.3 The Spin-Wave Spectra

We calculated the spectral functions $A(\vec{k},\omega)$ and the averaged density of states $\rho(\omega)$ for a ferromagnetic binary alloy having the simple cubic lattice structure. The magnetic atoms are assumed to have spins 1/2 and 1. In Figs.5.1-5.3 behaviour of the spectral functions is studied for various values of x and $\vec{k}$ keeping the exchange integrals fixed. The energy is expressed in units of $2S_A J_{AA} Z$. As expected the spectral functions are very sharp in the low energy region and correspond to well defined spin waves. For low concentration of B spins, the spectral functions at higher values of k are very broad and even some satellite peaks appear in the high energy region (Fig.5.1). As the concentration of B spins is increased (Figs.5.1 and 5.2), the spectral functions corresponding to large k values get comparatively sharper apart from tailing at the low energy side. This can be understood in the following way. For higher energies, the spin-wave function has larger amplitude on B sites and thus it suffers comparatively less scattering as the concentration of A spins is decreased. The spectral functions shift towards higher energies as the concentration of B spins is increased (Fig.5.3). In general the shape of the spectral functions is similar to those of Tsukada[177] and Harris et al[184] obtained for the diluted ferromagnets. A detailed comparison of our work with the earlier theories is not possible as most of these deal with

diluted system. As far as we are aware, ours is the first self-consistent calculation for mixed ferromagnetic systems where both the diagonal and off-diagonal disorders are considered on an equal footing.

In Figs.5.4-5.6 we show the variations of the spectral functions as the values of the exchange integrals J_{AB} and J_{BB} are varied, the concentration being fixed at $x = 0.4$. The low k spectral functions remain very sharp in all the cases, but high k spectral functions become comparatively sharper as J_{BB} is decreased. In Fig.5.7 we have plotted the spin wave energies in the (1,1,1) direction for the entire range of concentration. The exchange integrals are kept the same as in Figs.5.1-5.3. We have not shown the results for very low values of k because the Goldstone theorem is not satisfied. In this region our theory does not give good results and moreover there are numerical problems due to which spectral functions have more than one peak. In Fig.5.8 we have shown the variation of the stiffness constant D defined as

$$D = \frac{1}{2} \frac{\partial^2 \omega(k)}{\partial k^2}\Big|_{k=o} \quad . \qquad \ldots (5.19)$$

This result is compared with the variational theory of Murray[182] whose results are shown by the broken line. Our results lie below the variational estimate which is a rigorous upper bound for spin-wave energy.

Figures 5.9 and 5.10 show representative plots of the averaged densities of states. In Fig.5.9 exchange integrals are

kept fixed at values same as in Fig.5.1 and the variation with concentration is studied. At low concentrations, there is some structure at high energy end. These correspond to the resonance modes of B spins. The oscillations at the low energy side are due to numerical difficulties and no physical significance need be attached to these. Such difficulties have also been encountered in the work of Theumann and Tahir-Kheli[185] on the diluted ferromagnets. As the concentration is increased, the band edge at the low energy end shifts away from zero. As discussed earlier, this arises due to the use of normalized spin deviation operators for which Goldstone theorem is not obeyed. In Fig.5.10 we have shown the variation of the density of states as the values of exchange integrals are varied. The concentration of B spins is kept fixed at x = 0.4. As expected, the width of the band depends upon the largest exchange integral.

From this analysis we can say that our theory describes well the mixed Heisenberg ferromagnets in the whole energy region except at very low energies and at very low concentrations. As far as the low concentration limit is concerned, we can introduce a term in the effective medium Hamiltonian corresponding to an effective interaction between the second nearest neighbours as done in the case of electrons. This additional matrix element can be determined self-consistently in our formulation by supplementing the equation (5.18) by the condition $\langle T^{c}_{ss} \rangle = 0$. This theory can also be easily extended to the mixed antiferromagnets for which extensive experimental results are available.

FIGURE CAPTIONS

Fig.5.1 Spin wave spectral functions of the disordered Heisenberg ferromagnetic binary alloy for various values of the wave vector $\vec{k}$. $x = 0.2$, $J_{AA} = 1.0$, $J_{AB} = 1.25$, $J_{BB} = 1.5$, $S_A = 0.5$ and $S_B = 1.0$.

Fig.5.2 Spin wave spectral functions for $x = 0.5$. Other parameters are same as in Fig.5.1.

Fig.5.3 Spin wave spectral functions for $x = 0.8$. Other parameters are same as in Fig.5.1.

Fig.5.4 Spin wave spectral functions for various values of wave vector $\vec{k}$. $S_A = 0.5$, $S_B = 1.0$, $J_{AA} = 1.0$, $J_{AB} = 0.75$, $J_{BB} = 0.5$ and $x = 0.4$.

Fig.5.5 Spin wave spectral functions for $J_{AA} = 1.0$, $J_{AB} = 1.25$ and $J_{BB} = 0.75$. Other parameters are same as in Fig.5.4.

Fig.5.6 Spin wave spectral functions for $J_{AB} = 0.75$, and $J_{BB} = 1.5$. Other parameters are same as in Fig.5.4.

Fig.5.7 Spin wave dispersion relations in the (111) direction for various values of impurity concentration. Other parameters are the same as in Fig.5.1.

Fig.5.8 Plot of stiffness constant vs. concentration. The broken line corresponds to Murray's results. $J_{AA} = 1.0$, $J_{AB} = 1.25$, $J_{BB} = 1.5$, $S_A = 0.5$ and $S_B = 1.0$.

Fig.5.9 Spin wave densities of states (a) $x = 0.1$, (b) $x = 0.3$, (c) $x = 0.5$, (d) $x = 0.7$ and (e) $x = 0.9$. Other parameters are the same as in Fig.5.1.

Fig.5.10 Spin wave densities of states (a) $J_{AB} = 1.25$, $J_{BB} = 1.5$, (b) $J_{AB} = 1.25$ and $J_{BB} = 0.75$, (c) $J_{AB} = 0.75$ and $J_{BB} = 0.5$. Other parameters are the same as in Fig.5.4.

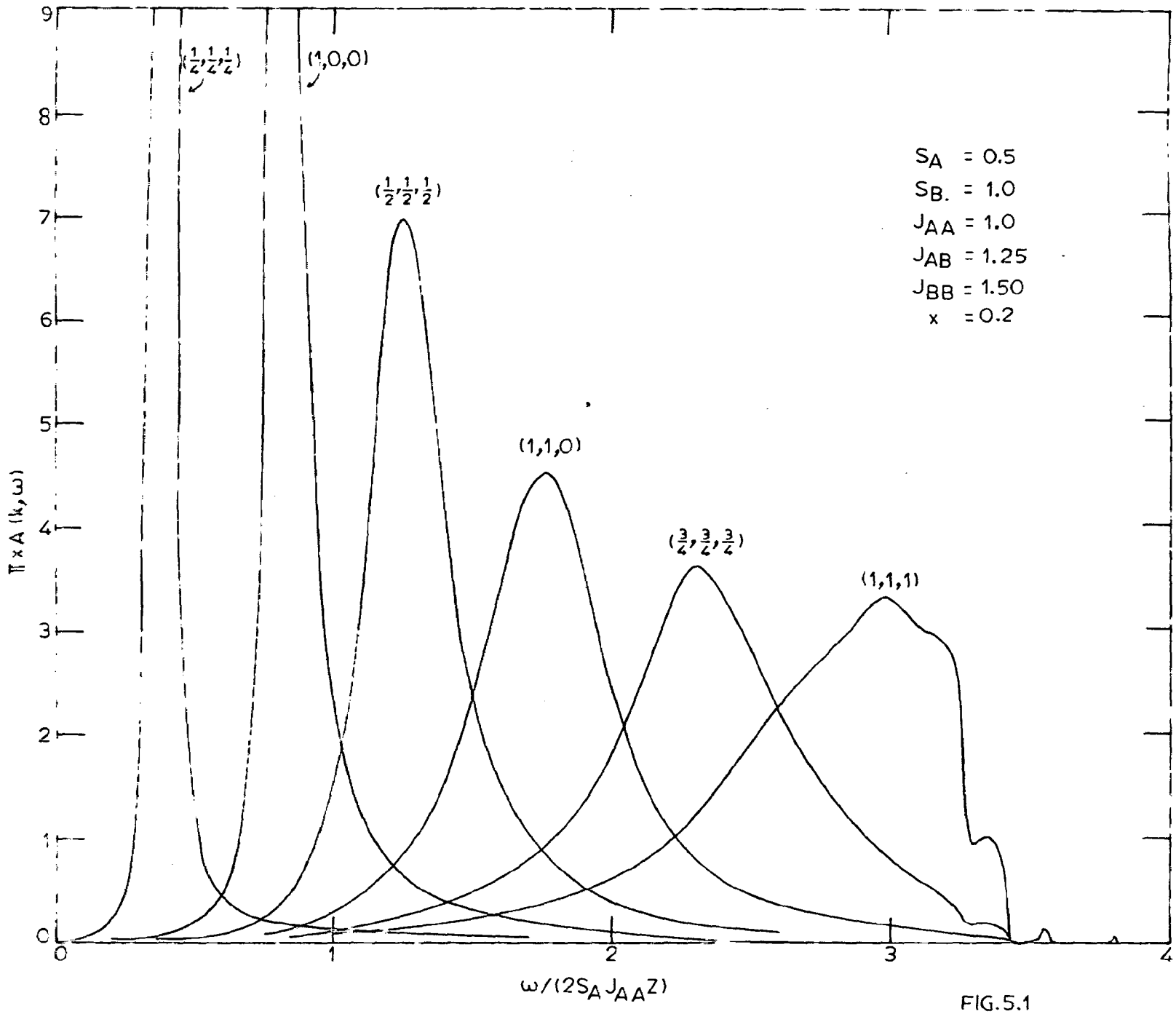
$(\frac{1}{2},\frac{1}{2},\frac{1}{2})$
(1,0,0)
$(\frac{1}{2},\frac{1}{2},\frac{1}{2})$
(1,1,0)
$(\frac{3}{4},\frac{3}{4},\frac{3}{4})$
(1,1,1)
$S_A = 0.5$
$S_B = 1.0$
$J_{AA} = 1.0$
$J_{AB} = 1.25$
$J_{BB} = 1.50$
$x = 0.2$
$\pi \times A(k,\omega)$
$\omega/(2S_A J_{AA} Z)$
0
1
2
3
4
5
6
7
8
9

FIG. 5.1

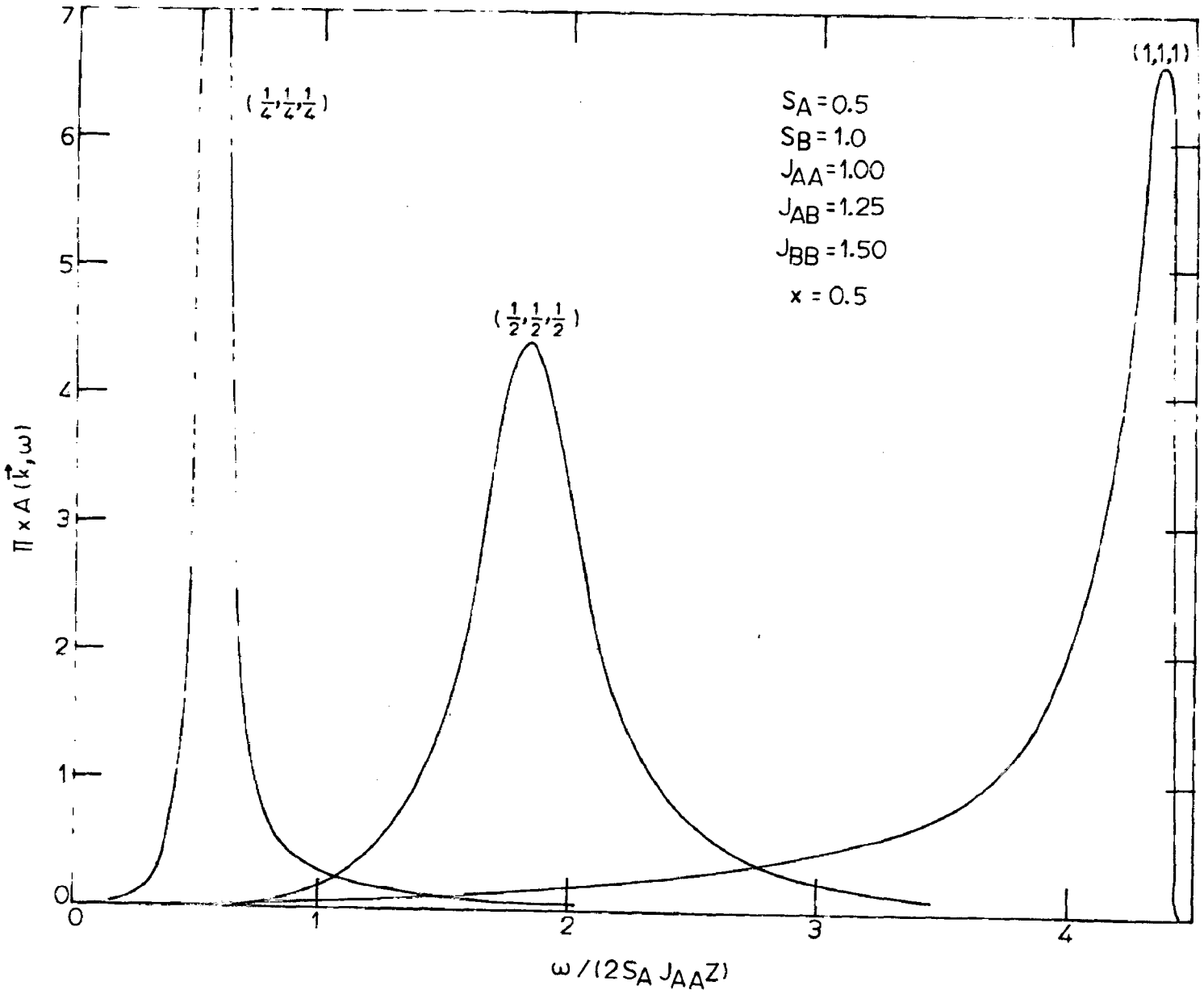
$(\frac{1}{4},\frac{1}{4},\frac{1}{4})$
$(\frac{1}{2},\frac{1}{2},\frac{1}{2})$
(1,1,1)
$S_A = 0.5$
$S_B = 1.0$
$J_{AA} = 1.00$
$J_{AB} = 1.25$
$J_{BB} = 1.50$
$x = 0.5$
$\pi \times A(\vec{k},\omega)$
$\omega/(2S_A J_{AA} Z)$
0
1
2
3
4
5
6
7

FIG. 5.2

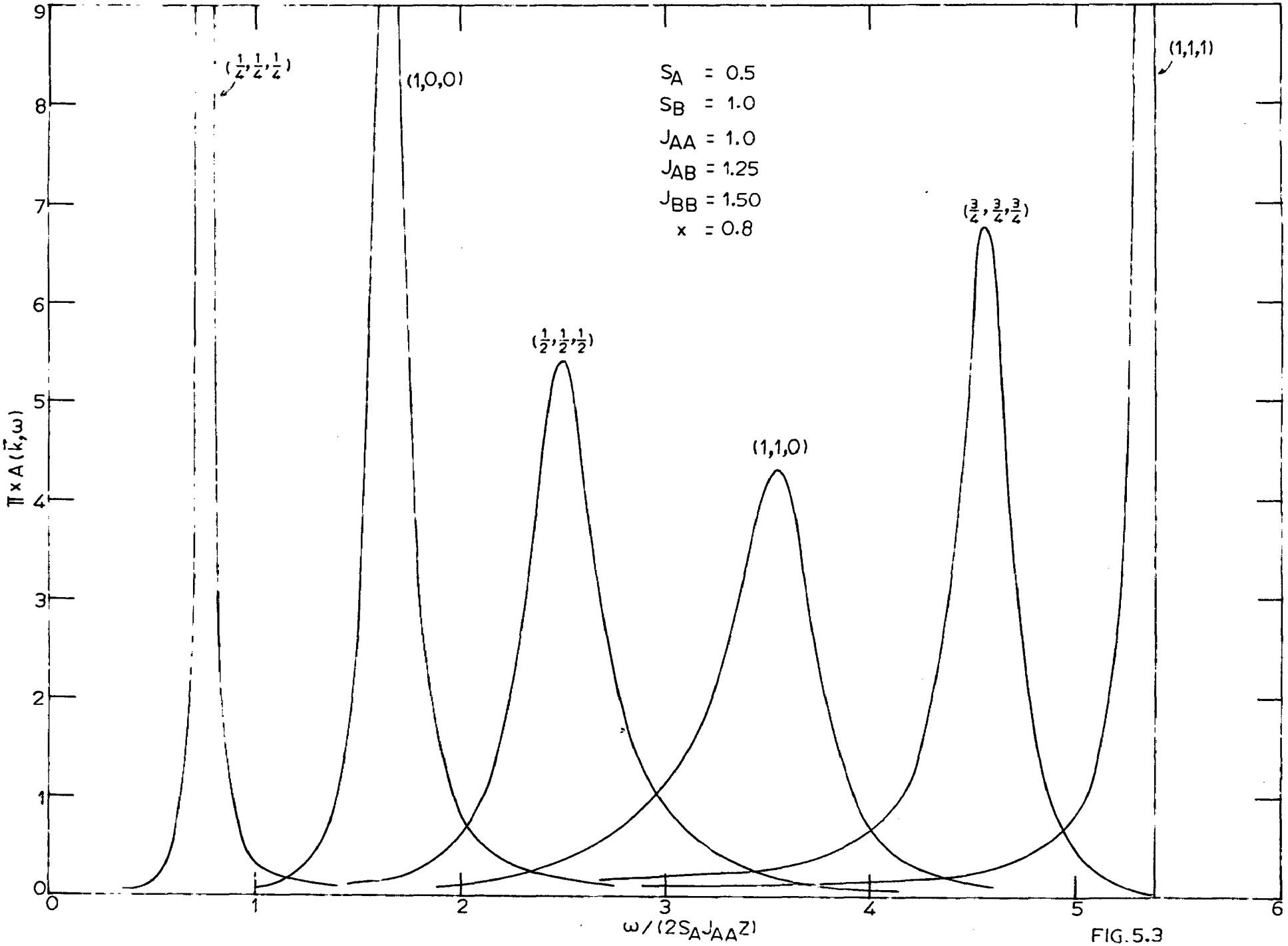
$S_A = 0.5$
$S_B = 1.0$
$J_{AA} = 1.0$
$J_{AB} = 1.25$
$J_{BB} = 1.50$
$x = 0.8$
$(\frac{1}{4},\frac{1}{4},\frac{1}{4})$
(1,0,0)
$(\frac{1}{2},\frac{1}{2},\frac{1}{2})$
(1,1,0)
$(\frac{3}{4},\frac{3}{4},\frac{3}{4})$
(1,1,1)
$\pi \times A(\vec{k},\omega)$
$\omega/(2S_AJ_{AA}Z)$
0
1
2
3
4
5
6
7
8
9

FIG. 5.3

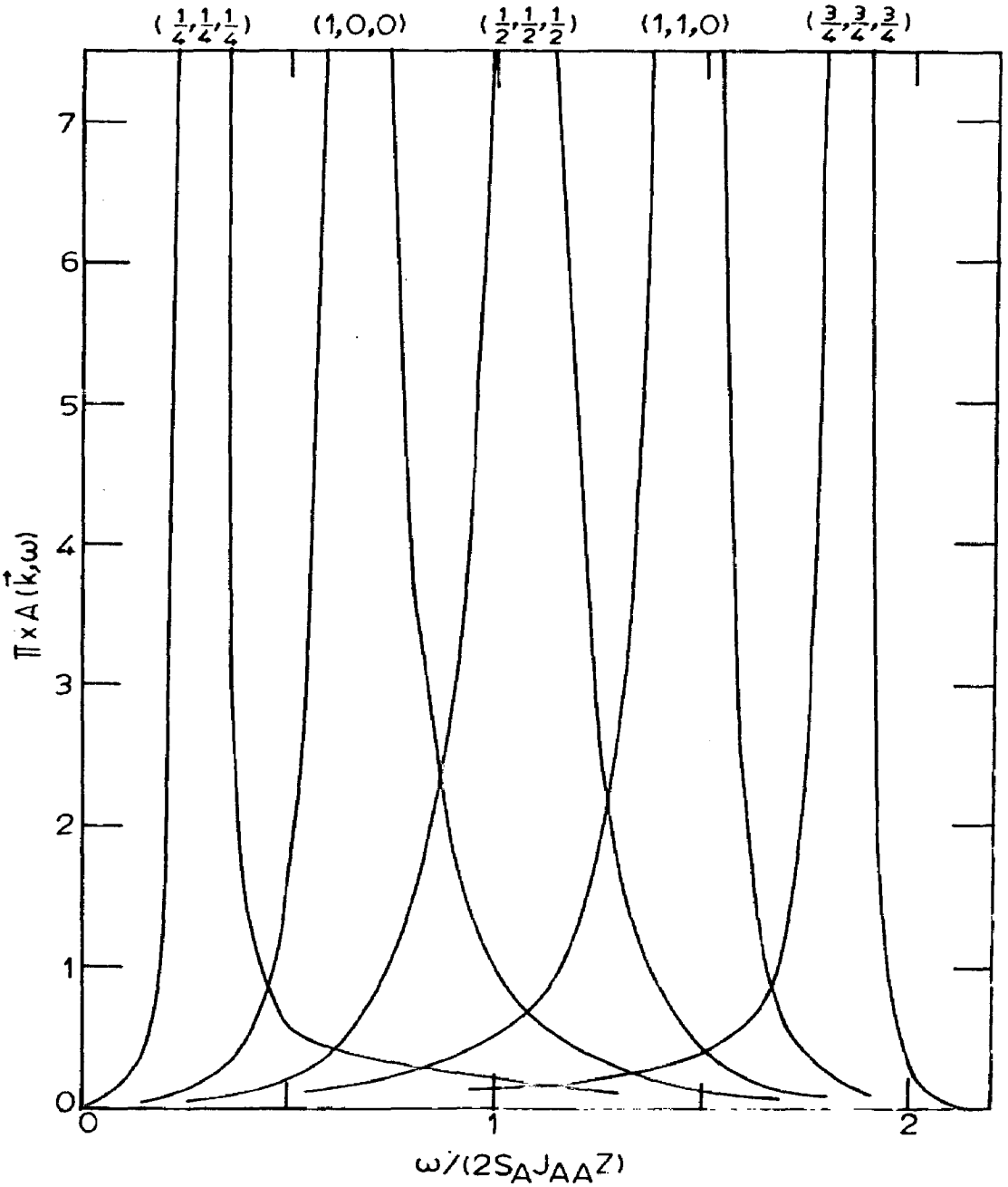
$(\frac{1}{4},\frac{1}{4},\frac{1}{4})$
(1,0,0)
$(\frac{1}{2},\frac{1}{2},\frac{1}{2})$
(1,1,0)
$(\frac{3}{4},\frac{3}{4},\frac{3}{4})$
$\pi \times A(\vec{k},\omega)$
0
1
2
3
4
5
6
7
0
1
2
$\omega/(2S_A J_{AA} z)$

FIG. 5.4

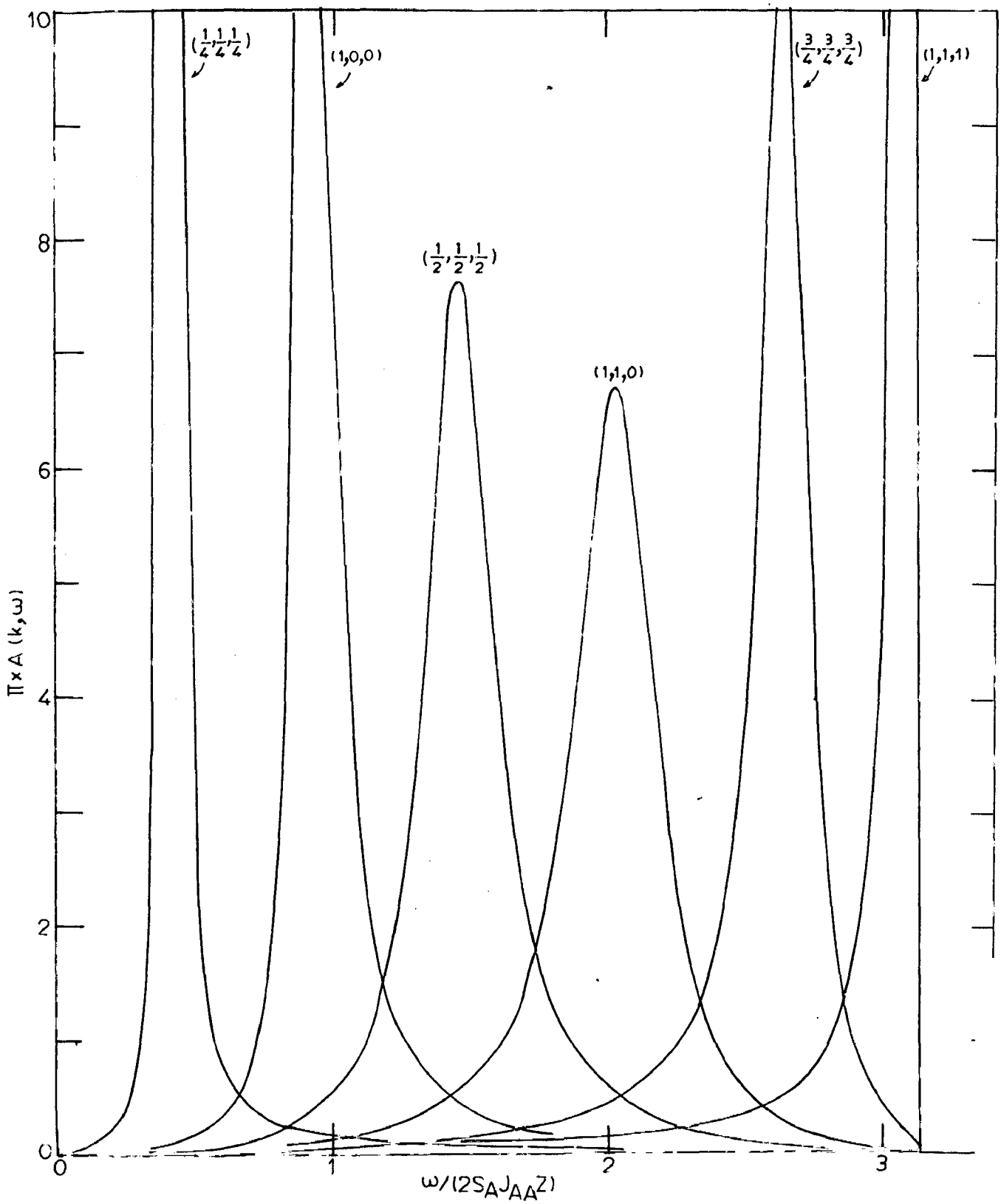
10
8
6
4
2
0
$\pi \times A(k,\omega)$
$(\frac{1}{4},\frac{1}{4},\frac{1}{4})$
(1,0,0)
$(\frac{1}{2},\frac{1}{2},\frac{1}{2})$
(1,1,0)
$(\frac{3}{4},\frac{3}{4},\frac{3}{4})$
(1,1,1)
0
1
2
3
$\omega/(2S_AJ_{AA}z)$

FIG. 5.5

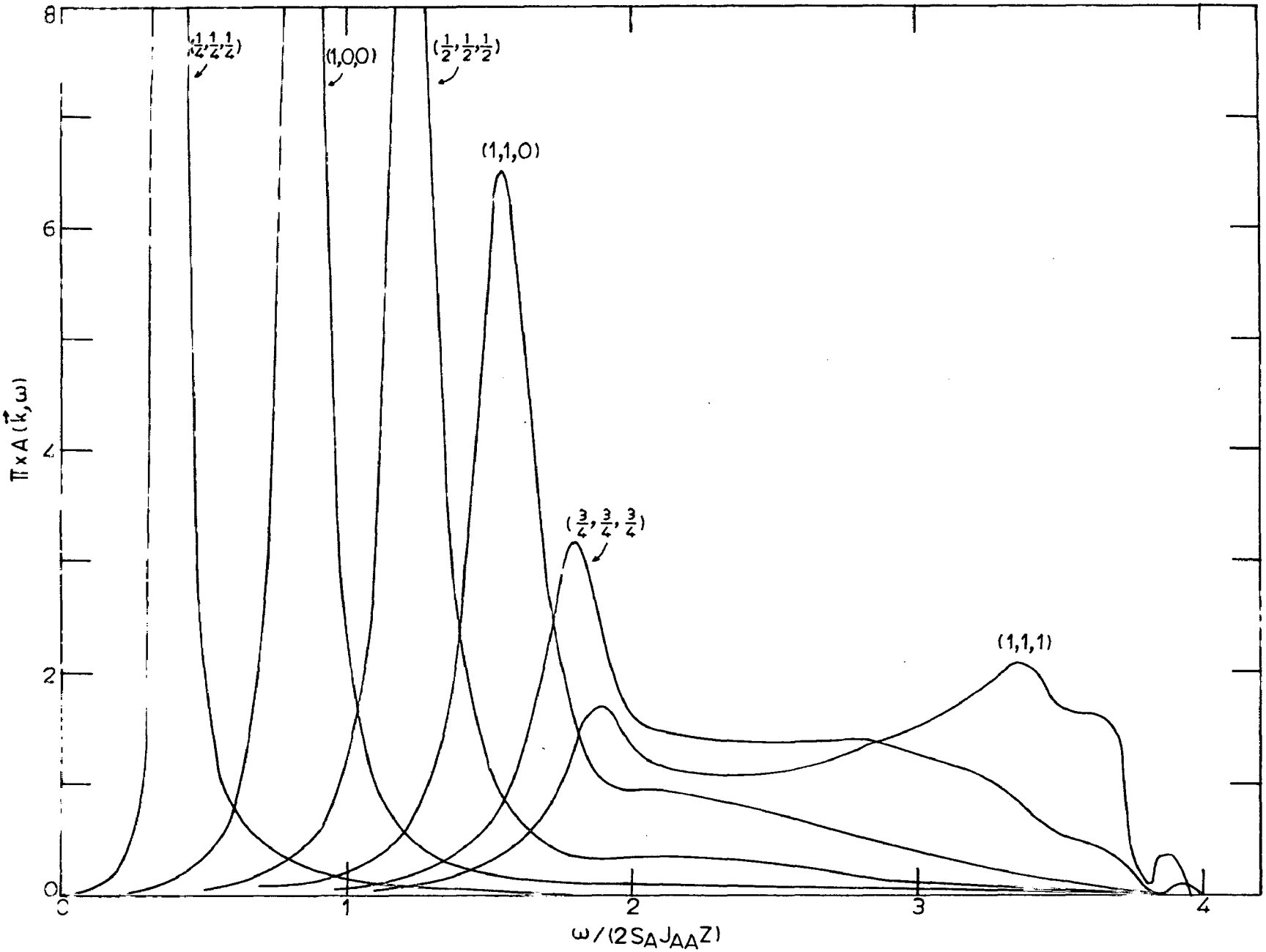
8
6
4
2
0
0
1
2
3
4
$\pi \times A(\vec{k},\omega)$
$\omega/(2S_A J_{AA} Z)$
$(\frac{1}{2},\frac{1}{2},\frac{1}{2})$
(1,0,0)
$(\frac{1}{2},\frac{1}{2},\frac{1}{2})$
(1,1,0)
$(\frac{3}{4},\frac{3}{4},\frac{3}{4})$
(1,1,1)

FIG. 5.6

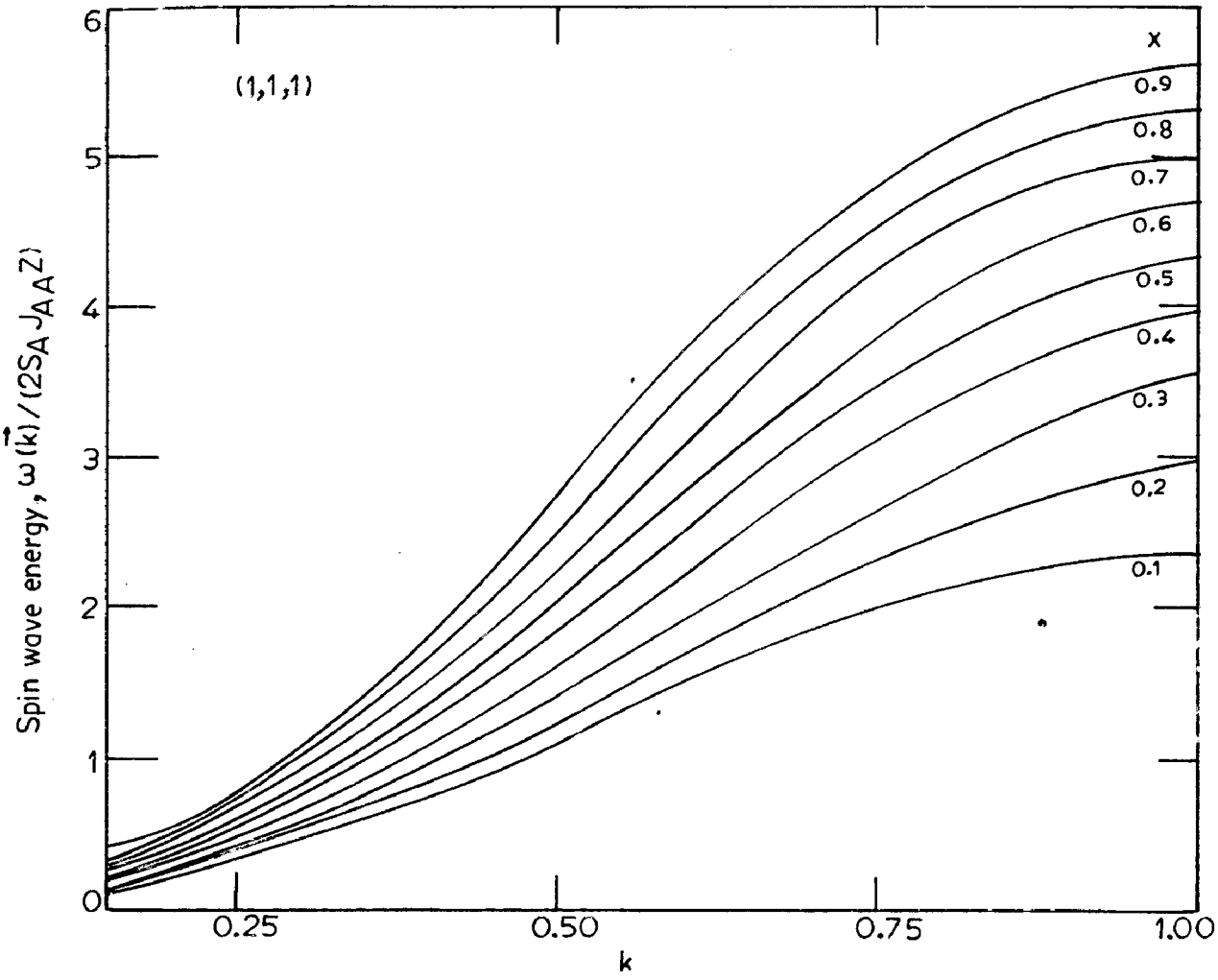
(1,1,1)
x
0.9
0.8
0.7
0.6
0.5
0.4
0.3
0.2
0.1
Spin wave energy, $\omega(\vec{k})/(2S_A J_{AA} Z)$
0
1
2
3
4
5
6
0.25
0.50
0.75
1.00
k

FIG. 5.7

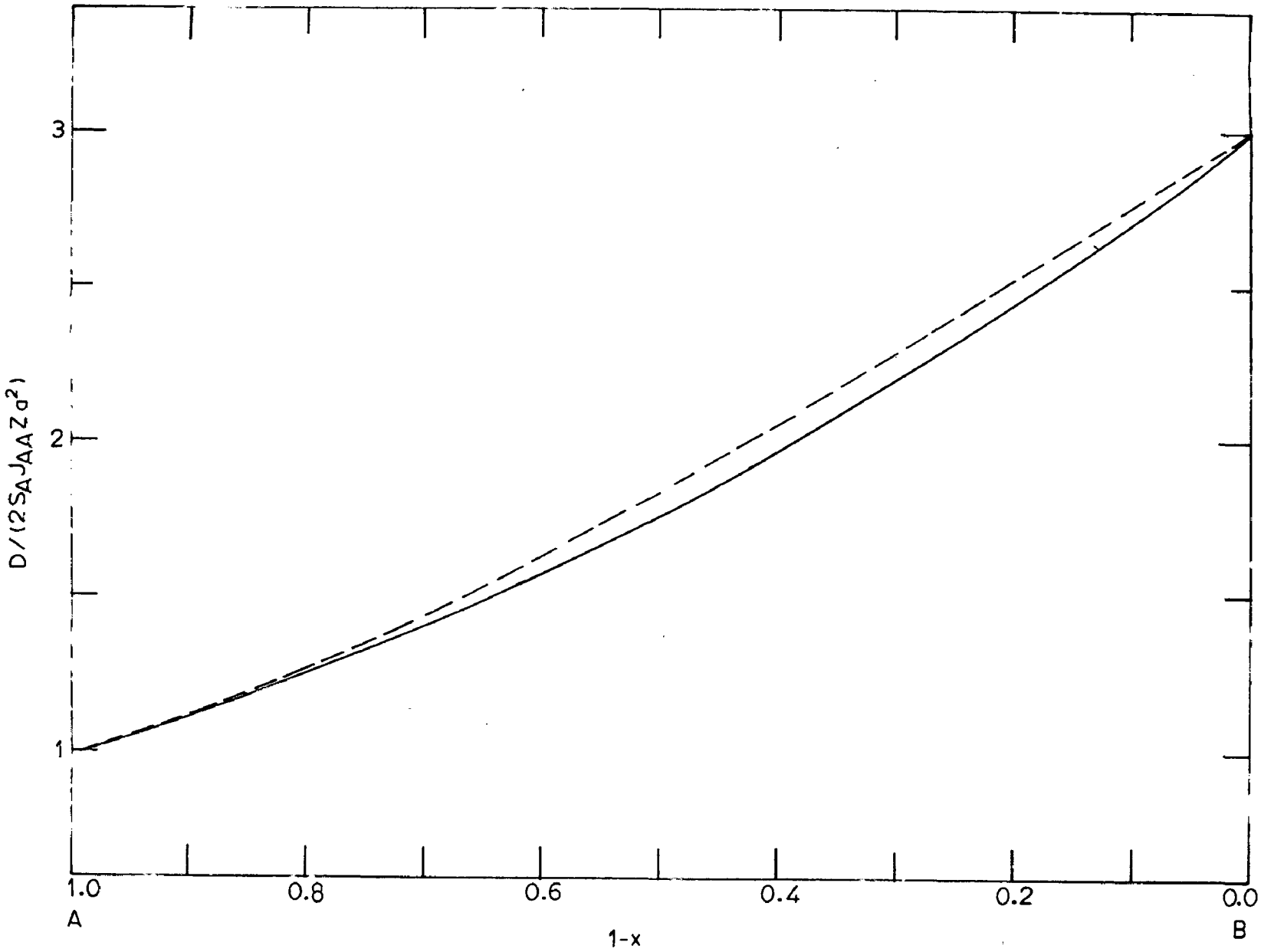

FIG. 5.8

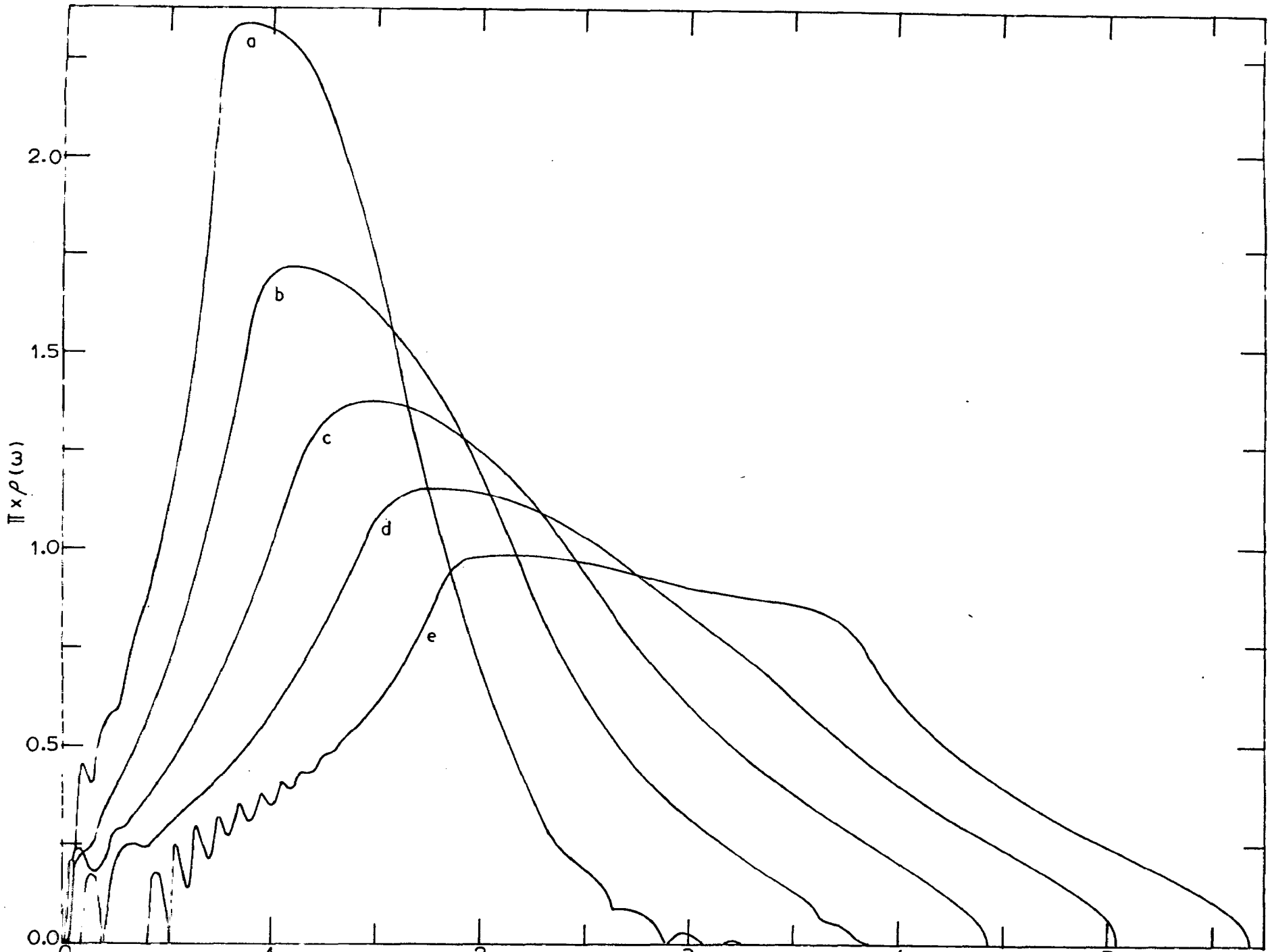

FIG. 5.9

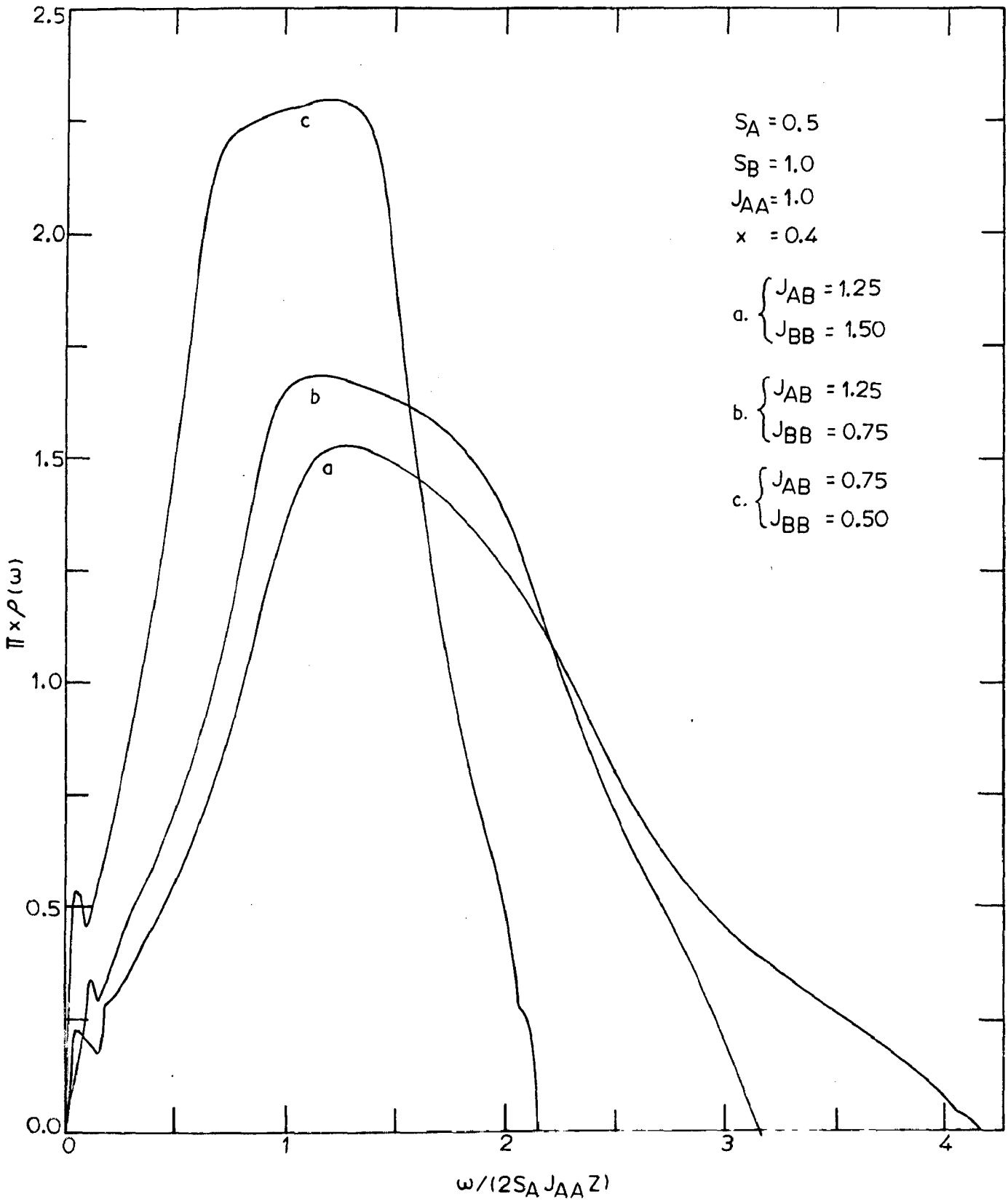
2.5
2.0
1.5
1.0
0.5
0.0
0
1
2
3
4
$\pi x \rho(\omega)$
$\omega/(2S_A J_{AA} Z)$
c
b
a
$S_A = 0.5$
$S_B = 1.0$
$J_{AA} = 1.0$
$x = 0.4$
a. $J_{AB} = 1.25$, $J_{BB} = 1.50$
b. $J_{AB} = 1.25$, $J_{BB} = 0.75$
c. $J_{AB} = 0.75$, $J_{BB} = 0.50$

FIG. 5.10

PART II

SURFACE SEGREGATION IN ALLOYS

CHAPTER VI

REGULAR SOLUTIONS

§ 6.1 The Model

We first assume that the binary alloy is a solid solution in thermodynamic equilibrium. It could be obtained, say, by first preparing the liquid alloy and then cooling it slowly, such that at every stage the solution is in equilibrium. In this process it is assumed that the surface is produced in vacuum. The presence of some environment such as the gasious environment is also considered in a heuristic manner in a later section. If a surface is produced in a solid alloy by cleavage, the question of surface relaxation of atoms poses a difficult problem. We have ignored such non-equilibrium processes.

We shall always remain above the critical order-disorder transition temperature, so that the alloy is completely random. The bulk composition is a known factor. Further, depending upon the bulk concentration and temperature, the equilibrium lattice structure is known. We assume that the surface is atomistically plane, although in reality this has been shown[186] not to be the case.

The phenomenon of surface segregation and its temperature dependence indicates that in the socalled random alloys there is a configuration dependence of internal energy. Since the short-range-order in such alloys is negligible at ordinary temperatures, the energy difference between various configurations must be small compared with thermal energy kT.

Here we assume a simple model for configuration energy. We assume that only nearest neighbour atom pairs interact and the total configuration energy may be taken as a sum of interaction energies of nearest neighbour atom pairs. A similar model has also been employed by Williams and Nason[96]. The pair energies depend only on the type of atoms occupying the pair of sites. Such a model has been extensively used[187,188] for discussing order-disorder transitions in alloys. However, the present problem is different from the usual Ising problem of order-disorder transition. We are always in the disordered regime, so the question of assigning sublattices to different components does not arise, rather we fix the overall bulk concentration by an external constraint. In the Ising model language, this external constraint is like an external magnetic field.

Let $\{N_{AA}, N_{BB}, N_{AB}\}$ denote a configuration with N_{AA}, AA pairs etc. If on the whole there are N atoms, the extrinsic configuration energy is given by

$$U_N(N_{AA}, N_{AB}, N_{BB}) = \varepsilon_{AA}N_{AA} + \varepsilon_{BB}N_{BB} + \varepsilon_{AB}N_{AB} \qquad \ldots (6.1)$$

where we have assigned energies ε_{AA} to AA pairs etc.

In general this is a degenerate state. The configuration parameters $\{N_{AA}, N_{BB}, N_{AB}\}$ are not all independent, but are related according to[189]

$$\begin{aligned} ZN_A &= 2N_{AA} + N_{AB} \\ ZN_B &= 2N_{BB} + N_{AB} \\ N &= N_A + N_B \end{aligned} \qquad \ldots (6.2)$$

where Z is the number of nearest neighbours.

Substituting back into (6.1) we get

$$U_N(N_A, N_{AA}) = (\varepsilon_{AA} + \varepsilon_{BB} - 2\varepsilon_{AB}) N_{AA} + (\varepsilon_{AB} - \varepsilon_{BB}) ZN_A + \tfrac{1}{2} Z\varepsilon_{BB} N. \qquad \ldots (6.3)$$

The last term is irrelevant because it does not depend on configurations and it can be eliminated by a suitable choice of energy origin.

Let us now divide the semi-infinite system lattice into layers parallel to our planar surface and number the layers as $\lambda = 0,1,2,\ldots\xi$, $\lambda = 0$ being the surface which we shall also call the first layer. The intrinsic assumption of our model is that the concentration varies normal to our planar surface only. This assumption is reasonable for a semi-infinite system with a planar surface. Since the environments of points on the same layer parallel to the surface are equivalent, there seems no reason why composition should vary along a layer.

Let there be N^λ sites on the λ^{th} layer of which N_A^λ, N_B^λ are occupied by A and B atoms respectively,

$$N_A^\lambda + N_B^\lambda = N^\lambda \quad ; \quad \sum_{\lambda=0}^{\xi} N^\lambda = N. \qquad \ldots (6.4)$$

A site on the λ^{th} layer has $Z_{\lambda\lambda}$ nearest neighbours on the same layer and $Z_{\lambda\mu}$ nearest neighbours on the neighbouring layer μ so that

$$Z_{\lambda\lambda} + \sum_{\mu\neq\lambda} Z_{\lambda\mu} = Z_{\lambda}. \qquad \ldots (6.5)$$

This Z_{λ} on the surface layer is different from the other lower layers. The external constraint is

$$\sum_{\lambda=o}^{\xi} N_A^{\lambda} = N_A \quad , \quad \sum_{\lambda=o}^{\xi} N_B^{\lambda} = N_B. \qquad \ldots (6.6)$$

If $N_{AA}^{\lambda\lambda}$ and $N_{AA}^{\lambda\mu}$ etc. refer to pairs in the same and adjacent layers respectively, the internal energy can be written as

$$U_N(N_A^{\lambda}, N_{AA}^{\lambda\lambda}, N_{AA}^{\lambda\mu}) = (\varepsilon_{AA} + \varepsilon_{BB} - 2\varepsilon_{AB})\Big(\sum_{\lambda=o}^{\xi} N_{AA}^{\lambda\lambda} + \frac{1}{2}\sum_{\lambda}\sum_{\mu\neq\lambda} N_{AA}^{\lambda\mu}\Big) + (\varepsilon_{AB} - \varepsilon_{BB})\sum_{\lambda=o}^{\xi} Z_{\lambda} N_A^{\lambda}. \qquad \ldots (6.7)$$

Here we have assumed that the pair bond energies ε_{AA}, ε_{AB} and ε_{BB} do not change as we move from the bulk to the surface.

Define now

$$\frac{N_A^{\lambda} - N_B^{\lambda}}{N^{\lambda}} = m_{\lambda} \Rightarrow N_A^{\lambda} = \frac{1}{2}N^{\lambda}(m_{\lambda}+1). \qquad \ldots (6.8)$$

m_{λ} is a direct measure of local concentration x_{λ} of a constituent in the λ^{th} layer by the relation

$$m_{\lambda} = 2x_{\lambda} - 1 = 1 - 2y_{\lambda}. \qquad \ldots (6.9)$$

Further the ratios

$$\frac{N_{AA}^{\lambda\lambda}}{\frac{1}{2}Z_{\lambda\lambda}N^{\lambda}} = \frac{1}{2}(\sigma_{\lambda\lambda}+1) \qquad \ldots (6.10a)$$

$$\frac{N_{AA}^{\lambda\mu}}{\frac{1}{2}Z_{\lambda\mu}(N^{\lambda}+N^{\mu})} = \frac{1}{2}(\sigma_{\lambda\mu}+1) \qquad \lambda \neq \mu \qquad \ldots (6.10b)$$

measure the fraction of AA pairs on the same layer and in two adjacent layers.

We shall now make a 'Bragg-Williams approximation' which states that the probability of finding an AA pair on neighbouring sites i and j, is the probability of independently finding an A atom each on sites i and j; the same holds for BB and AB pairs. In essence, this implies that there is no short-range-order. For binary alloys with very little short-range-order, this approximation is reasonable. The case of non-regular solutions where some short-range may exist will be treated in the next chapter. Within this approximation

$$\begin{aligned}(\sigma_{\lambda\lambda}+1) &\simeq \frac{1}{2}(m_{\lambda}+1)^2 \\ (\sigma_{\lambda\mu}+1) &\simeq \frac{1}{2}(m_{\lambda}+1)(m_{\mu}+1).\end{aligned} \qquad \ldots (6.11)$$

The set $\{m_{\lambda}\}$ now completely determines a configuration and we can write

$$U_N(\{m_{\lambda}\}) = -\frac{1}{2}\varepsilon \sum_{\lambda=0}^{\xi} \sum_{\mu=\lambda-1}^{\lambda+1} N^{\lambda}Z_{\lambda\mu}m_{\lambda}m_{\mu} - B\sum_{\lambda=0}^{\xi} N^{\lambda}Z_{\lambda}m_{\lambda} \qquad \ldots (6.12)$$

where

$$\varepsilon = \frac{1}{2}\left(\varepsilon_{AB} - \frac{\varepsilon_{AA} + \varepsilon_{BB}}{2}\right) \qquad \ldots (6.13)$$

and $$B = \frac{1}{4}(\varepsilon_{BB} - \varepsilon_{AA}). \qquad \ldots (6.14)$$

The parameters ε and B are the only parameters which are to be known in our formalism. These have simple thermodynamic interpretation. $Z\varepsilon$ may be identified with the heat of mixing, while the parameter B is related to the difference in the heats of vaporization of the two pure constituents. In the present theory $Z_m B$ where Z_m is the number of missing neighbours for the surface atoms, plays the role of the surface tension difference of the two pure metals. Thus both the parameters can, in simple cases, be estimated from the experimental data. One particular difficulty arises in cases when the atoms of the constituents being alloyed have appreciably different sizes. In such cases, the parameters B and ε will not have the above simple interpretation, but should incorporate some energy changes arising due to the size difference. Further, both the heat of mixing and the heat of vaporization are somewhat temperature dependent quantities. So their correspondence with ε and B is not quite precise.

The alloy has some crystal structure and the constituents that make up the alloys may have different crystal structures from that of the alloy. In the calculation of the surface segregation, we have to know A-A and B-B bond strengths in the alloy. These should be calculated from the heats of vaporization of the pure constituents having the alloy crystal

structure rather than the normal constituent crystal structure. Kaufmann and Bernstein[190] have calculated such heats of vaporization for a number of elements. However, most of the alloys of catalytic interest have the same structure as their constituents.

The intrinsic configuration energy per atom is given by

$$U(\{m_\lambda\}) = \sum_{\lambda=0}^{\xi} \frac{N^\lambda}{N}\left(-\frac{\varepsilon}{2}\sum_{\mu=\lambda-1}^{\lambda+1} Z_{\lambda\mu}m_\mu - BZ_\lambda\right) m_\lambda. \qquad \ldots (6.15)$$

In the thermodynamic limit $N \to \infty$, $N^\lambda \to \infty$, $\xi \to \infty$, but the sums of the type

$$\sum_{\lambda=0}^{\xi}, \quad \frac{N^\lambda}{N}\phi_\lambda$$

remain finite, since $N^\lambda/N \approx O(1/\xi)$. This configuration energy is degenerate for all configurations sharing the same $\{m_\lambda\}$. The thermodynamic probability of a configuration is given by

$$P_N(\{m_\lambda\}) = \prod_{\lambda=0}^{\xi} \frac{N^\lambda!}{\frac{1}{2}N^\lambda(1+m_\lambda)!\,\frac{1}{2}N^\lambda(1-m_\lambda)!} \qquad \ldots (6.16)$$

and is related to the intrinsic entropy

$$S(\{m_\lambda\}) = (k/N)\ln[P_N(\{m_\lambda\})] \qquad \ldots (6.17)$$

where k is the Boltzmann constant. When N^λ is very large, we may use Sterling's formula to get

$$S(\{m_\lambda\}) = -\sum_{\lambda=0}^{\xi} \frac{N^\lambda}{N}\left[k\left(\frac{1+m_\lambda}{2}\ln\frac{1+m_\lambda}{2} + \frac{1-m_\lambda}{2}\ln\frac{1-m_\lambda}{2}\right)\right] \ldots (6.18)$$

The free energy per atom in the thermodynamic limit becomes

$$F = U-TS = \underset{(\text{therm})}{\text{Limit}} \sum_{\lambda=o}^{\xi} \frac{N^{\lambda}}{N}\Big[-\frac{\varepsilon}{2}\sum_{\mu=\lambda-1}^{\lambda+1} Z_{\lambda\mu}m_{\lambda}m_{\mu} - BZ_{\lambda}m_{\lambda} + kT\Big(\frac{1+m_{\lambda}}{2}\ell n\,\frac{1+m_{\lambda}}{2} + \frac{1-m_{\lambda}}{2}\ell n\,\frac{1-m_{\lambda}}{2}\Big)\Big] . \quad \ldots (6.19)$$

The external constraint fixing the overall bulk concentration is

$$\frac{N_A-N_B}{N} = M = \sum_{\lambda=o}^{\xi} \frac{N^{\lambda}}{N} m_{\lambda}. \quad \ldots (6.20)$$

To determine the equilibrium configuration we have to minimise (6.19) with respect to $\{m_{\lambda}\}$, under the constraint (6.20). Using a Lagrangian multiplier η we obtain the $(\xi+1)$ equations

$$\tanh^{-1}m_{\lambda} = \Big(\varepsilon \sum_{\mu=\lambda-1}^{\lambda+1} Z_{\lambda\mu}m_{\mu} + BZ_{\lambda}+\eta\Big)/kT. \quad \ldots (6.21)$$

The $(\xi+2)$ equations (6.20) and (6.21) are sufficient to determine the $(\xi+2)$ variables $\{m_{\lambda}\}$ and η. The determination of the local concentrations in various layers reduces to the solution of these equations. In a semi-infinite system it is to be expected that $m_{\lambda} \to m_b$ in the bulk fairly rapidly. The Lagrangian multiplier η can rather be deduced from

$$\tanh^{-1}m_b = \Big(Z\varepsilon\, m_b + ZB + \eta\Big)/kT \quad \ldots (6.22)$$

where m_b is related to the overall bulk composition and Z describes the bulk environment. We may then put $m_{\lambda} = m_b$ for λ sufficiently large, say λ_j, and solve the set of λ_j simultaneous nonlinear equations

§ 6.2 Face-Centered Cubic Model Calculations

To illustrate our theory we performed numerical calculations on a face centered cubic lattice. To begin with we assume that m_λ approaches m_b, the bulk value, rather fast. This will be justified later by our numerical results. Considering the concentration variation in the first three layers we can write equations (6.20) and (6.21) as

$$\tanh^{-1}m_o = (\varepsilon m_o Z_L + \varepsilon m_1 Z_{IL} + BZ_o + \eta)/kT$$

$$\tanh^{-1}m_1 = (\varepsilon m_1 Z_L + \varepsilon m_2 Z_{IL} + \varepsilon m_o Z_{IL} + BZ + \eta)/kT$$

$$\tanh^{-1}m_2 = (\varepsilon m_1 Z_{IL} + \varepsilon m_2 Z_L + \varepsilon m_b Z_{IL} + BZ + \eta)/kT$$

$$\tanh^{-1}m_b = (\varepsilon m_b Z + ZB + \eta)/kT \qquad \ldots (6.23)$$

where we have defined Z_L and Z_{IL} respectively to be the number of nearest neighbours in a layer and in two neighbouring layers (IL stands for interlayer). When $m_b = \pm 1$ i.e. for a pure solid ($x = 0$ or $y = 0$), it is easy to check that all $m_\lambda = \pm 1$ as it should be. For $-1 < m_b < 1$ these equations are solved for three surfaces (100), (110) and (111) of a face centered cubic lattice. The results are shown in figures 6.1-6.5. In figure 6.1 we have plotted the first layer composition m_o against m_b for different values of temperature. ε and B are chosen such that $\varepsilon/k = 10$ K and $B/k = 75$ K. For ideal solutions ε is zero and in this case the alloy composition differs only in the first layer. The broken straight line in the graphs denotes that the bulk and the surface compositions are the same. Since B is positive, the pair bond

in the second, third and further layers as well. In figure 6.5 we have studied the behaviour of varying B on the (111) face at T = 773 K. As the value of B/k is increased from 75 to 122 K segregation of the B component increases at the surface. We have not plotted the composition in the second and the third layers for all the cases studied here because these are only a little different from the bulk.

§ 6.3 Chemisorption and Surface Relaxation Effects

a. Chemisorption

So far we have considered the solid binary alloy with the surface contiguous to vacuum (clean surfaces). If the alloy is prepared in the presence of some gas, e.g. O,H,S, CO etc., then chemical adsorption of the molecules of the gas will take place on the alloy surface. As discussed in the introduction, this can change the surface composition very much. We can extend the formalism of Sec. 6.1 to take in account this effect easily. Let Z_A and Z_B be the coordination number of the A and B atoms at the surface with the chemisorbed species M. If ε_{AM} and ε_{BM} are the pair bond energies of the A-M and the B-M bonds respectively, then the internal energy can be written as

$$U_N(\{N_A^\lambda,\ N_{AA}^{\lambda\lambda},\ N_{AA}^{\lambda\mu}\}) = \Big[\sum_{\lambda=0}^{\xi} N_{AA}^{\lambda\lambda} + \frac{1}{2}\sum_{\lambda=0}^{\xi}\sum_{\substack{\mu=\lambda-1\\ \mu\neq\lambda}}^{\lambda+1} N_{AA}^{\lambda\mu}\Big](\varepsilon_{AA}+\varepsilon_{BB}-2\varepsilon_{AB})$$

$$+(\varepsilon_{AB}-\varepsilon_{BB})\sum_{\lambda=0}^{\xi} Z_\lambda N_A^\lambda + \varepsilon_{AM} Z_A N_A^o + \varepsilon_{BM} Z_B N_B^o. \qquad \ldots (6.24)$$

Proceeding parallel to the procedure of Section § 6.1 we shall obtain the following final form for U_N

$$U_N(\{m_\lambda\}) = \sum_{\lambda=0}^{\xi} \frac{N^\lambda}{N}\left[-\frac{\varepsilon}{2}\sum_{\mu=\lambda-1}^{\lambda+1} Z_{\lambda\mu} m_\lambda m_\mu - BZ_\lambda m_\lambda\right] - \frac{1}{2}(\varepsilon_{BM}Z_B - \varepsilon_{AM}Z_A)\frac{N^o}{N} m_o. \quad \ldots (6.25)$$

In this expression we have again dropped the constant terms. Now minimizing the free energy with the help of the Lagrangian multiplier we obtain a set of four equations. The first is

$$\tanh^{-1} m_o = [\varepsilon m_o Z_L + \varepsilon m_1 Z_{IL} + BZ_o + (\varepsilon_{BM}Z_B - \varepsilon_{AM}Z_A)/2 + \eta]/kT \quad \ldots (6.26)$$

and the remaining three are the same as in equation (6.23).

In our calculations we have taken $Z_A = Z_B = Z_{IL}$ and defining $X = (\varepsilon_{BM} - \varepsilon_{AM})/2K$ the surface concentration against the bulk concentration is plotted in figure 6.6 for two values of X. The central full curve corresponds to the clean surface. For positive values of X we see that the surface segregation decreases whereas for negative values of X, it increases. It can be understood easily because when X is positive, then the ε_{AM} bond is stronger than the ε_{BM} bond and therefore it tries to drive more A atoms on the surface and therefore the net effect is a reduction in the surface concentration of B atoms. The reverse of this statement is true for a case where X is negative.

b. Surface relaxation

In the derivation of equation (6.21) it was assumed that the pair bond energies do not change as we move from the bulk to the surface. In practice there may be surface relaxation effects which will change the pair bond energies of the atoms in the regime of the surface. Here we shall assume that only atoms on the surface layer are affected. If the fractional change in all the pair bond energies is denoted by a relaxation parameter δ, then the first equation in the set of equations (6.23) will become

$$\tanh^{-1} m_o = [\bar{\varepsilon}(1+\delta) m_o Z_L + \varepsilon m_1 Z_{IL} + B(1+\delta) Z_L + BZ_{IL} + \eta]/kT. \quad \ldots (6.27)$$

The remaining three equations will be unchanged. The surface composition has been calculated with 15% surface relaxation in the pair bond energies and is shown in figure 6.7. The parameter δ can be either positive or negative. For positive δ the surface segregation effect is reduced whereas for negative δ, the segregation at the surface increases. The surface relaxation also affects the second layer composition but the change is very small and we have not plotted it in the figure.

§6.4 Application to Ni-Au System

Williams and Boudart[78] have studied the surface composition of the Ni-Au system by Auger-electron spectroscopy. Their experimental results reflect the segregation of gold at the surface of the Ni-Au solid solution. Our calculation give results which agree with these experiments and are shown in

figures 6.8 and 6.9. The parameters ε/kT and B/kT were calculated from data tabulated by Hultgren et al[191] and have the values -0.075 and 0.3083 respectively. We have calculated surface composition for (111), (110) and (100) faces of Ni-Au system. Maximum segregation occurs at the (110) face. The compositions in the second and third layers also differ from the bulk composition and are shown in figure 6.8. In the first layer segregation of Au occurs whereas in the second layer Ni content is greater than in the bulk. This is because ε now has a negative value which means that the Ni-Au bond is stronger and therefore the excess of Au atoms in the first layer pulls Ni atoms in the second layer and we obtain an excess of Ni atoms in the second layer. The change in the third layer is not appreciable. We have not shown the experimental points of Williams and Boudart[78] since they have not mentioned the surface which they have studied. They have also reported that oxygen or hydrogen chemisorption on the sample leads to Ni-enrichment at the surface. Since the oxygen-nickel or hydrogen-nickel bond is stronger than oxygen-gold or hydrogen-gold bond respectively, we can argue on the basis of our results of §6.3a that nickel enrichment should occur at the surface.

§ 6.5 Discussion

The results of the earlier sections show that this simple model can explain the important and broad features of the phenomenon of surface segregation. Clearly the model is only qualitative and for any real system such simplistic assumptions

about configuration energy will not suffice. It is quite conceivable that the bond energies themselves are composition dependent. The thermodynamic data[101] on heat of mixing for several alloys like Au-Ni, Ni-Pt etc. indicate that the present model is fairly reasonable, while for several other alloys more complex behaviour is observed. It is not unlikely that even some of the other features may be understood by including (i) interactions among second nearest and farther atoms and (ii) improving upon the statistical calculation of entropy. This has been studied in the next chapter where we have applied the Bethe-Peierls approximation to calculate the free energy. In this approximation we can consider the short-range-order that may be present in the bulk alloy and its influence on the surface composition. When the atomic size difference is significant, in our formalism, we shall have to adjust the parameters B and ε, to incorporate the size aspect. This only shows that the thermodynamic calculation of the parameters ε and B, as mentioned in § 6.1 is not always reliable.

A more basic question is concerned with the pair bonding assumption involved in the calculation of configuration energy. When can such an approach be justified on microscopic principles? Such a question can be investigated by considering a simple tight binding model description for the alloys.

FIGURE CAPTIONS

Fig.6.1 First layer composition against the bulk composition for different temperatures on (a) (100) face, (b) (110) face and (c) (111) face of an FCC lattice. The broken line corresponds to no segregation. $B/k = 75$ K and $\varepsilon/k = 10$K.

Fig.6.2 Comparison of the first layer composition on the (110), (——); (100), (---); and (111), (—·—·—) faces. T = 600 K, $B/k = 75$ K and $\varepsilon/k = 10$K.

Fig.6.3 Variation of composition on the first (——) and second (---) layers of the (110) face with the bulk composition. T = 600 K, $B/k = 75$K and $\varepsilon/k = 10$K. (— —) corresponds to no segregation.

Fig.6.4 Plots of $\ell n\left[(x^s/y^s)/(x^b/y^b)\right]$ against 1/T for (110), (—·—·—); (100), (---) and (111), (——) surfaces. The bulk composition for all surfaces is fixed at $m_b = 0.5$, $B/k = 75$ K, $\varepsilon/k = 10$K.

Fig.6.5 Composition on the first layer of (111) face for various values of B/k. T = 773 K, $\varepsilon/k = 10$K.

Fig.6.6 First layer composition of (111) face against bulk composition. (——), clean surface; (——), X = -30K; (—·—·—), X = 30K. $B/k = 122$K, T = 773K and $\varepsilon/k = 10$K.

Fig.6.7 Surface relaxation effects on the composition of the first layer of (111) face (——), clean surface with no surface relaxation; (——), $\delta = -0.15$; (—·—·—), $\delta = 0.15$, $B/k = 122$K, T = 773K and $\varepsilon/k = 10$K.

Fig.6.8 Variation of the composition in the first three layers on the (100) face with the bulk composition of Ni-Au alloys. (---) corresponds to no segregation.

Fig.6.9 The first layer composition on the (111), (—·—·—); (100), (——) and (110), (---) faces of Ni-Au alloys. The surface is assumed to be clean

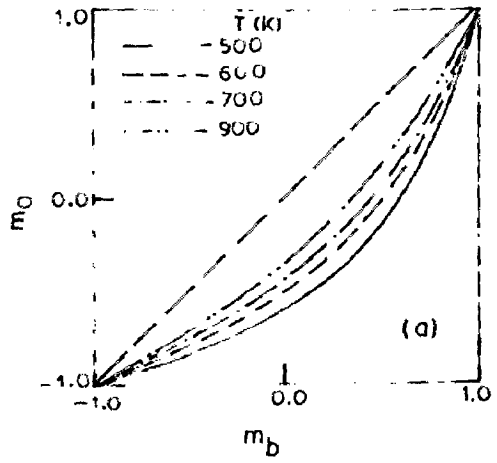

FIG. 6.1

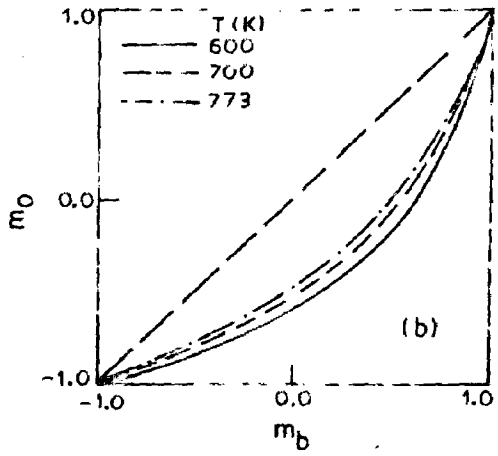

FIG. 6.1

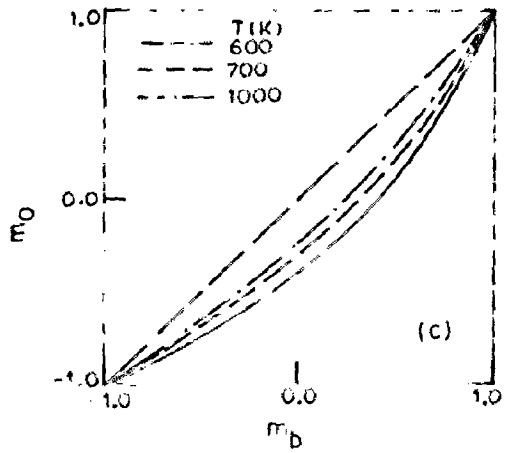

FIG. 6.1

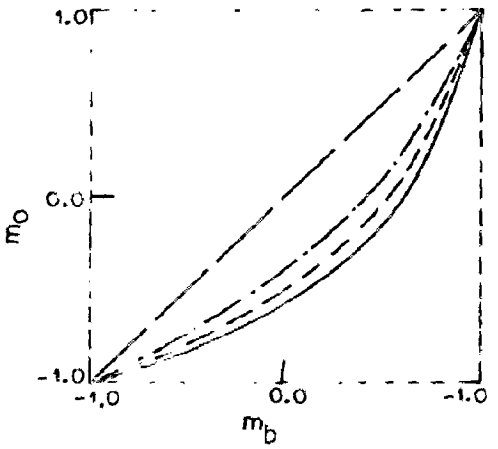

FIG. 6.2

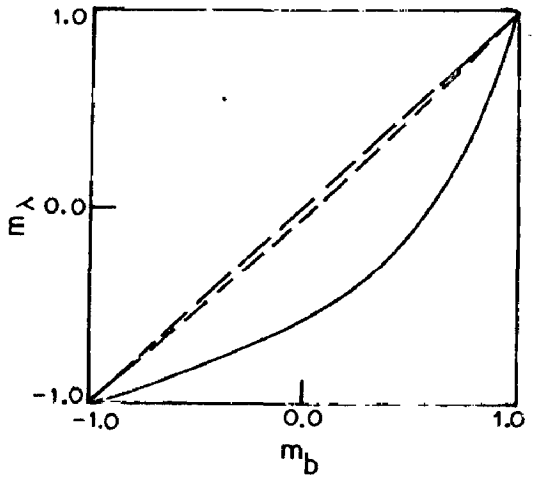

FIG. 6.3

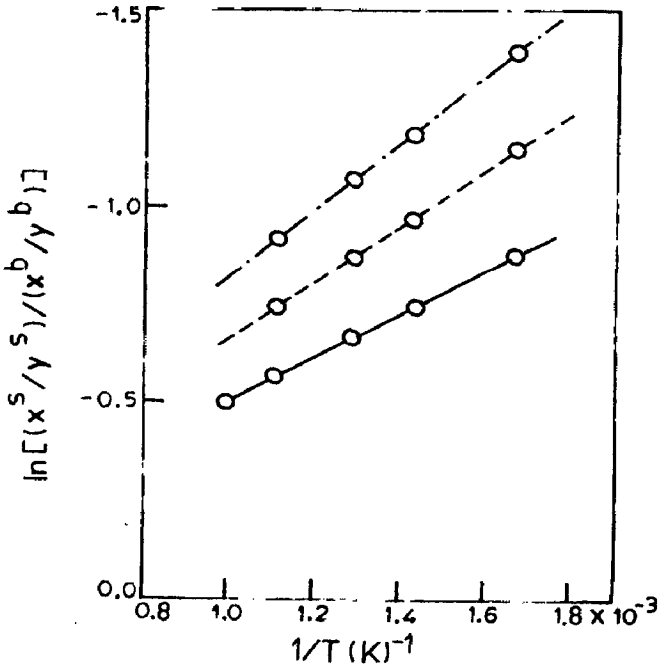

FIG. 6.4

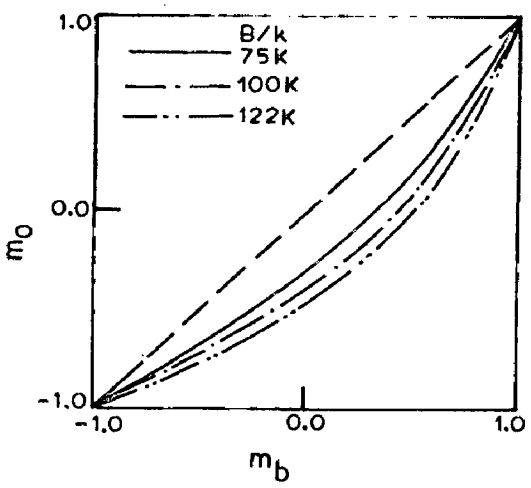

FIG. 6.5

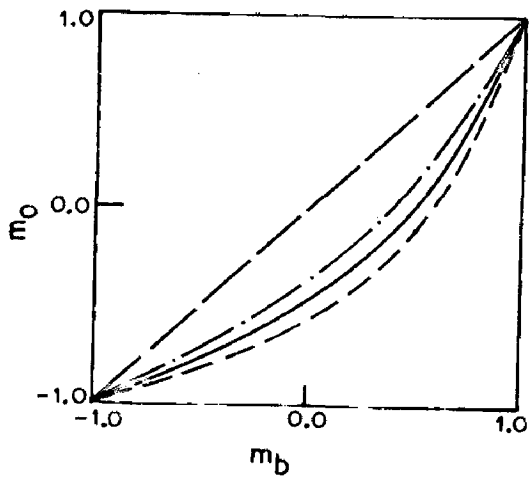

FIG. 6.6

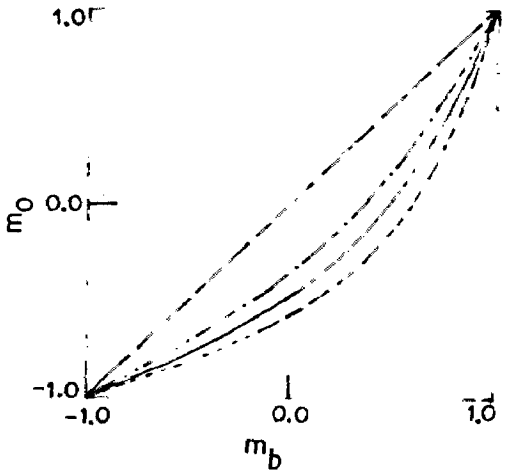

FIG. 6.7

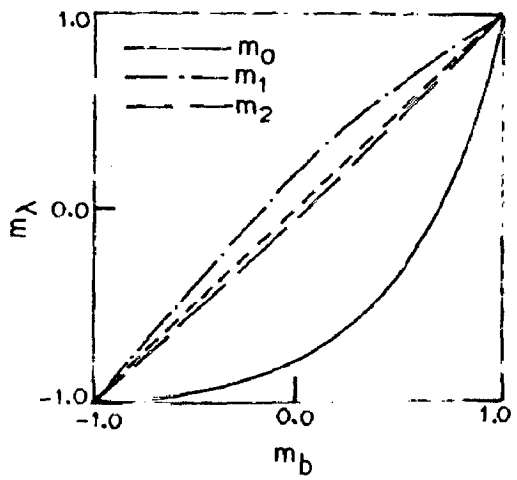

FIG. 6.8

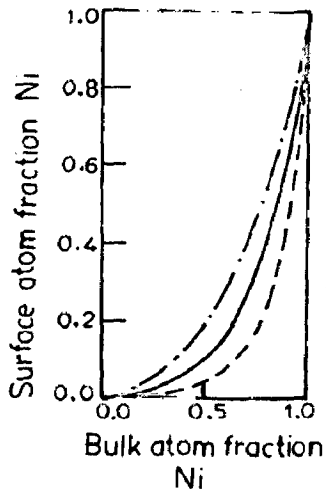

FIG. 6.9

CHAPTER VII

NON-REGULAR SOLUTIONS

Almost all the theories of surface segregation todate assume an alloy to be either an ideal solution or a regular-solution. In many cases this gives a reasonably good agreement with the experiments. But most solutions do not fall into the category of either ideal or regular solutions. From the phase diagrams of entropy and free energy of various metallic alloys, it has been observed that the excess entropy of mixing and the heat of formation are nonzero for these solutions. This suggests that there is deviation from perfect randomness of the distribution of atoms in the system, and there exist some short-range-order. There is experimental evidence based on diffuse X-ray scattering which shows that there is considerable short-range-order in many alloys.

This ordering phenomena is more likely in alloys whose constituents have significantly different atomic radii because this leads to excess thermodynamic quantities. Further for alloys having short-range-order, the parameter ε is not a constant but changes with concentration and temperature. We have extended our formulation of Chapter VI for non-regular solutions. We have introduced surface short-range-order parameters which will in general be different from their bulk value. These can be determined with a knowledge of bulk thermodynamic data. We have taken into account the temperature and concentration dependence of the parameter ε using the method

of Averbach[192]. In this way we are able to take into account to some extent the vibrational contribution to free energy, which are otherwise neglected in the model.

§ 7.1 General Formulation

We consider a semi-infinite solid binary alloy in thermodynamic equilibrium. The configuration energy is still given by equation (6.1). We again divide the system into layers parallel to the planar surface and number the layers $\lambda = 0,1,2,\ldots\xi$ as before. Using the notations of the last chapter, the relations (6.2) can be generalized as follows for surfaces:

$$Z_{\lambda\lambda}N_A^\lambda = 2N_{AA}^{\lambda\lambda} + N_{(AB)}^{\lambda\lambda} \quad \ldots (7.1a)$$

$$Z_{\lambda\lambda}N_B^\lambda = 2N_{BB}^{\lambda\lambda} + N_{(BA)}^{\lambda\lambda} \quad \ldots (7.1b)$$

$$Z_{\lambda\mu}N_A^\lambda = N_{AA}^{\lambda\mu} + N_{AB}^{\lambda\mu} \quad \ldots (7.1c)$$

$$Z_{\lambda\mu}N_B^\lambda = N_{BB}^{\lambda\mu} + N_{BA}^{\lambda\mu} \quad \ldots (7.1d)$$

Here (AB) denotes pairs of both the types AB and BA. Next we introduce the short-range-order parameters in the usual manner of solid solution theory. We write

$$N_{(AB)}^{\lambda\lambda} = 2x_\lambda y_\lambda \alpha_\lambda N^{\lambda\lambda} \quad \ldots (7.2a)$$

$$N_{AA}^{\lambda\lambda} = x_\lambda(1-\alpha_\lambda y_\lambda)N^{\lambda\lambda} \quad \ldots (7.2b)$$

$$N_{BB}^{\lambda\lambda} = y_\lambda(1-\alpha_\lambda x_\lambda)N^{\lambda\lambda}, \quad \ldots (7.2c)$$

where $x_\lambda = N_A^\lambda/N^\lambda$ and $y_\lambda = N_B^\lambda/N^\lambda$. α_λ is the short-range-order parameter for the λ^{th} layer. It will vary from layer to layer. Since the concentration x_λ is to vary with λ, we shall require

two more short-range-order parameters to obtain similar expressions for interlayer pairs. Thus we have

$$N_{AB}^{\lambda\lambda+1} = x_\lambda y_{\lambda+1}\beta_\lambda N^{\lambda\ \lambda+1} \qquad \ldots (7.3a)$$

$$N_{BA}^{\lambda\lambda+1} = y_\lambda x_{\lambda+1}\beta'_\lambda N^{\lambda\ \lambda+1} \qquad \ldots (7.3b)$$

$$N_{AA}^{\lambda\lambda+1} = x_\lambda(1-\beta_\lambda y_{\lambda+1}) N^{\lambda\ \lambda+1} \qquad \ldots (7.3c)$$

$$N_{BB}^{\lambda\lambda+1} = y_\lambda(1-\beta'_\lambda x_{\lambda+1}) N^{\lambda\ \lambda+1} \qquad \ldots (7.3d)$$

Here β_λ is the short-range-order parameter associated with the probability of finding a B atom in the $(\lambda+1)$th layer nearest neighbour to an A atom in the λ^{th} layer. whereas β'_λ is the short-range-order parameter associated with the probability of finding an A atom in the $(\lambda+1)^{th}$ layer nearest neighbour to a B atom in the λ^{th} layer. As the concentration in various layers is different, these two parameters have different values, but we shall see that these are not independent. The relation between them follows from the constraint.

$$N_{AA}^{\lambda\lambda+1} + N_{BA}^{\lambda\lambda+1} = Z_{IL} N_A^{\lambda+1} . \qquad \ldots (7.4)$$

This can be simplified using the definitions (7.3) to obtain

$$x_\lambda - x_{\lambda+1} = x_\lambda y_{\lambda+1}\beta_\lambda - y_\lambda x_{\lambda+1}\beta'_\lambda . \qquad \ldots (7.5)$$

The configuration energy (6.1) can now be expressed in terms of layer parameters

$$\begin{aligned} U_N = {} & \varepsilon_{AA} \sum_{\lambda=0}^{\xi} (N_{AA}^{\lambda\lambda} + N_{AA}^{\lambda\lambda+1}) \\ & + \varepsilon_{AB} \sum_{\lambda=0}^{\xi} (N_{(AB)}^{\lambda\lambda} + N_{AB}^{\lambda\lambda+1} + N_{BA}^{\lambda\lambda+1}) \\ & + \varepsilon_{BB} \sum_{\lambda=0}^{\xi} (N_{BB}^{\lambda\lambda} + N_{BB}^{\lambda\lambda+1}) . \end{aligned} \qquad \ldots (7.6)$$

Now using the definitions (7.2) and (7.3) this can be easily reduced to the following form

$$U_N(\{N_A^\lambda, N_{AA}^{\lambda\lambda}, N_{AA}^{\lambda\lambda+1}\}) = (\varepsilon_{AA} + \varepsilon_{BB} - 2\varepsilon_{AB}) \sum_{\lambda=0}^{\xi} (N_{AA}^{\lambda\lambda} + N_{AA}^{\lambda\lambda+1}) + (\varepsilon_{AB} - \varepsilon_{BB}) \sum_{\lambda=0}^{\xi} (Z_{\lambda\lambda} N_A^\lambda + Z_{\lambda\lambda+1} N_A^\lambda + Z_{\lambda\lambda+1} N_A^{\lambda+1}) . \quad \ldots (7.7)$$

Here again we have dropped the constant terms. Now using the relations (7.2b), (7.3c) and the fact that $N_A^\lambda = x_\lambda N^\lambda$ we can rewrite (7.7) in the form

$$U_N(\{x_\lambda, \alpha^\lambda, \beta_\lambda\}) = 2\varepsilon \sum_{\lambda=0}^{\xi} \{Z_{\lambda\lambda} x_\lambda y_\lambda \alpha_\lambda N^\lambda + Z_{\lambda\lambda+1} N^\lambda (x_\lambda y_{\lambda+1} \beta_\lambda + x_{\lambda+1} y_\lambda \beta_\lambda')\} - 2B \sum_{\lambda=0}^{\xi} N^\lambda (Z_{\lambda\lambda} x_\lambda + Z_{\lambda\lambda+1} x_\lambda + Z_{\lambda\lambda+1} x_{\lambda+1}), \quad \ldots (7.8)$$

where the expressions for ε and B are given by (6.13) and (6.14) respectively.

The configurational entropy is given by (6.17), but now the thermodynamic probability of a configuration is given by

$$P_N = \prod_{\lambda=0}^{\xi} \frac{N^{\lambda\lambda}!}{N_{AA}^{\lambda\lambda}!\, N_{AB}^{\lambda\lambda}!\, N_{BA}^{\lambda\lambda}!\, N_{BB}^{\lambda\lambda}!} \times \frac{N^{\lambda\lambda+1}!}{N_{AA}^{\lambda\lambda+1}!\, N_{AB}^{\lambda\lambda+1}!\, N_{BA}^{\lambda\lambda+1}!\, N_{BB}^{\lambda\lambda+1}!} \times \left(\frac{N_A^\lambda!\, N_B^\lambda!}{N^\lambda!}\right)^{Z_\lambda - 1}, \quad \ldots (7.9)$$

where Z_λ denotes the number of nearest neighbours of an atom in the λ^{th} layer. The configurational entropy is therefore

$$S = \frac{k}{N}\Big[\sum_{\lambda=o}^{\xi} \ell n\, N^{\lambda\lambda}! + \ell n\, N^{\lambda\lambda+1}! + \ell n\, A_\lambda - \ell n\, N_{AA}^{\lambda\lambda}!$$

$$- \ell n\, N_{AB}^{\lambda\lambda}! - \ell n\, N_{BA}^{\lambda\lambda}! - \ell n\, N_{BB}^{\lambda\lambda}! - \ell n\, N_{AA}^{\lambda\lambda+1}!$$

$$- \ell n\, N_{AB}^{\lambda\lambda+1}! - \ell n\, N_{BA}^{\lambda\lambda+1}! - \ell n\, N_{BB}^{\lambda\lambda+1}!\Big]$$

where $A_\lambda = \left(\frac{N_A^\lambda!\, N_B^\lambda!}{N^\lambda!}\right)^{Z_\lambda - 1}$.

In the limit of large N^λ, $N^{\lambda\lambda}$, $N^{\lambda\lambda+1}$, we can use the Sterling's approximation to write

$$S = k\sum_{\lambda=o}^{\xi} \frac{N^\lambda}{N}\Big[(Z_\lambda - 1)(x_\lambda \ell n\, x_\lambda + y_\lambda \ell n\, y_\lambda)$$

$$- \tfrac{1}{2} Z_{\lambda\lambda}\{x_\lambda(1-\alpha_\lambda y_\lambda)\ell n\, x_\lambda(1-\alpha_\lambda y_\lambda)$$

$$+ 2x_\lambda y_\lambda \alpha_\lambda \ell n\, x_\lambda y_\lambda \alpha_\lambda + y_\lambda(1-\alpha_\lambda x_\lambda)\ell n\, y_\lambda(1-\alpha_\lambda x_\lambda)\}$$

$$- Z_{\lambda\lambda+1}\{x_\lambda(1-\beta_\lambda y_{\lambda+1})\ell n\, x_\lambda(1-\beta_\lambda y_{\lambda+1})$$

$$+ x_\lambda y_{\lambda+1}\beta_\lambda \ell n\, x_\lambda y_{\lambda+1}\beta_\lambda + y_\lambda x_{\lambda+1}\beta_\lambda' \ell n\, x_{\lambda+1} y_\lambda \beta_\lambda'$$

$$+ y_\lambda(1-\beta_\lambda' x_{\lambda+1})\ell n\, y_\lambda(1-\beta_\lambda' x_{\lambda+1})\}\Big]. \qquad \ldots (7.10)$$

The quantities quantities x_λ, α_λ, β_λ are now obtained by minimizing the free energy per atom F= U-TS with the constraint that the overall concentration of various constituents in the alloy is fixed. Mathematically this constraint is

$$\sum_{\lambda=o}^{\xi} N^\lambda x_\lambda = N_A. \qquad \ldots (7.11)$$

This minimization procedure leads to the following set of

equations:

$$\frac{2\varepsilon}{kT}\Big[Z^{o}\alpha_{\lambda}(y_{\lambda}-x_{\lambda})+Z^{1}(\beta_{\lambda}y_{\lambda+1}-\beta'_{\lambda}x_{\lambda+1}+y_{\lambda-1}\beta'_{\lambda-1}$$
$$-x_{\lambda-1}\beta_{\lambda-1})\Big]-\frac{2BZ_{\lambda}+\eta}{kT}-(Z_{\lambda}-1)\ell n\,(x_{\lambda}/y_{\lambda})$$

$$+\frac{1}{2}Z^{o}\Big[\{1-\alpha_{\lambda}(y_{\lambda}-x_{\lambda})\}\ell n\,x_{\lambda}(1-\alpha_{\lambda}y_{\lambda})$$
$$-\{1+\alpha_{\lambda}(y_{\lambda}-x_{\lambda})\}\ell n\,y_{\lambda}(1-\alpha_{\lambda}x_{\lambda})$$
$$+2\alpha_{\lambda}(y_{\lambda}-x_{\lambda})\ell n\,\alpha_{\lambda}x_{\lambda}y_{\lambda}\Big]$$

$$+Z^{1}\Big[\ell n\,\frac{(1-y_{\lambda+1}\beta_{\lambda})x_{\lambda}}{y_{\lambda}(1-\beta'_{\lambda}x_{\lambda+1})}+y_{\lambda+1}\beta_{\lambda}\ell n\,\frac{y_{\lambda+1}\beta_{\lambda}}{1-y_{\lambda+1}\beta_{\lambda}}$$
$$-x_{\lambda+1}\beta'_{\lambda}\ell n\,\frac{x_{\lambda+1}\beta'_{\lambda}}{1-x_{\lambda+1}\beta'_{\lambda}}+y_{\lambda-1}\beta'_{\lambda-1}\ell n\,\frac{x_{\lambda}\beta'_{\lambda-1}}{1-x_{\lambda}\beta'_{\lambda-1}}$$
$$-x_{\lambda-1}\beta_{\lambda-1}\ell n\,\frac{y_{\lambda}\beta_{\lambda-1}}{1-y_{\lambda}\beta_{\lambda-1}}\Big]=0 \qquad \ldots\ (7.12a)$$

$$\frac{2\varepsilon}{kT}+\frac{1}{2}\ell n\,\frac{\alpha_{\lambda}^{2}x_{\lambda}y_{\lambda}}{(1-\alpha_{\lambda}y_{\lambda})(1-\alpha_{\lambda}x_{\lambda})}=0 \qquad \ldots\ (7.12b)$$

and

$$\frac{2\varepsilon}{kT}+\frac{1}{2}\ell n\,\frac{\beta_{\lambda}y_{\lambda+1}\beta'_{\lambda}x_{\lambda+1}}{(1-y_{\lambda+1}\beta_{\lambda})(1-x_{\lambda+1}\beta'_{\lambda})}=0 \qquad \ldots\ (7.13c)$$

Here η is a Lagrangian multiplier and it can be determined from

$$\frac{2\varepsilon Z}{kT}-\alpha_{b}(y_{b}-x_{b})-\frac{2BZ+\eta}{kT}-(Z-1)\ell n(x_{b}/y_{b})$$
$$+\frac{1}{2}Z\Big[\{1-\alpha_{b}(y_{b}-x_{b})\}\ell n\,x_{b}(1-y_{b}\alpha_{b})-\{1+\alpha_{b}(y_{b}-x_{b})\}\,x$$
$$\ell n\,y_{b}(1-\alpha_{b}x_{b})+2(y_{b}-x_{b})\alpha_{b}\ell n\,\alpha_{b}x_{b}y_{b}\Big]=0. \qquad \ldots\ (7.14)$$

This equation has been obtained from (7.12a) by replacing the surface variables by their corresponding bulk value. In the limit of perfectly random alloy (α=1) equations (7.12a) and (7.14) reduces to equations (6.21) and (6.22) respectively. (7.12b) and (7.12c) are the generalizations of the familiear relationship for the bulk[192].

$$\frac{2\varepsilon}{kT} + \frac{1}{2}\ell n \frac{\alpha_b^2 x_b y_b}{(1-\alpha_b y_b)(1-\alpha_b x_b)} = 0. \qquad \ldots (7.15)$$

Equations (7.13) and (7.14) can further be simplified to obtain the following expressions:

$$\begin{aligned}
&\frac{2\varepsilon Z^1}{kT}(\beta_\lambda y_{\lambda+1} - x_{\lambda+1}\beta'_\lambda + y_{\lambda-1}\beta'_{\lambda-1} - x_{\lambda-1}\beta_{\lambda-1}) \\
&- \frac{2BZ_\lambda + \eta}{kT} + \frac{Z^o}{2}\ell n \frac{1-\alpha_\lambda y_\lambda}{1-\alpha_\lambda x_\lambda} + Z^1\Big[\ell n \frac{1-\beta_\lambda y_{\lambda+1}}{1-\beta'_\lambda x_{\lambda+1}} \\
&+ y_{\lambda+1}\beta_\lambda \ell n \frac{y_{\lambda+1}\beta_\lambda}{1-y_{\lambda+1}\beta_\lambda} - x_{\lambda-1}\beta_{\lambda-1}\ell n \frac{y_\lambda \beta_{\lambda-1}}{1-y_\lambda\beta_{\lambda-1}} \\
&+ y_{\lambda-1}\beta'_{\lambda-1}\ell n \frac{x_\lambda \beta'_{\lambda-1}}{1-x_\lambda\beta'_{\lambda-1}} - x_{\lambda+1}\beta'_\lambda \ell n \frac{x_{\lambda+1}\beta'_\lambda}{1-x_{\lambda+1}\beta'_\lambda}\Big] \\
&- (Z_\lambda - \frac{Z^o}{2} - Z^1 - 1)\ell n(x_\lambda/y_\lambda) = 0 \qquad \ldots (7.16a)
\end{aligned}$$

$$\alpha_\lambda = \frac{-1+\sqrt{1+4\gamma x_\lambda y_\lambda}}{2x_\lambda y_\lambda \gamma} \qquad \ldots (7.16b)$$

$$\beta_\lambda = \frac{-\{1+\gamma(x_{\lambda+1}-x_\lambda)\} + \sqrt{[1+\gamma(x_{\lambda+1}-x_\lambda)]^2 + 4\gamma x_\lambda y_{\lambda+1}}}{2\gamma x_\lambda y_{\lambda+1}} \qquad \ldots (7.16c)$$

where $\gamma = (e^{4\varepsilon/kT} - 1)$. $\qquad \ldots (7.17)$

For brevity we have replaced $Z_{\lambda\lambda}$ and $Z_{\lambda\lambda+1}$ by Z° and Z^{1} respectively, because these will be the same for all the layers. For η the final equation is

$$\frac{\eta + 2BZ}{kT} = \left(\frac{Z}{2} - 1\right) \ell n(x_b/y_b) - \frac{1}{2} Z \ell n \frac{1-y_b\alpha_b}{1-x_b\alpha_b}. \qquad \ldots (7.18)$$

As we did in the case of random alloys, here also we can consider first two or three layers in which the concentration is different from the bulk. Then it can be assumed that all the remaining layers have the bulk concentration. For each layer we have to determine three parameters.

§ 7.2 Preliminary Results for Ag-Au Alloys

Recently Overbury and Somarjai[85] have studied the surface composition of Au-Ag alloys using Auger electron spectroscopy. They have compared their experimental data with the monolayer regular solution model. They find that the monolayer regular solution theory predicts much more segregation for Ag at the surface than is found experimentally. The heat of mixing of these alloys and the difference in the heats of vaporization of pure Ag and Au is quite large. Further there is experimental evidence based on X-ray scattering that there is considerable short-range-order in these alloys. Thus it is expected that the monolayer regular solution model will not be appropriate for Ag-Au alloys.

Here we have calculated the quantities ε and α_b from the data on heats of mixing of these alloys using the method of

Averback[192]. Now ε and α_b are concentration (x_b) and temperature (T) dependent. For Ag-Au alloys these are tabulated in the table 7.1. The temperature dependence of ε is easily understood as being due to vibrational contributions to the heat of mixing. The concentration dependence is presumably related to three body forces and long range forces in the alloys. As discussed in Chapter VI, B is proportional to the difference in the heats of vaporizations of the pure constituents A and B. This has been taken constant. Using the data tabulated by Hultgren et al[191] we find that NB = -1678 Cal/mol. at 800°K. The numerical solutions of equation (7.16) are obtained following the method of Chapter VI. We assume that x_λ etc. attain the bulk value after the first three layers. Then equation (7.16) is written explicitly for the first three layers which are then solved simultaneously. Here, we present some of our results in the absence of short-range-order (though it has been taken into account in the calculation of ε). The complete solution of (7.16) is in progress. Our calculation shows that a rather heavy enrichment of Ag occurs at the top layer. However, the variation of concentration with layers is not monotonic, for in the second layer, there is a slight enrichment of Au. In the third layer again enrichment of Ag occurs. This sort of oscillation is to be expected as ε is negative for these alloys, so that unlike pairs have stronger bonds. The results are shown in figure 7.1. Our results for the segregation on the top layer are much higher than those observed experimentally by AES. However, an AES experiment probes not just the topmost layer but a few of

Table 7.1

Values of parameters $\varepsilon = u + j(x) + gT$ and α_b for Ag-Au alloys at T = 800°K

x_{Au}	N(u+j(x)) Cal/mol	Ng Cal/mol°K	α_b	Nε Cal/mol
0.1	-384.4556	0.0867	1.0356	-315.0956
0.2	-368.0235	0.0779	1.0614	-305.7035
0.3	-356.7311	0.0713	1.0790	-299.6911
0.4	-347.6946	0.0674	1.0885	-293.7746
0.5	-339.4583	0.0660	1.0900	-286.6583
0.6	-336.1584	0.0694	1.0846	-280.6384
0.7	-333.1505	0.0749	1.0720	-273.2305
0.8	-331.3079	0.0826	1.0533	-265.2279
0.9	-332.8094	0.0908	1.0294	-260.1694

the layers near the surface depending on the incident electron energy. For the sake of comparison with AES experiment, we should calculate the average concentration over the top few layers. Figure 7.2 shows the average of Ag concentration on first three layers and its comparison with the results of manolayer model. Our results are closer to experimental values. We think that the AES results should be taken for various incident electron energy. Then by knowing the attenuation depth of electrons of various energies one can calculate an average concentration on those layers from the present model and a comparison can be made with the experiments. Also so far we have not come across any experimental results on surface short-range-order parameter. The most suitable experiment for this will be LEED. We feel that the short-range-order may have significant effect on the surface segregation and the surface short-range-order parameter may be quite different from its bulk value. These quantities will naturally play an important role in determining the behaviour of various elementary excitation near surfaces of alloys.

FIGURE CAPTIONS

Fig.7.1 Plots of surface concentration $m_\lambda = x_\lambda - y_\lambda$ vs. bulk concentration ($m_b = x^b - y^b$). (——), (---) and (-·-) denote respectively the first layer, the second layer and the third layer composition. T = 800°K.

Fig.7.2 Plot of the surface composition of Ag vs. the bulk Ag concentration. The full line denotes the averaged surface concentration of Ag which is the mean over the first three layers. The broken line denotes the corresponding result obtained from the monolayer model.

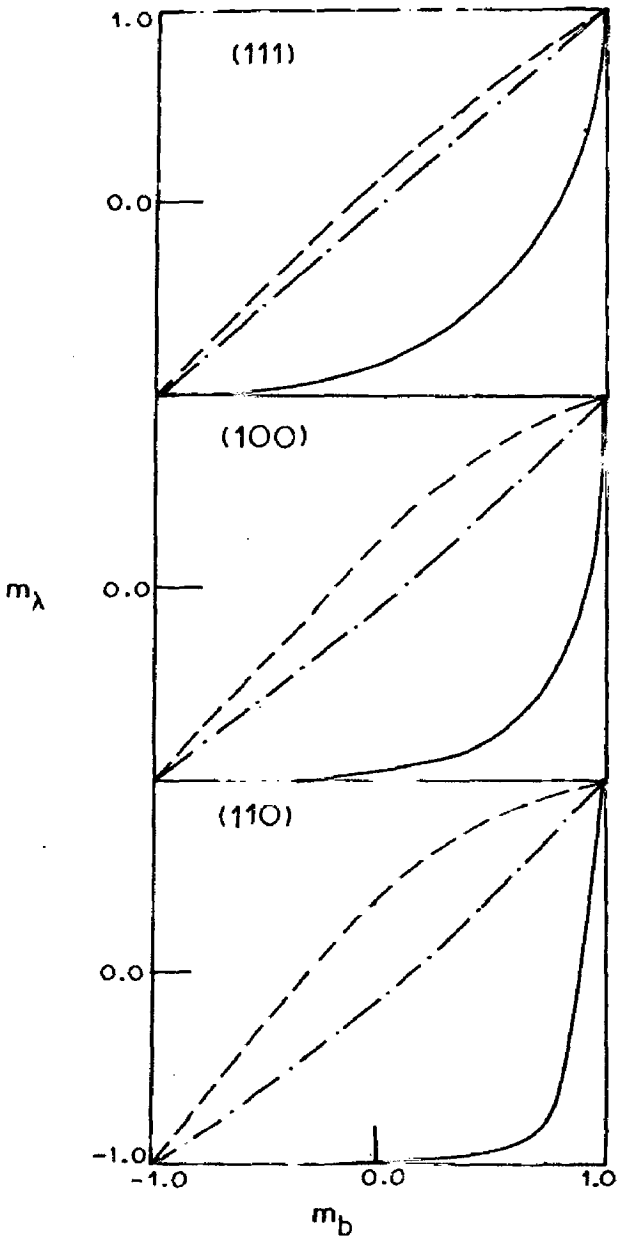
1.0
(111)
0.0
(100)
m_λ
0.0
(110)
0.0
-1.0
-1.0
0.0
1.0
m_b

FIG. 7.1

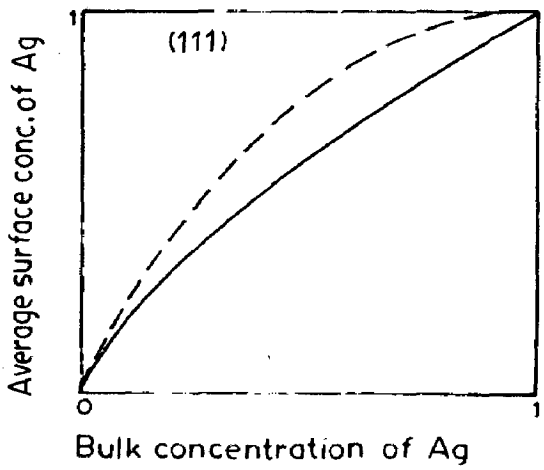
1
(111)
Average surface conc. of Ag
0
1
Bulk concentration of Ag

FIG 7.2

APPENDIX A

Single Particle Green's Function

For a given alloy configuration described by H, the single particle Green's function is defined as

$$G(z) = (z-H)^{-1} \qquad \ldots (A.1)$$

where $z = E \pm i\gamma$ is the complex energy having an infinitesimal imaginary part γ.

(A.1) may be rewritten in the following form

$$G(z) = \int_{-\infty}^{\infty} d\eta \, \frac{1}{z-\eta} \, \delta(\eta-H). \qquad \ldots (A.2)$$

Using the identity

$$\lim_{\gamma \to 0} \frac{1}{E-\eta \pm i\gamma} = P \frac{1}{E-\eta} \mp i\pi\delta(E-\eta) \qquad \ldots (A.3)$$

We have

$$G(E \pm io) = \int_{-\infty}^{\infty} d\eta \left[P \frac{1}{E-\eta} \mp i\pi\delta(E-\eta) \right] \delta(\eta-H). \qquad \ldots (A.4)$$

Here P denotes the principal value part.

Therefore,

$$\delta(E-H) = (2\pi i)^{-1} \left[G(E-io) - G(E+io) \right]. \qquad \ldots (A.5)$$

The spectral density operator A(E) defined as $A(E) = \langle \delta(E-H) \rangle$ is therefore

$$A(E) = (2\pi i)^{-1} \langle G(E-io) - G(E+io) \rangle \qquad \ldots (A.6)$$

which shows that the configurationally averaged spectral density of states operator is related to the discontinuity

of the configurationally averaged Green's function across the real axis. From equation (A.4) it follows that G(E+i0) and G(E-i0) are complex conjugate to each other and therefore

$$\langle G(E-i0) - G(E+i0) \rangle = -2i \, \mathrm{Im} \langle G(E+i0) \rangle . \qquad \ldots (A.7)$$

Hence

$$A(E) = -\frac{1}{\pi} \mathrm{Im} \langle G(E+i0) \rangle . \qquad \ldots (A.8)$$

The significance of the spectral density operator is clarified if it is expressed as a matrix element with respect to a configuration independent set of states $|\vec{k}\rangle$ appropriate to a perfect crystal;

$$\begin{aligned} A(\vec{k},E) &= \langle \vec{k}| \langle \delta(E-H) \rangle |\vec{k}\rangle \\ &= -\frac{1}{\pi} \mathrm{Im} \langle \vec{k}| \langle G(E+i0) \rangle |\vec{k}\rangle . \end{aligned} \qquad \ldots (A.9)$$

The spectral functions $A(\vec{k},E)$ gives information about the energy and the life time of excitations. Another quantity of main interest in disordered systems is the averaged density of states per atom which is related to the trace of the spectral density operator A.

$$\rho(E) = \frac{1}{N} \sum_{\vec{k}} A(\vec{k},E) = N^{-1} \mathrm{Tr} [\underline{A}(E)] \qquad \ldots (A.10)$$

Therefore $\rho(E) = -\frac{1}{\pi N} \mathrm{Im}\, \mathrm{Tr} \langle G(E+i0) \rangle = -\frac{1}{\pi} \mathrm{Im} \langle 0| \langle G \rangle |0\rangle$

$$\ldots (A.11)$$

which shows that the trace of the imaginary part of the configurationally averaged Green's function gives information about the density of states.

APPENDIX B

Exact Results in Dilute Limit

We consider a single impurity in a simple cubic crystal. In the subspace of the Wannier states spanned by the impurity site and the six nearest neighbours, the impurity potential in a single s-band model can be written in the following form:

$$V = \begin{pmatrix} \delta_0 & \delta_1 & \delta_1 & \delta_1 & \delta_1 & \delta_1 & \delta_1 \\ \delta_1 & \delta_2 & 0 & 0 & 0 & 0 & 0 \\ \delta_1 & 0 & \delta_2 & 0 & 0 & 0 & 0 \\ \delta_1 & 0 & 0 & \delta_2 & 0 & 0 & 0 \\ \delta_1 & 0 & 0 & 0 & \delta_2 & 0 & 0 \\ \delta_1 & 0 & 0 & 0 & 0 & \delta_2 & 0 \\ \delta_1 & 0 & 0 & 0 & 0 & 0 & \delta_2 \end{pmatrix} \qquad \ldots (B.1)$$

where $\langle 0|V|0\rangle = \delta_0$, $\langle 1|V|0\rangle = \delta_1$, $\langle 1|V|1\rangle = \delta_2$, and $|1\rangle$ is any nearest neighbour site.

In forming this potential, diagonal perturbations (δ_2) on the nearest-neighbour sites have been included. This matrix can be block diagonalized using the unitary transformation S discussed by Wolfram and Callaway[193],

$$S = \begin{pmatrix} 1 & 0 & 0 & 0 & 0 & 0 & 0 \\ 0 & a & b & 0 & 0 & 0 & d \\ 0 & a & -b & 0 & 0 & 0 & d \\ 0 & a & 0 & b & 0 & c & e \\ 0 & a & 0 & -b & 0 & c & e \\ 0 & a & 0 & 0 & b & -c & e \\ 0 & a & 0 & 0 & -b & -c & e \end{pmatrix} \quad \ldots \text{ (B.2)}$$

where $a = 1/\sqrt{6}$, $b = 1/\sqrt{2}$, $c = \frac{1}{2}$, $d = 1/\sqrt{3}$, and $e = 1/\sqrt{12}$. Under this transformation, the potential becomes[159]

$$V' = S^{\dagger} V S = \begin{pmatrix} \begin{pmatrix} \delta_0 & \sqrt{6}\delta_1 \\ \sqrt{6}\delta_1 & \delta_2 \end{pmatrix} & 0 & 0 \\ 0 & \begin{pmatrix} \delta_2 & 0 & 0 \\ 0 & \delta_2 & 0 \\ 0 & 0 & \delta_2 \end{pmatrix} & 0 \\ 0 & 0 & \begin{pmatrix} \delta_2 & 0 \\ 0 & \delta_2 \end{pmatrix} \end{pmatrix} \quad \ldots \text{ (B.3)}$$

The first block operates on the two s-states, the second on the three p-states and the third on the two d states. The same unitary transformation block-diagonalizes the Green's function giving

$$G' = S^{\dagger} G S = \begin{pmatrix} \begin{pmatrix} G_{oo} & \sqrt{6}\, G_{ol} \\ \sqrt{6}\, G_{ol} & G_s \end{pmatrix} & 0 & 0 \\ 0 & \begin{pmatrix} G_p & 0 & 0 \\ 0 & G_p & 0 \\ 0 & 0 & G_p \end{pmatrix} & 0 \\ 0 & 0 & \begin{pmatrix} G_d & 0 \\ 0 & G_d \end{pmatrix} \end{pmatrix} \qquad \ldots \text{(B.4)}$$

where,

$$G_s(E) = \frac{6}{N} \sum_{\vec{k}} \frac{s^2(\vec{k})}{E - E_{\vec{k}}}, \qquad G_{oo} = \frac{1}{N} \sum_{\vec{k}} \frac{1}{E - E_{\vec{k}}},$$

$$G_p(E) = \frac{1}{N} \sum_{\vec{k}} \frac{(1 - s(2\vec{k}))}{E - E_{\vec{k}}}, \qquad G_{ol} = \frac{1}{N} \sum_{\vec{k}} \frac{s(\vec{k})}{E - E_{\vec{k}}},$$

$$G_d(E) = \frac{1}{N} \sum_{\vec{k}} \frac{\frac{3}{2}(1 + s(2\vec{k}) - 2s^2(\vec{k}))}{E - E_{\vec{k}}}$$

and $s(\vec{k}) = \frac{1}{3}(\cos k_x a + \cos k_y a + \cos k_z a)$.

The T-matrix can now be written in block diagonal form, with the three blocks

$$t_s(E) = \left[\begin{pmatrix} 1 & 0 \\ 0 & 1 \end{pmatrix} - \begin{pmatrix} \delta_o & \sqrt{6}\, \delta_1 \\ \sqrt{6}\delta_1 & \delta_2 \end{pmatrix} \begin{pmatrix} G_{oo} & \sqrt{6}\, G_{ol} \\ \sqrt{6}\, G_{ol} & G_s \end{pmatrix} \right]^{-1} \begin{pmatrix} \delta_o & \sqrt{6}\, \delta_1 \\ \sqrt{6}\, \delta_1 & \delta_2 \end{pmatrix}, \qquad \ldots \text{(B.5a)}$$

$$t_p(E) = \left[1 - \delta_2 G_p(E) \right]^{-1} \delta_2 \begin{pmatrix} 1 & 0 & 0 \\ 0 & 1 & 0 \\ 0 & 0 & 1 \end{pmatrix}, \qquad \ldots \text{(B.5b)}$$

$$t_d(E) = [1-\delta_2 G_d(E)]^{-1} \delta_2 \begin{pmatrix} 1 & 0 \\ 0 & 1 \end{pmatrix} . \qquad \ldots (B.5c)$$

As Stern[160] has pointed out, the diagonal-disorder model contains, necessarily, only s-wave scattering by each defect, and hence has only a single phase shift to satisfy the Friedel sum rule. When the off-diagonal disorder is included ($\delta_1 \neq 0$) but $\delta_2 = 0$, we see from Eq.(B.5) that only the s-wave scattering is non-zero. It is, therefore, clear that the mere existence of some off-diagonal disorder is not sufficient for p- and d-wave scattering by a defect to occur. Rather it is required that the perturbing potential on the neighbouring sites also be nonzero. For example $\delta_2 \neq 0$ is sufficient. Thus the standard model of off-diagonal disorder ($\delta_o \neq 0$, $\delta_1 \neq 0$) which has been in common use in various generalizations of the CPA for the electronic problem, clearly fails to produce more than simply s-wave scattering and hence does not have enough flexibility to satisfy the Friedel sum rule when self-consistency requirement on the potential is imposed. When only the s-wave scattering is non-zero, the diagonal element of the T-matrix in $\vec{k}$-space becomes

$$t^s_{\vec{k}\vec{k}} = \frac{\delta_o + 6\delta_1^2 G_s + 12\delta_1(1-6\delta_1 G_{o1})s(\vec{k}) + 36\delta_1^2 G_{oo} s^2(\vec{k})}{1-\delta_o G_{oo} - 12\delta_1 G_{o1} + 36\delta_1^2 G_{o1}^2 - 6\delta_1^2 G_{oo} G_s} . \qquad \ldots (B.6)$$

In the low concentration limit the self-energy is given by

$$\sum(\vec{k},z) = x\, t^s_{\vec{k}\vec{k}} . \qquad \ldots (B.7)$$

From Eqs.(B.6) and (B.7) it is clear that in order to achieve the proper dilute limit the self-energy should contain a term proportional to $s^2(\vec{k})$.

REFERENCES

1. N.F.Mott, Adv.Phys.16, 49(1967).

2. N.F.Mott and E.A.Davis 'Electronic Processes in Non-Crystalline Materials' Clarendon, Oxford(1971).

3. P.Dean, Rev. Mod. Phys.44, 127(1972).

4. R.J. Bell, Rep.Prog.Phys.35, 1315(1972).

5. R.A. Cowley and W.J.L. Buyers, Rev.Mod. Phys.44,406(1972).

6. R.J.Elliott, J.A.Krumhansl and P.L.Leath, Rev. Mod. Phys.46, 465(1974).

7. H. Ehrenreich and L.Schwartz, Solid State Physics 31, ed. by H.Ehrenreich, F.Seitz and D.Turnbull, Academic Press(1976).

8. Vijay Kumar and S.K. Joshi, 'The Electronic States in Disordered Alloys', in the Commemoration Volume of Indian Journal of Physics and the Proceedings of Indian Association for Cultivation of Science Part II (1977).

9. N.F.Mott and H.Jones, 'Theory of the Properties of Metals and Alloys', Oxford University Press 1936.

10. F.Seitz, 'The Modern Theory of Solids', McGraw Hill (1940).

11. J.M.Ziman, 'Principles of the Theory of Solids', Cambridge University Press 1973.

12. R.E. Borland, Proc. Roy. Soc.274A, 529(1964); F.J.Dyson, Phys.Rev.92, 1331(1953).

13. R.L. Agacy, Proc. Phys. Soc. Lond. 83, 591(1964).

14. H.Schmidt, Phys. Rev.105,425(1957).

15. J.Hori, 'Spectral Properties of Disordered Chains and Lattices', Pergamon Press, London (1968).

16. Calculations for three dimensional systems have been carried out by Payton and Visscher[17] for the vibrational problem and more recently by Alben et al[18,19] for the electronic problem.

17. D.N. Payton III and W.M. Visscher, Phys. Rev. 154, 802(1967); ibid.175, 1201(1968).

18. R.Alben, M.Blume, H.Krakauer and L.Schwartz, Phys. Rev.B12, 4090(1975).

19. R.Alben, H.Krakauer and L.Schwartz, Phys. Rev. B14, 1510 (1976).

20. J. Callaway, 'Energy Band Theory', Academic Press, N.Y. (1964).

21. J.M. Ziman, Solid State Phys. Vol.26, Ed.by H.Ehrenreich, F.Seitz and D.Turnbull; (Academic Press 1971).

22. F.Herman, Phys. Rev.95, 847(1954); J.Tauc and H.Abraham, J.Phys.Chem.Sol.20, 190(1961); F.Bassani and D.Brust. Phys.Rev.131, 1524(1963).

23. D.Strond and H.Ehrenreich, Phys.Rev.B2, 3197(1970).

24. M.Lax, Rev. Mod. Phys.23, 287(1951).

25. M.Lax, Phys. Rev.85, 621(1952).

26. D.N. Zubarev, Usp. Fiz.Nauk 71, 71(1960) [Sov.Phys.Usp.3, 320(1960)].

27. P.Soven, Phys.Rev.156, 809(1967).

28. D.W.Taylor, Phys.Rev.156, 1017(1967).

29. B.Velicky, S.Kirkpatrick, and H.Ehrenreich, Phys.Rev.175, 747(1968).

30. See review articles in refs.6-8.

31. Theodore Kaplan and Mark Mostoller, Phys. Rev.B9, 1783(1974).

32. W.A. Kamitakahara and D.W.Taylor, Phys. Rev.B10, 1190(1974).

33. W.J.L. Buyers, D.E. Pepper and R.J.Elliott, J.Phys.C5, 2611(1972).

34. W.J.L. Buyers, D.E. Papper and R.J.Elliott, J.Phys.C6,1933 (1973).

35. M.J.Zuckermann, Can.J.Phys.52, 2177(1974).

36. W.H.Butler, Phys.Rev.B8, 4499(1973).

37. D.S.Saxon and R.A.Hutner, Philips Res.Rep.4, 81(1949).

38. J.M. Luttinger, Philips Res. Rep.6, 303(1951).

39. I.M. Lifshitz, Adv.Phys.13, 483(1964); usp.Fiz.Nauk 83, 617(1964) [Sov.Phys.-Usp.7,549(1965)].

40. S.Kirkpatrick, B.Velicky, and H.Ehrenreich, Phys.Rev.B1, 3250(1970).

41. D.J. Thouless, J.Phys.C3,1559(1970).

42. G.M. Stocks, R.W.Williams and J.S.Faulkner, Phys.Rev. Lett. 26, 253(1971).

43. G.M. Stocks, R.W.Williams and J.S.Faulkner, Phys.Rev.B4, 4390(1971).

44. G.M. Stocks, R.W.Williams and J.S.Faulkner, J.Phys.F3, 1688(1973).

45. K.Levin and H.Ehrenreich, Phys.Rev.B3, 4172(1971).

46. L.M. Schwartz, F.Brouers, A.V.Vedyayev and H.Ehrenreich, Phys.Rev.B4, 3338(1971).

47. C.D.Gelatt. Thesis, Harvard University (1974),(Unpublished).

48. C.D.Gelatt and H.Ehrenreich, Phys.Rev. B10, 398(1974).

49. A. Bansil, H.Ehrenreich, L.Schwartz and R.E. Watson, Phys. Rev.B9, 445(1974).

50. A.Bansil, L.Schwartz and H.Ehrenreich, Phys. Rev.B12, 2893 (1975).

51. A. Bansil, Solid State Commun. 16,885(1975).

52. L.M. Schwartz and A.Bansil, Phys.Rev.B10, 3261(1974).

53. P.E.Mijnarends and A.Bansil, Phys.Rev. B13, 2381(1976).

54. B.L. Gyorffy and G.M. Stocks, J.Phys.(Paris) 35, 74(1974).

55. CPA has been formulated for muffin-tin potential model of alloys by Soven[56] and Shiba[57] but it has not so far been applied to realistic systems.

56. P.Soven, Phys.Rev.B2, 4715(1970).

57. H.Shiba, Prog. Theor. Phys.46, 77(1971).

58. A.Mookerjee, J.Phys. C6, L205(1973).

59. A.Mookerjee, J.Phys.C6, 1340(1973).

60. K.Niizeki, Prog. Theor. Phys.53, 54(1975).

61. Vijay Kumar, Deepak Kumar and S.K. Joshi, Phys.Rev.B11, 2831(1975).

62. S.H.Overbury, P.A.Bertrand and G.A.Somarjai, Chem.Rev.75, 547(1975).

63. P.J. Estrup. Physics Today (April), p.33(1975)

64. D.E.Eastman and M.I.Nathan, Phys. Today (April) 44(1975); T.C.Tracy,Nato Summer School on Electron Spectroscopy, Gent. Belgium, 1972.

65. J.W. Gibbs, Trans. Conn.Acad.Arts Sci 3, 108(1875/76), 343(1877/78).

66. G.A.Somarjai, 'Principles of Surface Chemistry', Prentice Hall, N.Y.1972.

67. R.Defay, I.Prigogine, A.Bellemans and D.H.Everett, 'Surface Tension and Adsorption, Wiley, N.Y.1966.

68. L.A.Harris, J.Appl.Phys.39, 1419(1968).

69. R.Bouwman, Ned.Tijdschrift Voor Vacuum Technick 11, 37 (1973).

70. M.L. Tarng and G.K. Wehner, J.Appl.Phys.42, 2449(1971).

71. D.T. Quinto, V.S.Sundaram, and W.D.Robertson, Surf.Sci. 28, 504(1971).

72. M.Ono, Y.Takasu, K.Nakayama and T.Yamashina, Surf. Sci. 26, 313(1971).

73. C.R.Helms, J.Catal.36,114(1975) and references therein.

74. K.Christmann and G.Ertl, Surf.Sci., 33, 254(1972).

75. R.Bouwman and W.M.H.Sachtler, J.Catal.25, 350(1972).

76. B.J.Wood and H.Wise, Surf.Sci. 52, 151(1975).

77. S.Berglund and G.A.Somarjai, J.Chem.Phys.59, 5537(1973).

78. F.L. Williams and M.Boudart, J.Catal.30, 438(1973).

79. J.J. Burton, C.R.Helms and R.S.Polizzotti, J.Vac.Sci. Technol.13, 204(1976); J.Chem.Phys.65, 1089(1976).

80. C.Leygraf, G.Hultquist, S.Ekelund and J.C.Ericksson, Surf. Sci. 46, 157(1974).

81. P.Braun and W.Farber, Surf.Sci.47, 57(1975).

82. R.A.Van Santen, L.H. Toneman and R.Bouwman, Surf.Sci. 47, 64(1975),

83. J.M. McDavid and S.C.Fain,Jr., Surf.Sci. 52, 161(1975).

84. H.C.Potter and J.M.Blakely, J.Vac. Sci. Technol.12, 635 (1975).

85. S.H.Overbury and G.A. Somarjai, Surf. Sci. 55, 209(1976).

86. R.Bouwman, L.H. Tonemann, M.A.M. Boersma and R.A.Van Santen, Surf.Sci.59, 72(1976).

87. G.Nelson, Surf. Sci.59.

88. S.H.Overbury and G.A.Somerjai, J.Chem.Phys.(in press).

89. C.T.H. Stodart, R.L. Moss and D.Pope, Surf.Sci. (in press).

90. F.J.Kuijers, R.P.Dessing and W.M.H. Sachtler, J.Catal.33, 316(1974).

91. R.Bouwman, L.H. Toneman and A.A.Holscher, Surf. Sci. 35, 8(1973).

92. R.Bouwman and P.Biloen, Surf. Sci. 41, 348(1974); Analytical Chem.46, 136(1974).

93. J.Ferrente, Acta Metall.19, 743(1971).

94. M.L.Tarng and G.K. Wehner, J.Appl. Phys.42, 2449(1971).

95. R.Bouwman and W.M.H.Sachtler, J.Catal.19,127(1970).

96. F.L. Williams and D.Nason, Surf.Sci.45, 377(1974).

97. J.J. Burton and E.Hyman, J.Catal.37, 114(1975).

98. J.J. Burton, E.Hyman and D.Fedak, J.Catal.37, 106(1975).

99. R.A. Van Santen and W.M.H. Sachtler, J.Catal.33, 202(1974).

100. Deepak Kumar, A.Mookerjee and Vijay Kumar, J.Phys.F6,725 (1976).

101. R.A.Swalin, 'Thermodynamics of Solids', Wiley, N.Y.1972.

102. D.McLean, 'Grain Boundaries in Metals', Oxford, Clarendon (1957).

103. M.P.Seah, Surf.Sci.53, 168(1975).

104. J.J.Burton and E.S.Machlin, Phys.Rev. Lett. 37, 1433(1976).

105. Vijay Kumar, Deepak Kumar and S.K. Joshi in the Proceedings of 'International Symposium on Solid State Physics', held at Calcutta Jan.10-14, 1977; Vijay Kumar, Deepak Kumar and S.K. Joshi, submitted to J.Phys.F.

106. P.W.Anderson and W.L.McMillan in 'Theory of Magnetism in Transition Metals', Proceedings of the International School of Physics, 'Enrio Fermi', Course 37, Edited by H.Suhl (Academic Press 1967).

107. S.F.Edwards, Phil.Mag.6, 617(1961).

108. J.L. Beeby and S.F.Edwards, Proc.Roy.Soc. Lond.274A,395 (1962).

109. See H.Ehrenreich in the proceedings of the Michigan State University Summer School on Alloys 1972.

110. L.M.Schwartz and H.Ehrenreich, Phys.Rev. B6, 2923(1972).

111. The CPA has been rederived independently by several workers using various different techniques. For a review of these we refer to review articles in refs. 6,8 and 112.

112. F.Yonezawa and K.Morigaki, Prog.Theor.Phys. Suppl.53,1(1973).

113. A.B.Chen, Phys.Rev.B7, 2250(1973).

114. S.F.Edwards, Proc. Roy.Soc. Lond.267A,518(1962).

115. J.Hubbard, Proc.Roy. Soc. Lond.276A, 238(1963).

116. V.Jaccarino and L.R.Walker, Phys.Rev. Lett. 15, 258(1965).

117. J.S.Kouvel and J.B.Comly, Phys.Rev. Lett. 24, 598(1970).

118. T.J.Hicks, B.Rainford, J.S.Kouvel, G.G.Low and J.B.Comly, Phys.Rev.Lett. 22, 531(1969).

119. J.P.Perrier, B.Tissier and R.F.Tournier, Phys.Rev.Lett. 24, 313(1970).

120. A.T.Aldred, B.D.Rainford, T.J.Hicks and J.S.Kouvel, Phys. Rev.B7, 218(1973).

121. M.Tsukada, J.Phys.Soc. Jap.26, 684(1969).

122. M.Tsukada, J.Phys.Soc.Jap.32, 1475(1972).

123. H.Matsuda, Prog.Theor. Phys.Suppl.36, 97(1966);H.Matsuda and N.Ogita, Prog.Theor. Phys.38, 81(1967); K.Okada and H.Matsuda, Prog.Theor. Phys.39, 1153(1968).

124. W.H. Butler and W.Kohn, J.Res. Natl. Bue.Stand.(U.S.)74A, 443(1970).

125. F.Ducastelle, J.Phys.C7,1795(1974).

126. W.H.Butler, Phys.Lett.39A,203(1972).

127. V.Capek, Phys.Status Solidi 52(b), 399(1972).

128. F.Brouers, M.Cyrot and F.Cyrot-Lackmann, Phys. Rev.B7, 4370(1973).

129. F.Brouers, F.Ducastelle, F.Gautier and J.Van der Rest, J.Phys.F3, 2120(1973).

130. F.Brouers, F.Ducastelle, F.Gautier and J.Van der Rest, J.Phys.(Paris) 35, Suppl.C4-89(1974).

131. H.Miwa, Prog.Theor.Phys.52, 1(1974).

132. H.Schmidt, Phys.Rev.105,425(1957).

133. B.G.Nickel and W.H.Butter, Phys.Rev.Lett.30, 373(1973).

134. For analytic properties of Green's function, see P.Nozieres, 'Interacting Fermi Systems', Benjamin Inc.N.Y.(1964).

135. Vijay Kumar and S.K. Joshi, J.Phys.C8, L 148(1975).

136. A.Mookerjee, J.Phys.C8, 29(1975).

137. A.Mookerjee, J.Phys.C8, 1524(1975).

138. Vijay Kumar and S.K. Joshi, Phys.Rev.(in press).

139. R.Haydock, V.Heino and M.J.Kelly, J.Phys.C5,2845(1972) and references therein.

140. M.C.Desjonqueres and F.Cyrot-Lackmann, Preprint.

141. E.Muller-Hartmann, Solid State Commun.12, 1269(1973).

142. B.G.Nickel and J.A.Krumhansl, Phys. Rev.B4, 4354(1971).

143. A.R.Bishop and A.Mookerjee, J.Phys.C7, 2165(1974).

144. P.W.Anderson, Phys. Rev.109, 1492(1958).

145. T.Kaplan and L.J.Gray, Phys.Rev.B14, 3462(1976); J.Phys. C9, L303(1976).

146. T.Kaplan and L.J.Gray, J.Phys.C9, L483(1976).

147. Vijay Kumar, A.Mookerjee and S.K. Joshi, unpublished.

148. P.L. Leath, Phys. Rev.B2, 3078(1970).

149. T.Matsubara,Prog.Theor.Phys.Suppl.46, 326(1970).

150. R.N.Aiyer, R.J.Elliott, J.A.Krumhansl, and P.L. Leath, Phys.Rev. 181, 1006(1969). F.Yonezawa and S.Homma, J.Phys. Soc. Jap. Suppl. 26, 68(1969); B.G.Nickel and J.A. Krumhansl, Phys.Rev.B4, 4354(1971); P.L. Leath. Phys. Rev.B5, 1643(1972).

151. F.Yonezawa, Prog.Theor.Phys.40, 734(1968). Also see ref.112.

152. J.P.Gaspard and F.Cyrot-Lackmann, J.Phys.C6, 3077(1973) and ref.8.

153. R.L. Jacobs, J.Phys.F3, 933(1973); G.Kerker, J.Phys.F6, L113(1976).

154. F.Cyrot-Lackmann and F.Ducastelle, Phys.Rev. Lett.27, 429(1971).

155. L.M.Schwartz and H.Ehrenreich, Phys.Rev.B6, 2923(1972).

156. F.Ducastelle, J.Phys.F2, 468(1972).

157. P.L. Leath, J.Phys.C6, 1559(1973); J.Phys.(Paris) 35, Suppl.au n°5, C4-99(1974).

158. G.Cubiotti, E.Donato and R.L. Jacobs, J.Phys.F5, 2068(1975).

159. R.Bass and P.L. Leath, Phys. Rev.B9, 2769(1974).

160. E.A. Stern, Phys.Rev. Lett.26, 1630(1971).

161. J.Friedel, Adv.Phys.3, 446(1954); Nuovo Cimento Suppl.7, 287(1958).

162. J.Rudnick and E.A. Stern, Phys.Rev.B7, 5062(1973).

163. J.A.Blackman, D.M. Esterling and N.F.Berk, Phys.Rev.B4, 2412(1971).

164. J.A.Blackman, J.Phys.F3, L31(1973).

165. H.Fukuyama, H.Krakauer and L.Schwartz, Phys.Rev.B10, 1173(1974).

166. J.Mertsching, Phys.Stat.Sol.(b) 63, 241(1974).

167. A.Gonis and J.W.Garland, Phys.Rev.(in press).

168. A.Gonis and J.W.Garland, Phys.Rev.(in press).

169. Vijay Kumar, Deepak Kumar and S.K.Joshi, J.Phys.C9, 2733(1976).

170. E.A.Stern and Avnar Zin, Phys.Rev.B9, 1170(1974).

171. S.M.Bose and E.Ni.Foo, J.Phys.(Paris) 35, C4-95(1974).

172. L.Schwartz, H.Krakauer and H.Fukuyama, Phys.Rev.Lett.30, 746(1973).

173. W.A.Kamitakahara and B.N.Brockhouse, Phys. Rev.B10, 1200(1974).

174. E.Ni.Foo and D.H.Wu, Phys.Rev.B5, 98(1972).

175. R.A.Tahir-Kheli, Phys.Rev.B6, 2808(1972).

176. R.J.Elliott and D.E.Pepper, Phys.Rev.B8, 2374(1973).

177. M.Tsukada, Z.Physik B21, 141(1975).

178. T.Kaneyoshi, Prog.Theor.Phys.42, 477(1969).

179. S.F.Edwardo and R.C.Jones, J.Phys.C4, 2109(1971).

180. R.C.Jones and G.J.Yates, J.Phys.C8, 1705(1975).

181. A.Theumann, J.Phys.C7, 2328(1974).

182. G.A.Murray, Proc. Phys.Soc.89, 111(1966).

183. Yu.Izyumov, Proc. Phys.Soc.87, 505(1966).

184. A.B.Harris, P.L. Leath, B.G.Nickel and R.J. Elliott, J.Phys.C7, 1693(1974).

185. A.Theumann and R.A.Tahir Kheli, Phys.Rev.B12, 1796(1975).

186. M.W.Finnis and V.Heine, J.Phys.F4, L37(1974).

187. T.Muto and Y.Takagi, in Solid State Physics Vol.1, Ed.by H.Ehrenreich, F.Seitz and D.Turnbull (Academic Press, N.Y.1955).

188. L.Guttman in Solid State Physics Vol.3 Ed.by H.Ehrenreich, F.Seitz and D.Turnbull (Academic Press, N.Y.1956).

189. K. Huang, 'Statistical Mechanics' (Wiley, N.Y.1963).

190. L.Kaufman and H. Bernstein, 'Computer Calculation of Phase Diagrams', (Academic Press, N.Y.1970).

191. R.Hultgren, R.Orr, P.Anderson and K.Kelley, 'Selected Values of Thermodynamic Properties of Metals and Alloys', (Wiley, N.Y.1963).

192. B.L. Averbach in 'Energetics in Metallurgical Phenomena', Vol.II, ed.by W.M.Mueller (Gordon and Breach, N.Y.1965).

193. T.Wolfram and J.Callaway, Phys.Rev.130, 2207(1963).

energy which is related to the heat of vaporization of the B component is less than that of A. From the graphs it is seen that the B component becomes enriched at the surface. These results are in agreement with several experimental observations and simple surface thermodynamic principles that the component with lower heat of vaporization or the surface tension gets enriched at the surface. From Figure 6.2, it is observed that the enrichment on the (110) face is the maximum among the three surfaces studied for the same values of parameters ε, B and T and is the least on the (111) face, which is a simple consequence of the fact that the segregation is larger, the larger the value of Z_{IL}. As the temperature is increased, the surface segregation decreases for all the three surfaces. The variation of the concentration in the different layers is shown in figure 6.3. The composition in the first layer is markedly different from that of the bulk whereas in the second layer this difference is very small. The composition in the third layer is almost the same as the bulk and therefore it is not shown explicitly in the graph. This also justifies our approximation that m_λ approaches rather fast to the bulk value for small values of ε, and this is consistent with the assumption regarding the absence of the short range order. In Fig. 6.4 we have plotted $\ell n\left[(x^s/y^s)/(x^b/y^b)\right]$ against 1/T for the three faces and we obtain straight lines. This shows that the simple thermodynamic monolayer model is consistent with our model. However, for larger values of ε one should expect appreciable deviation of composition